(12)

MARINE PHYSICAL LABORATORY

SCRIPPS INSTITUTION OF OCEANOGRAPHY

San Diego, California 92152

Analysis of 200 Hz CW Tone Propagation Signal Recorded During the September 1987 VLA Experiment

Jean-Marie Q.D. Tran and W. S. Hodgkiss

MPL TECHNICAL MEMORANDUM 418

MPL-U-7/90
September 1990

Approved for public release; distribution unlimited.

UNCLASSIFIED

SECURITY CLASSIFICATION OF THIS PAGE

REPORT DOCUMENTATION PAGE

Form Approved
OMB No. 0704-0188

1a. REPORT SECURITY CLASSIFICATION UNCLASSIFIED	1b. RESTRICTIVE MARKINGS
2a. SECURITY CLASSIFICATION AUTHORITY	3. DISTRIBUTION/AVAILABILITY OF REPORT Approved for public release; distribution unlimited.
2b. DECLASSIFICATION/DOWNGRADING SCHEDULE	
4. PERFORMING ORGANIZATION REPORT NUMBER(S) MPL Technical Memorandum 418 [MPL-U-7/90]	5. MONITORING ORGANIZATION REPORT NUMBER(S)
6a. NAME OF PERFORMING ORGANIZATION University of California, San Diego 6b. OFFICE SYMBOL (If applicable) MPL	7a. NAME OF MONITORING ORGANIZATION Office of Naval Research Department of the Navy
6c. ADDRESS (City, State, and ZIP Code) Marine Physical Laboratory Scripps Institution of Oceanography San Diego, California 92152	7b. ADDRESS (City, State, and ZIP Code) 800 North Quincy Street Arlington, VA 22217-5000
8a. NAME OF FUNDING/SPONSORING ORGANIZATION Office of Naval Research 8b. OFFICE SYMBOL (If applicable) ONR	9. PROCUREMENT INSTRUMENT IDENTIFICATION NUMBER N00014-89-K-0038
8c. ADDRESS (City, State, and ZIP Code) 800 North Quincy Street Arlington, VA 22217-5000	10. SOURCE OF FUNDING NUMBERS PROGRAM ELEMENT NO. / PROJECT NO. / TASK NO / WORK UNIT ACCESSION NO.

11. TITLE (Include Security Classification)
ANALYSIS OF 200 Hz CW TONE PROPAGATION SIGNALS RECORDED DURING THE SEPTEMBER 1987 VLA EXPERIMENT

12. PERSONAL AUTHOR(S)
Jean-Marie Q.D. Tran and W.S. Hodgkiss

13a. TYPE OF REPORT	13b. TIME COVERED	14. DATE OF REPORT (Year, Month, Day)	15. PAGE COUNT
technical memorandum	FROM _____ TO _____	September 1990	113

16. SUPPLEMENTARY NOTATION

17. COSATI CODES			18. SUBJECT TERMS (Continue on reverse if necessary and identify by block number)
FIELD	GROUP	SUB-GROUP	vertical line array, source tow modelling, sound speed profile

19. ABSTRACT

This technical report discusses the analysis of the 200 Hz CW tone signals recorded on Julian Day 270 and 272, during the September 1987 Single Vertical Line Array Experiment in the North East Pacific. On Julian Day 270, a 200 Hz CW tone was projected for various time lengths and three different source depths, 165 km from the Vertical Line Array (VLA). On Julian Day 272, the 200 Hz source was towed away from the VLA for 10 hours at a speed of 5 kts. The signals were received by the VLA, which extended from a depth of 400 m to 1300 m. Power spectra between 0 and 250 Hz are presented for selected channels of the array. Vertical distribution of power across the Vertical Line Array is obtained for the signal and noise at 200 Hz. Finally, arrival structures of the signal and of the noise at 200 Hz, are obtained using conventional beamforming techniques. Nine data tapes, recorded during these transmissions, were processed, and the results are presented in this report. The comprehensive environmental information, collected during the experiment, allows the successful acoustic modeling of both the fixed range case, where the source depth is varied and the fixed depth case, where range between the VLA and the source varied from 0 to 100 km. The CONGRATS ray-theory model of the GSM and the ATLAS normal mode model are used, produce similar results which are in good agreement with the experimental results.

20. DISTRIBUTION/AVAILABILITY OF ABSTRACT	21. ABSTRACT SECURITY CLASSIFICATION
☐ UNCLASSIFIED/UNLIMITED ■ SAME AS RPT. ☐ DTIC USERS	UNCLASSIFIED

22a. NAME OF RESPONSIBLE INDIVIDUAL	22b. TELEPHONE (Include Area Code)	22c. OFFICE SYMBOL
W. S. Hodgkiss	(619) 534-1798	MPL

DD Form 1473, JUN 86 *Previous editions are obsolete*

SECURITY CLASSIFICATION OF THIS PAGE
UNCLASSIFIED

Analysis of 200 Hz CW tone Propagation Signals Recorded During the September 1987 VLA Experiment

Jean-Marie Q.D. Tran
William S. Hodgkiss

Marine Physical Laboratory
Scripps Institution of Oceanography
San Diego, CA 92152

ABSTRACT

This technical report discusses the analysis of the 200 Hz CW tone signals recorded on Julian Day 270 and 272, during the September 1987 Single Vertical Line Array Experiment in the North East Pacific. On Julian Day 270, a 200 Hz CW tone was projected for various time lengths and three different source depths, 165 km from the Vertical Line Array (VLA). On Julian Day 272, the 200 Hz source was towed away from the VLA for 10 hours at a speed of 5 kts. The signals were received by the VLA, which extended from a depth of 400 m to 1300 m. Power spectra between 0 and 250 Hz are presented for selected channels of the array. Vertical distribution of power across the Vertical Line Array is obtained for the signal and noise at 200 Hz. Finally, arrival structures of the signal and of the noise at 200 Hz, are obtained using conventional beamforming techniques. Nine data tapes, recorded during these transmissions, were processed, and the results are presented in this report. The comprehensive environmental information, collected during the experiment, allows the successful acoustic modeling of both the fixed range case, where the source depth is varied and the fixed depth case, where range between the VLA and the source varied from 0 to 100 km. The CONGRATS ray-theory model of the GSM and the ATLAS normal mode model are used, produce similar results which are in good agreement with the experimental results.

Table of Contents

1. Introduction

This technical memorandum contains the analysis results of the conventional processing and the acoustic modeling of the 200 Hz CW tone propagation data, collected during the September 1987 Vertical Line Array (VLA) experiment in the North-East Pacific. The Marine Physical Laboratory (MPL) digital array long of 900 m and filled with 120 hydrophones with 7.5 m interelement spacing was deployed for several weeks from the R/P FLIP, approximately 400 km southwest of Monterey, CA. The R/P FLIP was in a three-point moor at 34°58.69′ N 123°58.43′ W. This work deals with the 200 Hz CW tone propagation data recorded by the VLA, first, when the source ship kept a fixed stations 89 nm from the R/P FLIP on Julian 271 and, second, when the ship towed the source away from the R/P FLIP for ten hours on Julian 272. In both cases, the top of the VLA was at a nominal depth of 400 m. The acoustic source was an HX90 deployed from the USNS NARRAGANSETT and projected the 200 Hz CW tone with a nominal source level of 184 dB ref 1 μPa at 1 m.

Fixed Station

On Julian Day 270, the 200 Hz CW tone was projected for various time lengths and various source depths, 89 nm (or 165.5 km) from the R/P FLIP. The first transmission with the source at a nominal depth of 300 m began at 20:50 GMT and lasted for 15 minutes. The corresponding data were stored on Tape 915 (which starts at 20:48:04 GMT). The source was raised to a depth of 150 m and the transmission resumed at 21:30 GMT for 10 minutes. The data were recorded on Tape 917 (which starts at 21:34:59 GMT). The source finally was raised to a depth of 20 m and projected for 18 minutes from 21:57 GMT. The data were recorded on Tape 918 (which starts at 21:58:27 GMT).

Environmental data were collected on the R/P FLIP. Swell heights on Julian Day 270 were visually measured between 5 and 10 feet. A northern wind was blowing with speeds between 20 and 25 kts. XBT casts were collected at the R/P FLIP before the

transmissions at 11:00 GMT on Julian Day 270 and after the transmissions at 03:00 GMT on Julian Day 271.

Source Tow

On Julian Day 272, the USNS NARRAGANSETT began a source tow for 10 hours, starting at 00:00 GMT. The HX90 source was towed at a nominal speed of 5 kts with 300 m of wire out (the probable source depth is 100 m). The ship was tracked by radar from the R/P FLIP during the first five hours of the transmission. Data were recorded continuously on 25 tapes from Tape 966 to 990 (each tape is worth 23 minutes and 28 seconds of data).

The swell heights recorded at the R/P FLIP were just below 5 feet and wind speeds were between 10 and 15 kts. An XBT cast was taken on the R/P FLIP at 03:00 GMT during the source tow.

2. Description of the Array

The characteristics of the MPL digital array are summarized below. More detailed information can be found in [Sotirin1988]. The vertical line array has 12 sections, each section contains 10 acoustic transducers and a microprocessor-based processor which samples and telemeters the data to topside on a serial link. The acoustic channels are numbered from bottom to top and a processor samples the 5 transducers immediately below and above, as indicated in Figure 1. The signal in a given channel is the output of a set of two Benthos Aquadyne AQ-1 hydrophones wired in series. The resulting acoustic transducer has a sensitivity of 197 dB // μPa. The transducer output, then, is amplified with a pre-amplification stage with gain of 40 dB and bandpass filtered between 10 and 220 Hz (with a nominal gain of 0 dB). A differential line driver transmits the signal to the processor producing a 6 dB gain. In the processor, the analog signal is amplified by a software controlled variable gain (selectable from 0 to 60 dB). The 10

acoustic channels are multiplexed and sampled by a 12 bit bipolar A/D converter. The reference voltages are ± 10 V. The sampling rate is 500 Hz. The digitization of the voltage signal into A/D counts corresponds to a gain of 46.23 dB. A summary of the gain chain is given in Figure 2.

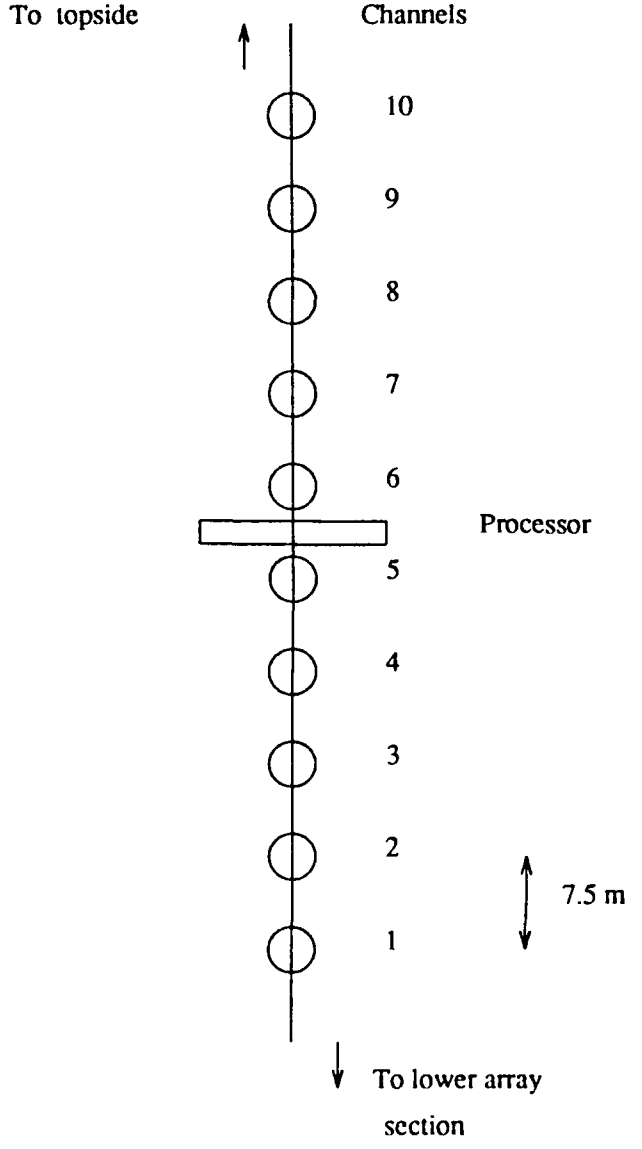

Figure 1: VLA section

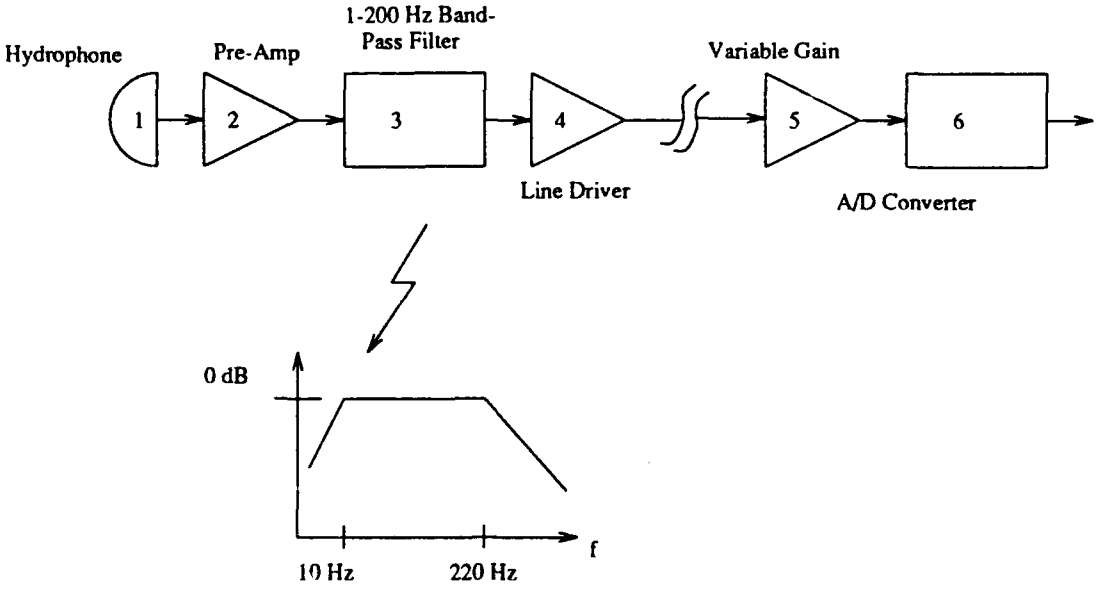

1: -197 dB re 1 μPa

2: 40 dB Gain

3: 0 dB from 0 to 220 Hz

4: 6 dB Gain

5: 0 to 60 dB Gain

6: 46.23 dB Gain (Range is ±10 V, 12 bits)

Figure 2: September 1987 VLA Experiment Gain Chain

3. Outline of the Processing

Power spectrum estimation is performed on the array data with the conventional methods based on the Fast Fourier Transform (FFT). The 0 - 250 Hz power spectrum is computed on two channels (#4 and #7 in Figure 1) of each section. The 120 channels of the array are numbered from bottom (# 1) to top (# 120). The power spectra for channels 4, 7, 14, 17 and so on to 114 and 117 are obtained by processing 64 K data points (1 K is 1024 points), or 2 minutes and 11 seconds worth of data. They are derived from the incoherent addition of 15, 50 % overlapped, 8192-point FFTs (61 mHz bin width). A Kaiser-Bessel window with α parameter of 2.5, yielding a sidelobe level of - 57 dB [Harris1978], weights the data prior to each FFT. Power values are properly calibrated and expressed in dB re 1 μPa, to yield the correct power for sinusoidal signals. The 90 % confidence interval for these power spectra is +2.0 dB / - 1.6 dB.

The distribution of power in the vertical, for several frequency bins at or around 200 Hz, is computed by incoherently averaging thirty 8192-point FFTs obtained by processing two segments of 64 K data point (two times 2 minutes and 11 seconds). As before, the data are weighted by a Kaiser-Bessel window with α parameter of 2.5 prior to the FFT. The 90 % confidence interval is in this case + 1.4 dB / - 1.2 dB.

The conventional FFT beamformer is used to process the data in order to obtain some information on vertical directionality. The along channel FFTs are 50 % overlapped and 8192 points in length. As before, a Kaiser-Bessel window with α parameter of 2.5 weights the data prior to each FFT. The cross-channel FFT is 1024 points in length where complex data, first, is windowed with a 120-point Kaiser-Bessel window with α parameter of 1.5 (yielding a sidelobe level of -35 dB) and, then, zero padded to the FFT length. The beamforming output is produced for several frequency bins at or around 200 Hz. It is properly calibrated in dB (re 1 μPa) to yield the power of discrete arrivals impinging on the vertical line array at various angles. The array is numbered from bot-

tom to top, so negative angles of arrival correspond to downlooking beams or upgoing sound, and positive angles of arrival correspond to uplooking beams or downgoing sound.

4. Fixed Station Analysis

4.1. Data Analysis Results

The analysis results for the Tapes 915, 917 and 918, corresponding to respectively source depths of 300 m, 150 m, and 20 m, are plotted in the Appendix 1. The power spectra computed for selected channels of the array indicate the good quality of the data recorded on those tapes. The 200 Hz tone is present as a strong line component. The 60 Hz line and its harmonics (120 Hz, 180 Hz and 240 Hz) are the result of power line contamination. By looking carefully at these spectra, one notes some variability in the noise levels reported at high frequency. For example, Channel 104 has, around 250 Hz, noise levels 10 dB higher than the other channels, for all three tapes. Channel 77 also has line components levels that are higher than the other channels. The self noise characteristics vary from channel to channel [Sotirin1989].

The distribution of power in the vertical is plotted for four FFT bins (Figures are in the Appendix 1). Table 1 provides the GMT time at which the 4 minutes and 22 seconds data segment starts in each case. Bins # 7373 and # 7374 correspond to the 200 Hz line component with real frequencies respectively equal to 199.951 Hz and 200.134 Hz. Bin # 7368 and # 7380 corresponds to the noise at frequencies equal to 199.646 Hz and 200.378 Hz. The maximum signal power varies between 80 and 90 dB re 1 μPa depending on the source depth. A source level of 184 dB // 1 μPa at 1 m should suffer first a spherical transmission loss over a range on the order of a water depth (5000 m) and a cylindrical loss over the remaining range. Then, it should appear at the array with a power on the order of 95 dB re 1 μPa. One note that when the source is raised to shal-

lower depths, the signal overall power across the array aperture increases.

The distribution of noise power across the array shows a somewhat large variability, with peaks 5 to 15 dB above a noise floor which is between 60 and 65 dB (re 1 μ Pa). The normalization factor to pass from the sinusoidal component normalization to a noise spectral density normalization is on the order of 10 dB. The noise level at 200 Hz is therefore between 70 and 75 dB // 1 μPa / $\sqrt{Hz}$. Such levels are consistent with the common noise levels summarized in [Urick1986] for the wind speeds observed at the R/P FLIP (20 to 25 kts). The peaks in the vertical distribution of noise power at 200 Hz are not the result of a statistical artefact since the 90 % confidence interval is +1.4 / -1.2 dB. As mentioned earlier, they correspond to channels with high self noise characteristics. One observes that the peaks, generally, correspond to the channels which are physically the closest or the farthest to the processors. In an array section, the transducers the closest to the processors (# 5 and # 6 in Figure 1) are used for the array navigation, which involves acoustic transponders operating around 12 kHz. These navigation channels do not have the anti-aliasing filter cut-off at 220 Hz in order to allow the recording of the 12 kHz navigation signals. The two channels that are the farthest from the processor (# 1 and # 10 in Figure 1) suffer the most cross-talk with other telemetry and transmission lines, especially a 1 MHz clock signal.

Tape number	GMT start time
915	20:51:53
917	21:34:59
918	22:09:22

Table 1: Reference GMT time for plots of power across the VLA

The FFT beamformer processes the four FFT bins already considered (the two signal bins 7373 and 7374 and the two noise bins 7368 and 7380) to obtain information on the vertical arrival structure. The array is cut for 100 Hz with an interelement spacing

of 7.5 m and is therefore spatially aliased at the operating frequency of 200 Hz. The beamforming results are thus plotted between ±30° with respect to the horizontal (Figures are in Appendix 1). The noise arrival structure is generally flat across ±30°. The signals are very strong with relative signal levels up to 30 dB. Sidelobe leakage is experienced although a Kaiser-Bessel window with 35 dB sidelobe rejection is used. The array beampattern is degraded because of phase and gain errors from channel to channel [Sotirin1989]. For each tape, the arrival structure is displayed in a waterfall plot referenced in GMT time. The number of incoherent averages used to produce a particular angular spectrum is given in Table 2. This table also contains the 90 % confidence interval associated to each angular spectrum. The arrival structure stays fairly stationary since the ship was keeping a fixed station, although slight variations in the angular spectra are observed for Tape 915. For Tape 915, the 200 Hz signal is received at full power starting at 20:51:53 GMT (the transmission started at 20:50 GMT and the propagation time for 165 km is approximately 1 minute and 50 seconds). The arrival structure is stable until 21:01:24 GMT where it begins to change slightly.

The arrival structure does not change dramatically for the arrivals with angle steeper that ±15° as the source is raised from 300 m to 150 m and then 20 m. These arrivals correspond to refracted surface reflected (RSR) paths. On the other hand, the arrival structure at low angle of arrival with respect to the horizontal changes dramatically with source depth. When the source is at 300 m multiple arrivals impinge on the array at low angle of arrival (between -15° and +15°). Acoutic energy is effectively coupled in the deep sound channel with multiple refracted-refracted (RR) paths. When the source is shallower (either at 150 m or at 20 m), no strong low angle arrivals can be identified. There are no refracted refracted paths and there is no coupling of sound in the deep sound channel like in the 300 m source case.

Tape 915			Tape 917			Tape 918		
GMT Time	Number of Averages	Confidence Interval (dB)	GMT Time	Number of Averages	Confidence Interval (dB)	GMT Time	Number of Averages	Confidence Interval (dB)
20:48:04	15	+2.0/-1.6	21:34:59	15	+2.0/-1.6	21:58:27	15	+2.0/-1.6
20:50:15	11	+2.5/-1.9	21:37:10	15	+2.0/-1.6	22:00:38	12	+2.5/-1.8
20:51:53	19	+1.8/-1.4	21:39:21	19	+1.8/-1.4	22:02:49	15	+2.0/-1.6
20:54:37	15	+2.0/-1.6	21:42:12	11	+2.5/-1.9	22:05:00	15	+2.0/-1.6
20:56:48	15	+2.0/-1.6	21:43:43	15	+2.0/-1.6	22:07:11	15	+2.0/-1.6
20:58:59	15	+2.0/-1.6				22:09:22	15	+2.0/-1.6
21:01:24	15	+2.0/-1.6				22:11:24	15	+2.0/-1.6
21:03:21	15	+2.0/-1.6				22:13:44	7	+3.3/-2.3
21:05:32	10	+2.6/-2.0				22:14:50	15	+2.0/-1.6
21:07:02	20	+1.8/-1.4				22:17:01	15	+2.0/-1.6
21:09:54	10	+2.6/-2.0				22:19:12	18	+1.8/-1.44

Table 2: Angular spectra waterfall plot information (fixed station)

4.2. Fixed Station Modeling

4.2.1. Sound Speed Profiles

A CTD was collected in the vicinity of the R/P FLIP on Julian Day 267, up to a depth of of 3885 m. Another CTD, collected at 37°04.19′ N 134°46.75′ W on Julian Day 264, was used to extend the FLIP CTD down to the nominal bottom depth at the R/P FLIP, 4667 m. The sound speed profile, based on the CTD, was derived using the UNESCO equations relating conductivity to practical salinity and sound speed to temperature, salinity and pressure [Fofonoff1983].

XBT casts were collected at the R/P FLIP before and after the fixed station transmissions on Julian Day 270 at 13:00 GMT (a 400 m XBT) and on Julian Day 272 at 03:00 GMT (a 750 m XBT). These XBT data were used in the state equation of [Mackenzie1981] to produce sound speed profiles. The top 750 m portion of these sound speed profiles are plotted in Figure 3. One observes a good similarity between the XBT sound speed profiles and also between the 750 m XBT sound speed profiles and the CTD profile

below 500 m. This information allows the synthesis of a sound speed profile that will be used with various acoustic models in what follows. A desampled version of the 400 m XBT sound speed profile is used from 0 to 250 m. Then, a desampled version of the 750 m XBT is used down to 700 m where it blends with the CTD sound speed profile. A desampled version of the CTD sound speed profile is then used down to the bottom. The model sound speed profile is plotted in Figure 4 for the whole water column and for the top 750 m. The two XBT sound speed profiles are also plotted in dashed lines. The composite sound speed profile, that will be used with the acoustic models, is given in Table 3. A 30 m deep mixed layer was observed at the R/P FLIP, followed by a shallow duct above 100 m, which evolves with time, as shown by the two XBT sound speed profiles taken only 14 hours apart. The environment has a double duct with a deep sound axis at a depth of about 550 m.

Depth (m)	Sound Speed (m/s)
0.	1507.7
31.000	1508.1
57.000	1496.0
68.400	1499.0
82.500	1498.1
93.400	1496.9
100.50	1493.1
115.80	1493.3
130.00	1491.0
138.00	1490.5
145.80	1488.6
150.30	1488.3
160.50	1487.6
175.10	1486.5
190.30	1486.2
215.00	1485.6
250.40	1484.4
276.20	1483.4
300.00	1482.7
366.20	1479.9
400.40	1479.4
455.40	1479.5
500.00	1479.0
543.70	1478.5
613.00	1478.6
631.00	1478.9
683.40	1478.9
717.50	1478.8
802.58	1479.6
891.57	1480.1
980.51	1480.8
1069.4	1481.4
1158.3	1482.0
1247.1	1482.8
1424.7	1484.5
1602.1	1486.3
1779.3	1488.3
1956.4	1490.5
2133.4	1492.9
2310.2	1495.6
2486.9	1498.3
2663.4	1501.1
2839.8	1504.0
3016.0	1506.9
3192.1	1509.8
3368.1	1512.8
3543.9	1515.8
3807.3	1520.4
4128.9	1526.2
4667.0	1536.4

Table 3: Sound speed profile at the R/P FLIP (fixed station)

4.2.2. Modeling with the GSM

The CONGRATS ray tracing program of the Generic Sonar Model [Weinberg1985] is utilized to model the sound field. The sound speed profile in Table 3 is used and the bottom corresponds to the GSM Province Type 3 where the loss in dB is given as a function of incidence angle in Table 4. The simulated receiving array has 120 elements with a 7.5 m interelement spacing and has its top element at 400 m depth, the nominal depth of the VLA during the experiment. The ray-diagrams in Figure 5 correspond to the three nominal source depths: 20, 150 and 300 m. In this deep water case, convergence zone propagation takes place with RSR rays. At 165 km from the source, the sound has travelled over 3 convergence zones. As the source is lowered in the water column, the ray-diagrams change and shift in range. The convergence zones widen when the source is lowered. When the source is at 300 m, the sound couples in the deep sound channel (the sound axis is around 550 m) and RR rays propagate through the water. Altough the nominal source level is 184 dB re 1 μPa at 1 m, the calibrated received levels obtained from the experimental data indicate that the source level is actually closer to 174 dB re 1 μPa at 1 m. This latter source level will be used in the following modeling efforts.

Angle (deg)	Loss (dB)
0°	0.0
10°	0.4
20°	3.2
30°	5.2
40°	6.8
50°	7.6
60°	8.2
70°	8.2
80°	8.2
90°	8.4

Table 4: Bottom Loss Table in dB (GSM Province Type 3)

Using a trial and error procedure, the source range and depth corresponding to the best fit between the modeling and the experimental data were determined for the

three source depths. The resulting distribution of power computed by the GSM is plotted in Figure 6. The best fit for Tape 918 (source at 20 m) corresponds to a range of 162 km. Like for the data, the power distribution exhibits a strong interference pattern. The best fit for Tape 917 (source at a nominal depth of 150 m) is obtained with a source at a depth of 170 m and at a range of 161.4 km. Once again, the GSM predicts an interference pattern similar to the data. Finally, Tape 915 is best modelled by a source at a depth of 330 m and at a range of 161.8 km. In this case, the modeling achieved by the GSM is not as good, power levels observed experimentally are lower and there is a lack of definite interference pattern. In all three cases, the source range is close the nominal range of 165.5 km (89 nm). While the GSM predicts a distribution of power in the vertical very close to what is observed experimentally in the two shallower cases, it produces only fair results when the source is deeper around 300 m depth. In this case the convergence zone is not well defined and sound is effectively coupled in the deep sound channel. One observes qualitatively that the GSM average power across the receiving array decreases for increasing source depth, which is consistent with the data processing results.

For those best fits, the eigenray angles, computed by the GSM at the sound axis (550 m), are plotted in Figure 7 for the three cases. One observes a good correspondance with the beamforming vertical arrival structure for the arrivals with steep angles with respect to the horizontal (i.e. steeper than ±10°). When the source is at 330 m depth, there are arrivals with lower angles with respect to the horizontal (between -10° and 10°) which correspond to RR rays. These arrival angles are very close to the experimental beamforming results. But the levels of the arrivals do not match as well. This disagreement is consistent with the (only) fair modeling that could be achieved for the distribution of power in the vertical. The eigenray information obtained from the GSM is given in Tables 5,6,7 for source depths of 20, 170 and 330 m.

Source at 20 m depth, Receiver at 550 m depth						
Time (s)	Source Angle (deg)	Target Angle (deg)	Loss (dB)	Phase (deg)	Number of Reflections (V = Vertex)	
					Surface	Bottom
107.4788	0.4985	11.3486	-134.649	-83.183	0	0
106.5570	11.2360	-15.9103	-142.719	115.332	0	1V
107.9667	0.4985	-11.3486	-131.232	-130.259	0	1V
106.7507	-11.2359	15.9102	-140.774	-260.798	2	1V
108.0871	-0.4985	11.3486	-130.493	-477.611	2	1V
107.8519	-11.2360	-15.9103	-138.051	-365.537	2	2V
108.5750	-0.4985	-11.3486	-129.515	-576.437	2	2V
108.0353	11.2360	15.9103	-145.994	-469.397	2	2
108.0353	11.2360	15.9103	-143.391	-338.176	2	2V
108.6945	0.4985	11.3486	-128.710	-575.207	2	2V
109.1366	11.2513	-15.9209	-122.987	-481.822	2	3
109.1273	9.4087	-14.6938	-99.459	-540.000	2	3V
109.1824	0.5528	-11.3511	-112.061	-622.323	2	3V
109.3306	-11.2934	15.9504	-119.620	-819.308	4	3
109.2933	-6.9982	13.2996	-97.701	-900.000	4	3V
109.3038	-1.5975	11.4483	-100.322	-984.205	4	3V
110.5074	-12.8865	-17.1005	-116.867	-720.000	4	4
109.8488	-3.6943	-11.9170	-132.737	-952.093	4	4V
109.8488	-3.6943	-11.9170	-127.907	-1038.448	4	4V
110.7071	13.1085	17.2662	-116.710	-720.000	4	4
112.1085	15.5624	-19.1716	-121.124	-720.000	4	5
112.3492	-15.8691	19.4180	-121.585	-1080.000	6	5
114.0114	-18.4711	-21.5692	-129.039	-1080.000	6	6
114.2671	18.7695	21.8219	-129.508	-1080.000	6	6

Table 5: GSM eigenrays at 162 km.

Source at 20 m depth, Receiver at 550 m depth						
Time (s)	Source Angle (deg)	Target Angle (deg)	Loss (dB)	Phase (deg)	Number of Reflections (V = Vertex)	
					Surface	Bottom
108.7142	13.4523	-14.7247	-101.124	-540.000	2	3V
108.7232	14.7566	-15.9208	-124.294	-481.621	2	3
108.7747	-14.7649	-15.9284	-122.928	-474.303	3	3
108.7971	-9.6403	-11.3629	-107.976	-603.168	3	3V
108.8377	-8.1543	-10.1376	-123.033	-417.711	3	3
108.8507	-7.6850	-9.7655	-124.355	-761.047	3V	3V
108.8849	6.1181	-8.5917	-122.345	-304.327	2V	3V
108.8912	9.6211	11.3467	-120.930	-528.433	3V	3V
108.8913	-6.1526	-8.6162	-122.163	-406.432	3V	3V
108.8930	9.6760	11.3930	-103.653	-608.269	3	3V
108.9120	14.7864	15.9483	-120.877	-459.731	3	3
108.9150	-9.6211	11.3467	-123.974	-630.302	4V	3V
108.9150	-11.3465	12.8370	-98.345	-897.540	4	3V
108.9315	7.6747	9.7574	-113.030	-482.688	3V	3V
108.9315	7.6747	9.7574	-121.997	-444.879	3V	3V
108.9463	-7.6639	9.7489	-122.972	-704.011	4V	3V
108.9637	-14.8013	15.9621	-120.207	-812.268	4	3
108.9676	-2.6097	-6.5811	-119.858	-415.557	3V	3V
108.9849	-0.2094	-6.0472	-118.794	-589.427	3V	3V
108.9849	-0.2094	-6.0472	-119.791	-428.676	3V	3V
109.0171	-2.5307	6.5503	-116.798	-539.796	4V	3V
109.0263	0.0000	6.0436	-117.058	-507.500	3V	3V
109.0263	0.0000	6.0436	-122.493	-526.582	4V	3V
109.1426	-1.5282	-6.2331	-119.872	-585.277	4V	4V
109.1426	-1.5282	-6.2331	-122.089	-766.036	4V	4V
109.1450	1.8761	-6.3270	-121.781	-664.941	3V	4V
110.1452	-16.0823	-17.1523	-117.763	-720.000	4	4
110.2937	16.2060	17.2679	-117.636	-720.000	4	4
111.6957	18.2365	-19.1795	-121.831	-720.000	4	5
111.9967	-18.5712	19.4968	-122.394	-1080.000	6	5

Table 6: GSM eigenrays at 161.4 km range

Source at 330 m depth, Receiver at 550 m depth						
Time (s)	Source Angle (deg)	Target Angle (deg)	Loss (dB)	Phase (deg)	Number of Reflections (V = Vertex)	
					Surface	Bottom
108.9497	14.5526	-14.9837	-101.752	-537.852	2	3V
109.0814	-10.7846	-11.3652	-106.804	-615.012	3	3V
109.1391	10.7990	11.3789	-104.768	-616.563	3	3V
109.1440	15.5370	15.9402	-121.738	-465.235	3	3
109.1992	-10.7651	11.3467	-121.503	-633.258	4V	3V
109.2007	-12.2086	12.7227	-99.986	-908.174	4	3V
109.2033	-11.0427	11.6101	-102.378	-984.456	4	3V
109.2185	-9.6649	10.3102	-113.703	-707.275	4V	3V
109.2509	-5.2373	-6.3566	-121.357	-379.216	3	3
109.2520	-15.5614	15.9640	-120.433	-811.277	4	3
109.2818	5.2503	6.3674	-119.431	-377.482	3	3
109.2818	5.2503	6.3674	-120.906	-587.726	3V	3V
109.2964	-5.2587	6.3743	-111.952	-451.173	4	3
109.3044	-4.5036	5.7680	-116.806	-519.090	4V	3V
109.3849	2.2846	-4.2693	-99.165	-594.025	3V	4V
109.3855	1.5981	-3.9452	-105.046	-601.755	3V	4V
109.3855	1.5981	-3.9452	-108.307	-518.728	3V	4V
109.3858	-0.9778	-3.7375	-96.869	-656.453	4V	4V
109.3858	-2.8454	-4.5934	-97.425	-652.922	4V	4V
109.3859	-2.0999	-4.1735	-96.915	-657.990	4V	4V
109.4022	0.4541	3.6359	-99.032	-647.220	4V	4V
109.4022	-0.2825	3.6186	-100.776	-753.765	5V	4V
109.4050	2.2371	4.2441	-107.407	-735.157	4V	4V
109.4050	2.2371	4.2441	-111.385	-605.608	4V	4V
109.4335	0.0000	-3.6075	-120.218	-786.163	5V	5V
109.4335	0.0000	-3.6075	-121.871	-758.230	4V	5V
109.4607	-6.5996	-7.5174	-121.517	-567.405	4V	4V
110.4341	-16.7864	-17.1587	-117.968	-720.000	4	4
110.5215	16.8532	17.2240	-117.892	-720.000	4	4
111.9171	18.7874	-19.1183	-121.897	-720.000	4	5

Table 7: GSM eigenrays at 161.8 km range

4.2.3. Modeling with ATLAS

The modeling is now performed with the ATLAS normal mode model [Gordon1984]. The environmental parameters are the same as with the GSM, the sound speed profile is given in Table 3, and the bottom loss table (in Table 4) corresponds to the GSM bottom Province Type 3. The source level is taken equal to 174 dB re 1 μPa at 1 meter.

The power as a function of range, computed by the ATLAS model, is plotted in Figure 8 for a receiver depth of 20 m, and the nominal source depths of 20, 150 and 300 m. One observes that convergence zone propagation takes place, and that as the source is lowered, the convergence zone widens. The sound propagates over 3 convergence zones from the source to the receiving array, 165 km away. When the source is at 20 m, the VLA is in the third convergence zone. As the source goes deeper, the convergence zone becomes broader and shifts slightly towards the source. The array can be thought of in the trailing edge of the convergence zone which is more diffuse as the source is moved deeper.

As with the GSM, source ranges and depths are determined so as to optimize the modeling of the experimental data. The distribution of power across the array, computed by the ATLAS model, is plotted in Figure 9 for the nominal source depths. The best fit is achieved for ranges of 161.4 km when the source is 20 m deep, 163.9 km when the source is 150 m deep and 160.5 when the source is 300 m deep. These ranges are close to the nominal source range of 165 km. As with the GSM, the modeling is excellent for source depths of 20 m and 150 m, and fair for a source depth of 300 m.

The ATLAS normal mode model also produces the complex wavefield which can be beamformed to yield the model vertical arrival structure. The wavefield corresponding to the array at 400 m is beamformed, like the experimental data, with a Kaiser-Bessel window with α parameter of 1.5 (yielding a side-lobe rejection of 35 dB). The model vertical arrival structure in each case is given in Figure 10. The best fit for the

vertical arrival structure is achieved for a range of 165 km when the source is at 20 m, 163.75 km when the source is at 150 m and 164.5 km when the source is at 300 m depth. One observe a very good match between the modeling and experimental results. The pair of arrival above 10° corresponds to downgoing sound, which is consistent with having the receiving array in the trailing edge of the third convergence zone. The ATLAS arrival structure for a source at 300 m yields low angle of arrival with levels which are slightly too high compared with the data.

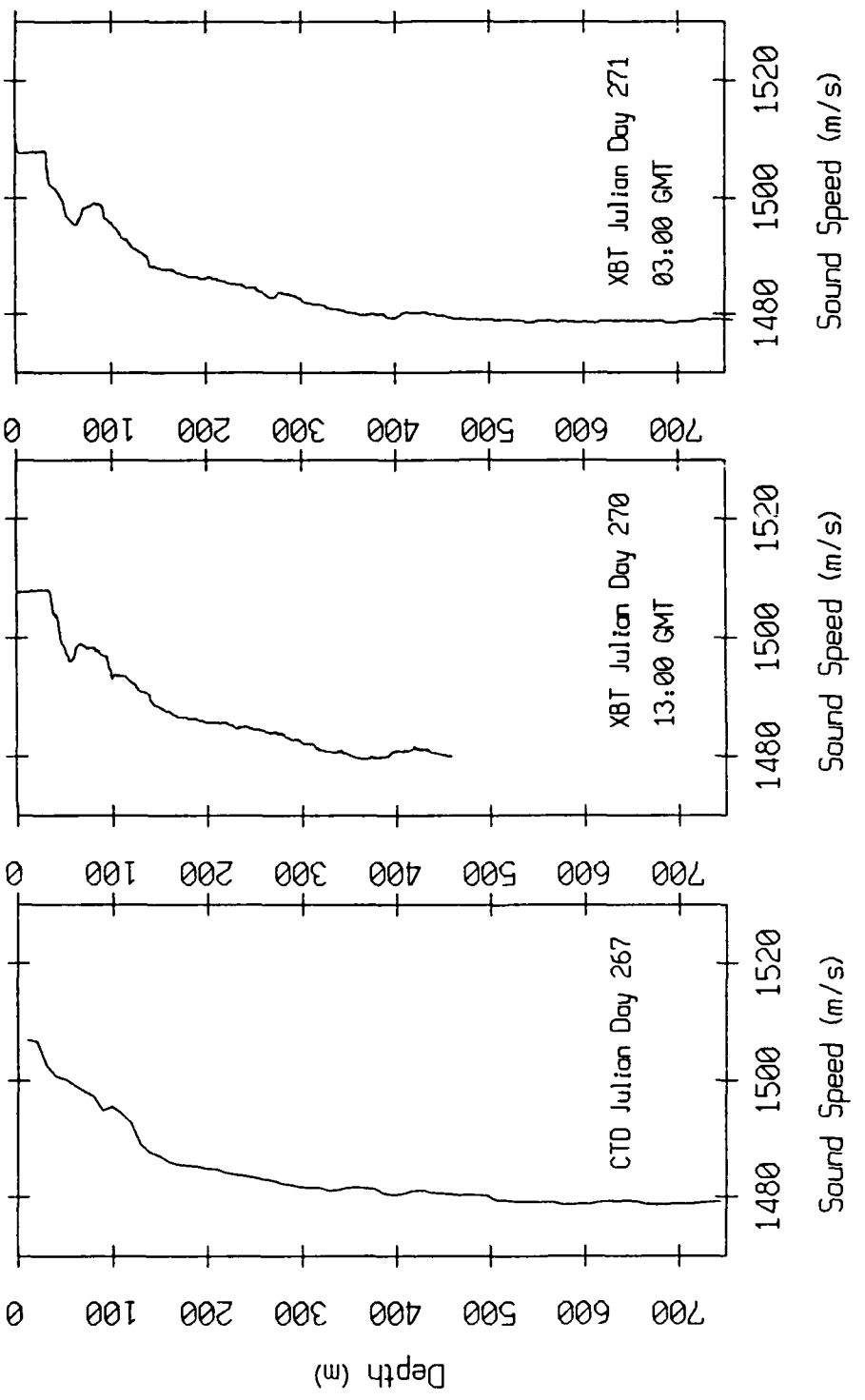

Figure 3: Fixed station sound speed profiles in the upper 750 m.

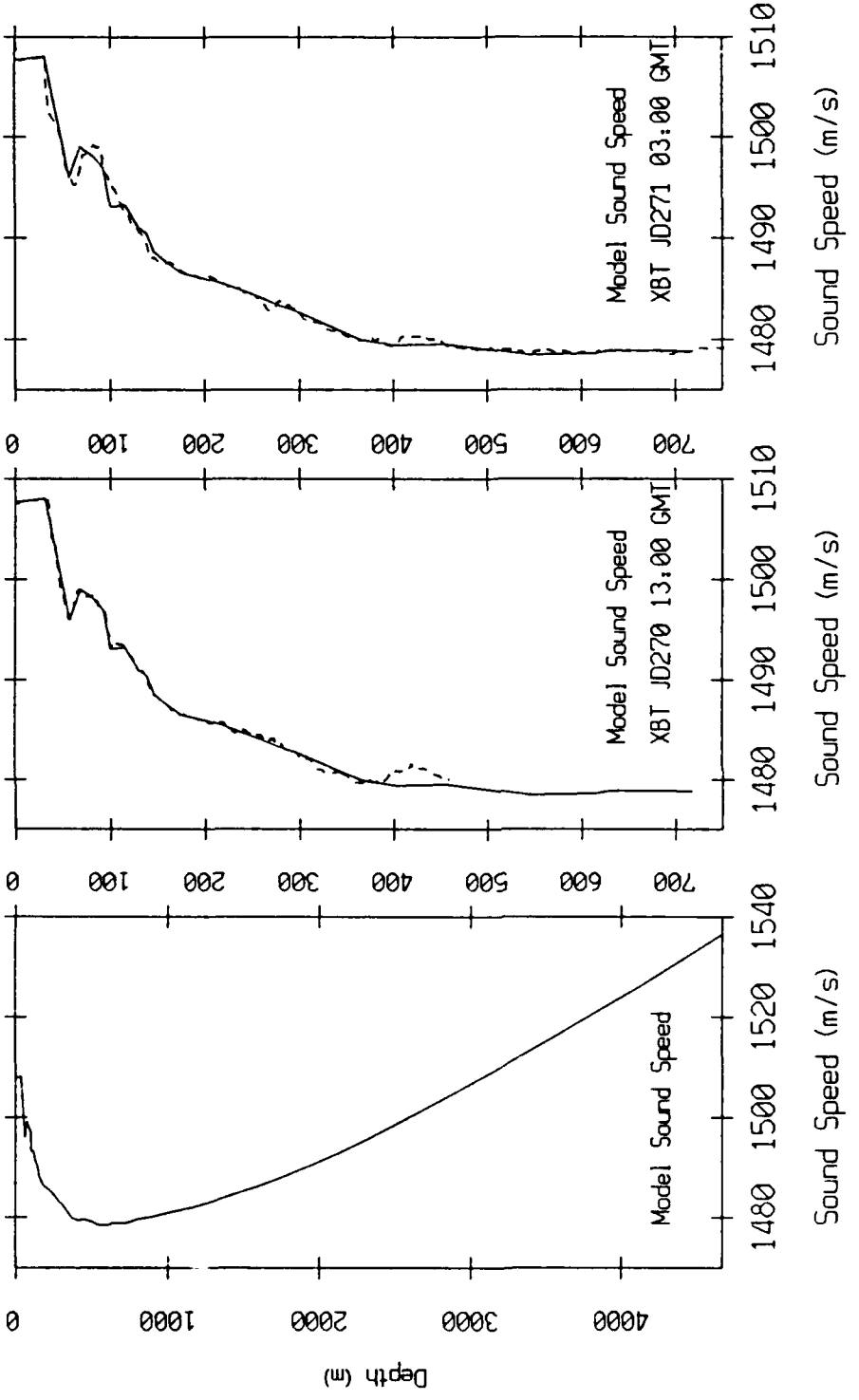

Figure 4: Fixed station model sound speed profile.

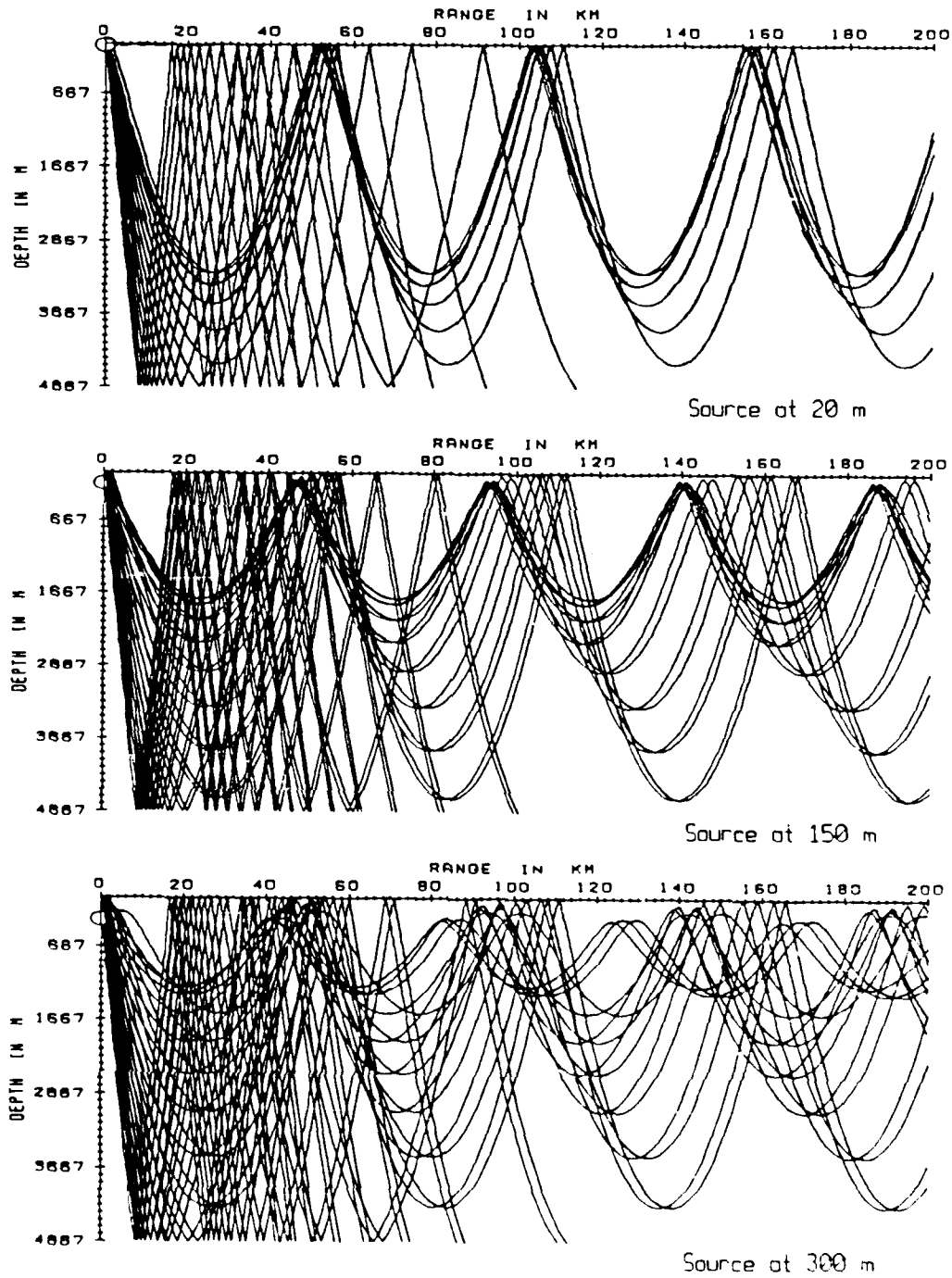

Figure 5: GSM ray traces.

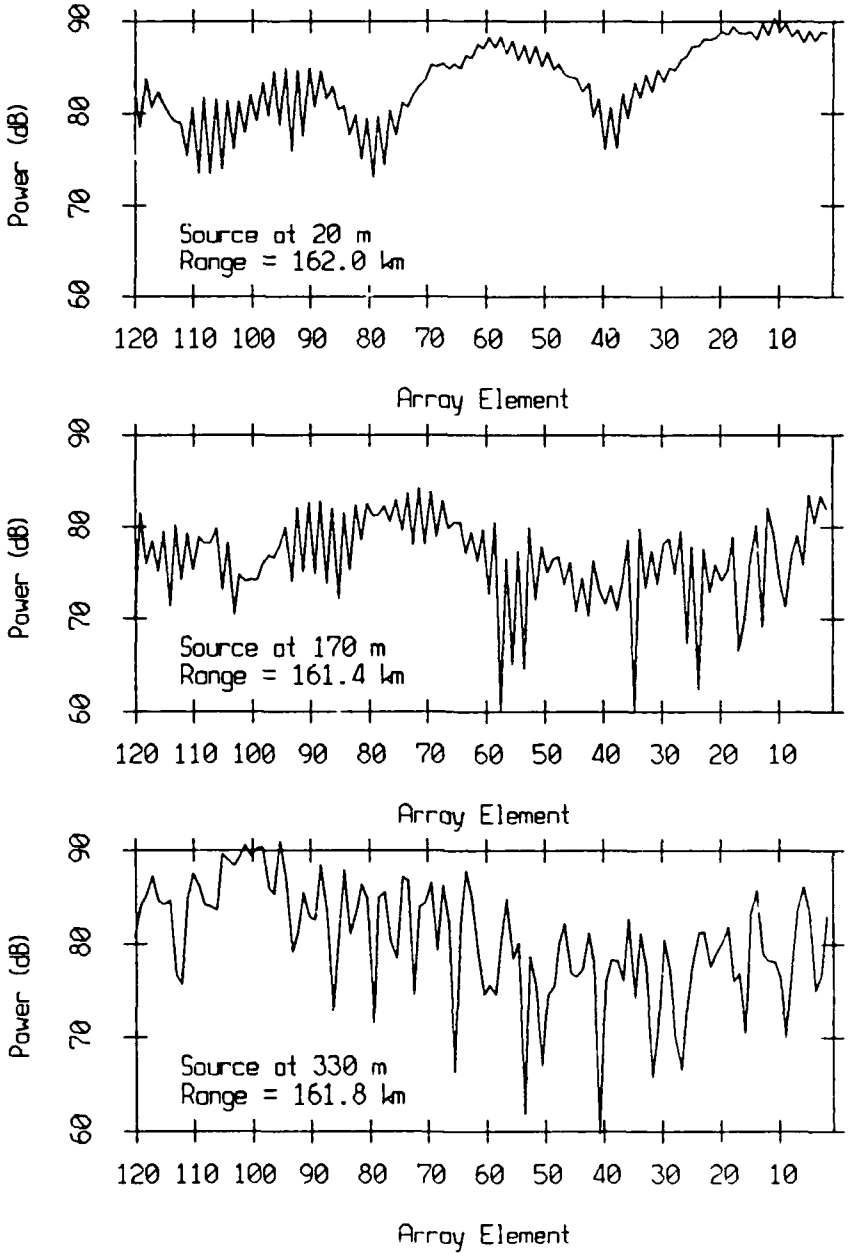

Figure 6: GSM distribution of power across the array.

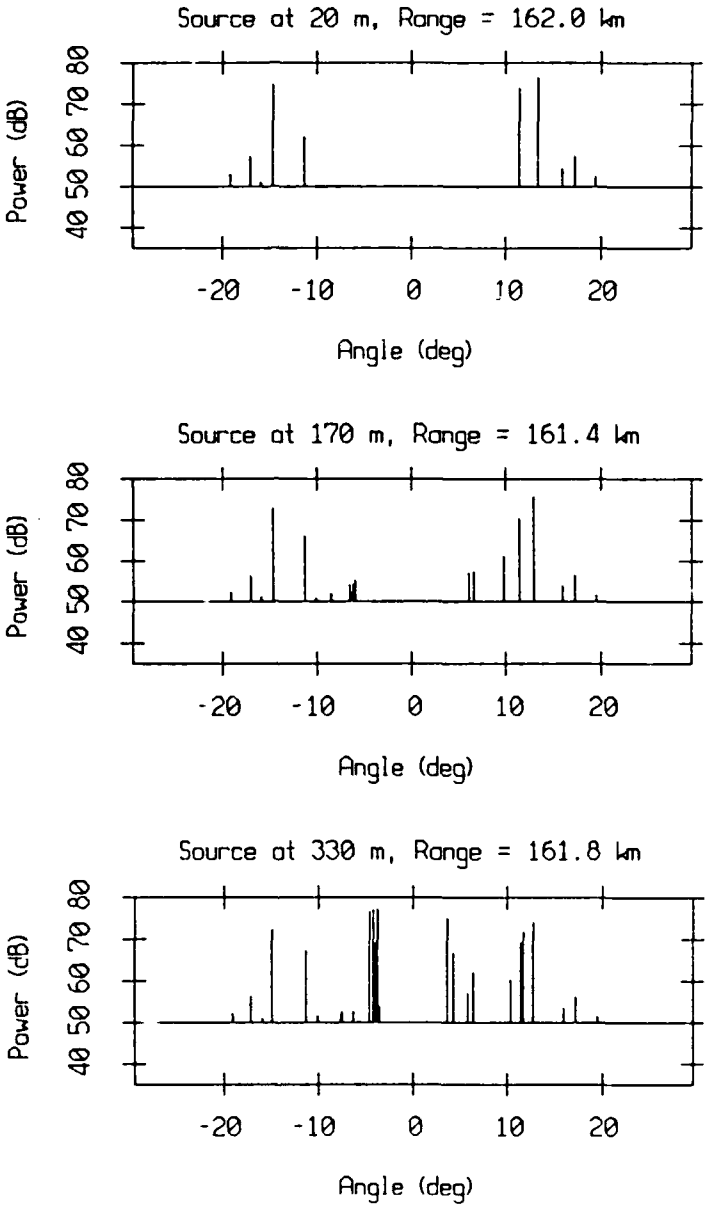

Figure 7: GSM Eigenrays at the sound axis.

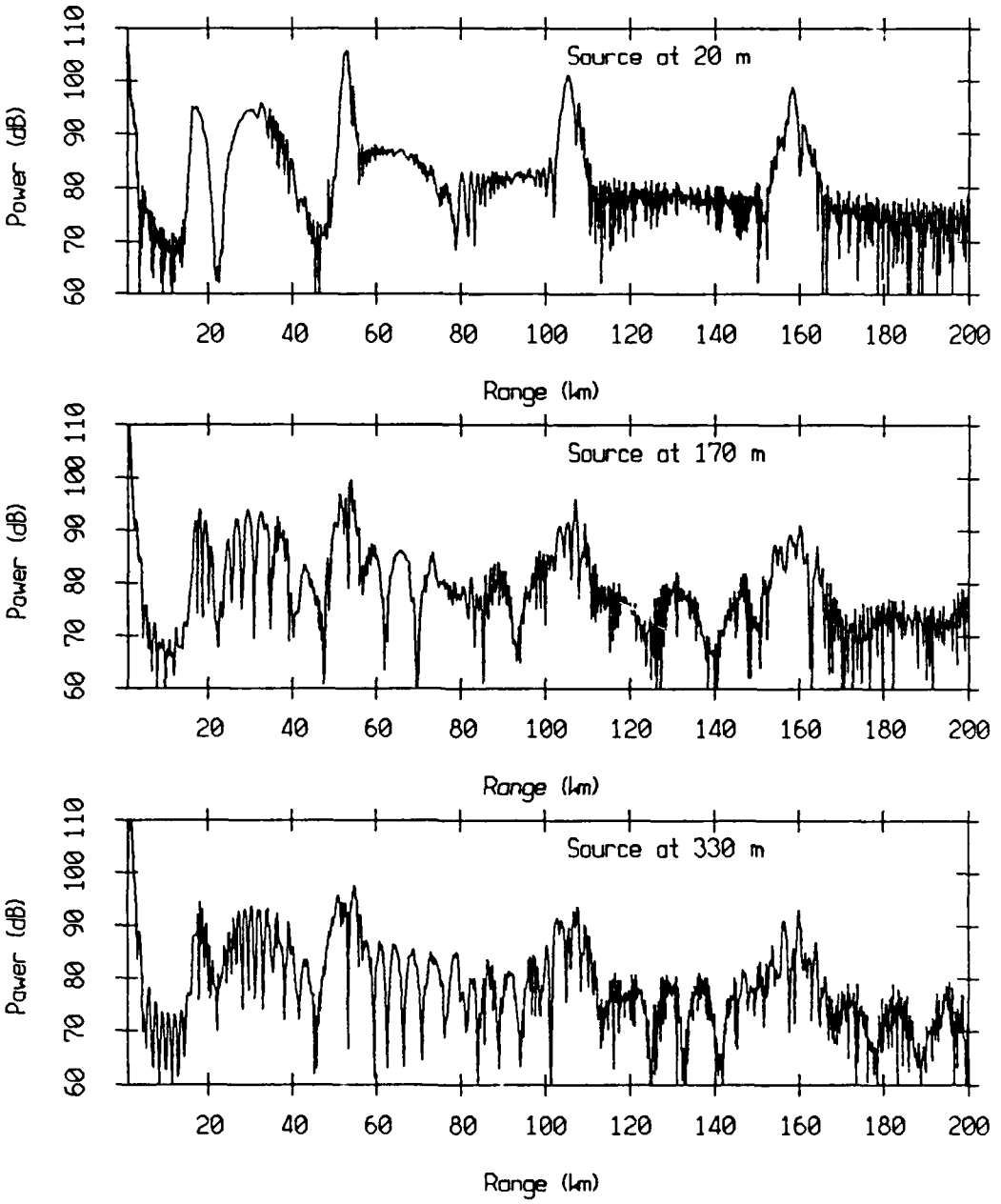

Figure 8: ATLAS transmission loss versus range.

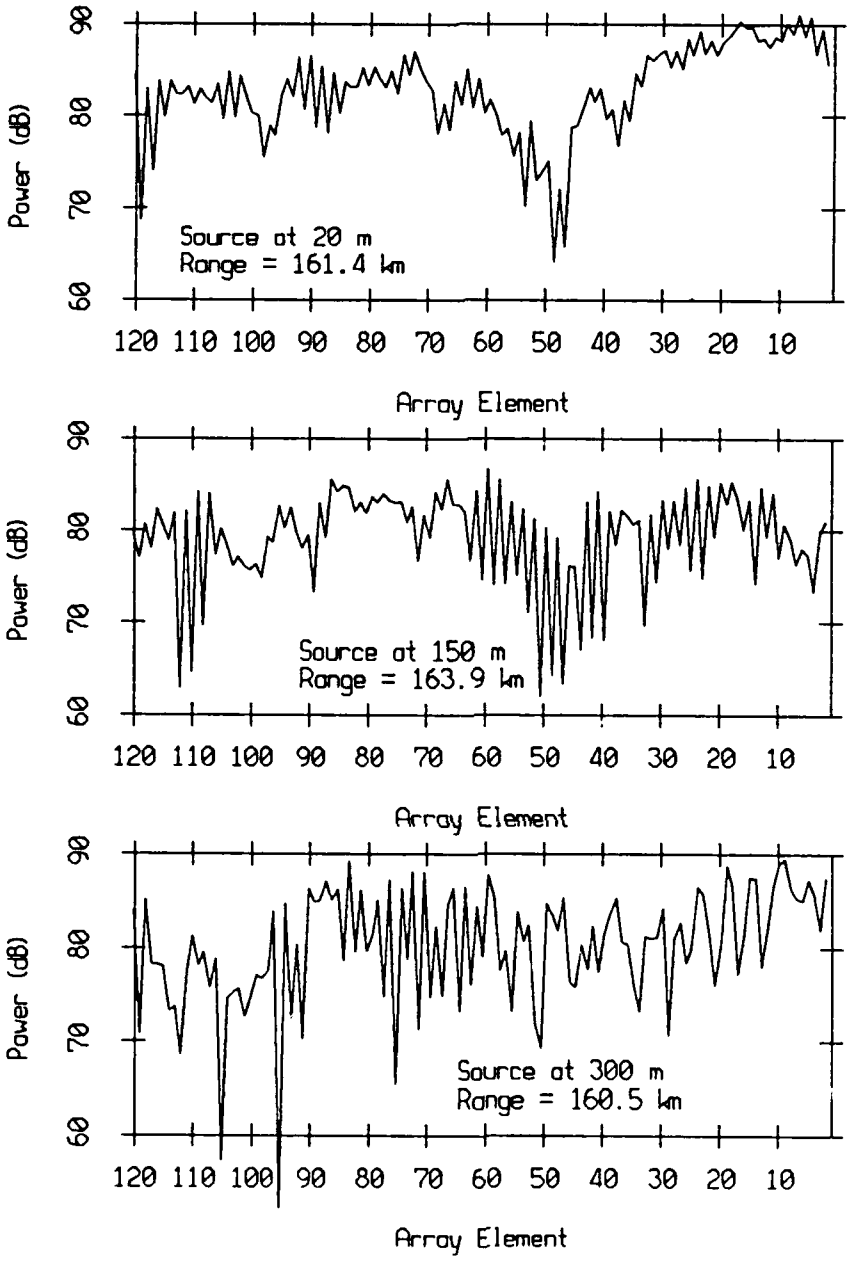

Figure 9: ATLAS distribution of power across the array.

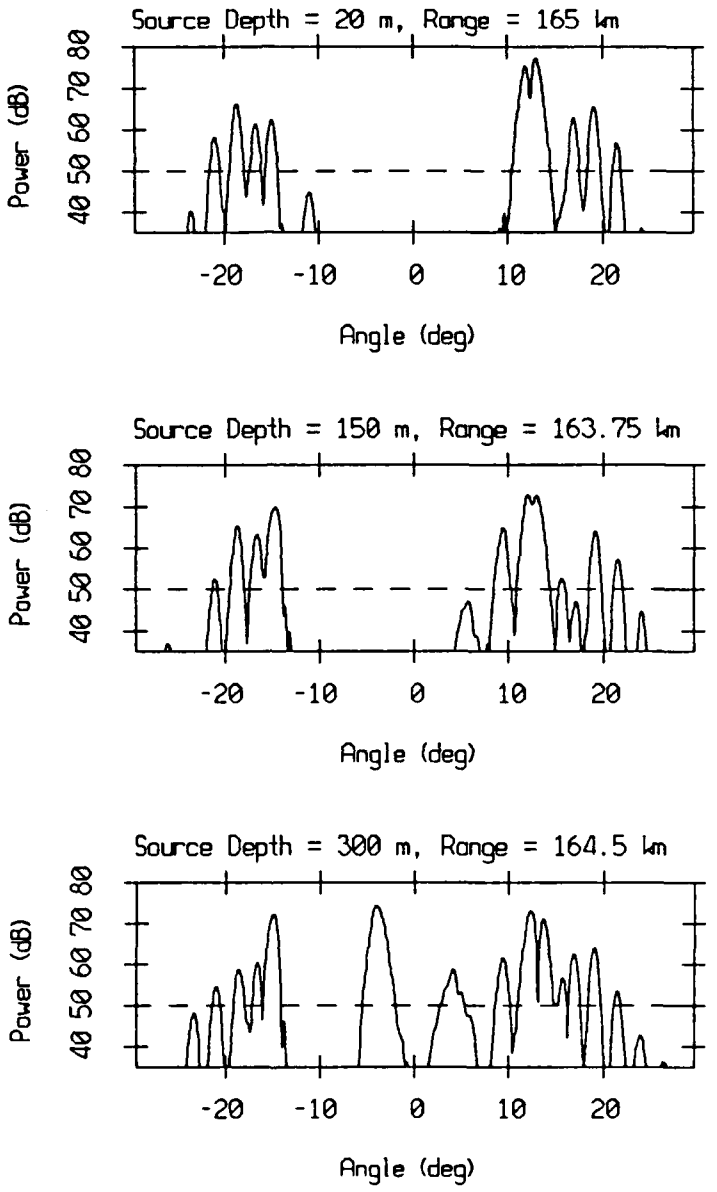

Figure 10: ATLAS angular spectra.

5. Source Tow Data Analysis

5.1. USNS NARRAGANSETT Tracking

The source tow began at 00:00 GMT on Julian Day 272. During the first four hours and fourty five minutes, the USNS NARRAGANSETT was tracked by radar on the R/P FLIP. The ship track, based on time, bearing and range information, is plotted in Figure 11. The speed of the ship varied slightly from the nominal speed of 5 knts. The radial speed, which depends on the instantaneous ship speed as well as on the ship bearing, varies from 3 to 4 knots in the first four hours and increases up to values between 5 and 6 knots near the end of the radar tracking at 04:45 GMT where the USNS NARRAGANSETT was 37 km from the R/P FLIP.

5.2. Selection of the Tapes To Process

The data tapes are selected so that characteristic propagation features are present in the data. In this propagation experiment, where the range between the source and the VLA array varies, the first convergence zone constitutes a reference. The following section, devoted to acoustic modeling, will help in the interpretation of the processed data, by providing information on the first convergence zone and as well as prediction of the variations of the arrival structure with range.

5.3. Source Tow Modeling

5.3.1. Sound Speed Profile

An XBT cast was collected at the R/P FLIP during the source tow, on Julian Day 272 at 03:00 GMT. This 750 m XBT data were utilized with the state equation of [Mackenzie1981] to produce the sound speed profile plotted in Figure 12. The environment at the R/P FLIP is one of a double duct with a large and well defined surface duct in the top hundred meters. The estimated depth of the towed source is 100 m, right at the boundary

of the two waveguides. Therefore, this situation may be difficult to model. The sound speed profile across the water column is synthesized by using a desampled version of the 750 m XBT sound speed profile and by blending it in a desampled version of the deep CTD at the R/P FLIP (the one used in the fixed station modeling). The desampled XBT sound speed profile in the top 750 m and the synthetic sound speed across the whole water column are also plotted in Figure 12. The sound speed profile used in the modeling is given in Table 8. The depth of the sound axis is 500 m . For consistency with the fixed station modeling, the deep sound axis will be considered at 550 m.

Depth (m)	Sound Speed (m/s)
0.	1508.4
18.100	1508.0
31.700	1508.1
49.700	1499.1
70.300	1494.7
87.600	1493.7
104.90	1497.9
122.20	1491.4
139.40	1489.5
156.60	1487.5
173.80	1486.5
190.90	1485.7
208.10	1485.7
225.10	1485.1
242.20	1484.5
259.20	1484.0
276.20	1483.1
293.10	1483.1
310.10	1482.6
327.00	1481.1
343.80	1480.8
360.60	1479.7
377.40	1479.5
394.20	1479.7
445.50	1480.0
499.60	1478.8
606.90	1479.0
739.00	1479.7
802.58	1479.6
891.57	1480.1
980.51	1480.8
1069.4	1481.4
1158.3	1482.0
1247.1	1482.8
1424.7	1484.5
1602.1	1486.3
1779.3	1488.3
1956.4	1490.5
2133.4	1492.9
2310.2	1495.6
2486.9	1498.3
2663.4	1501.1
2839.8	1504.0
3016.0	1506.9
3192.1	1509.8
3368.1	1512.8
3543.9	1515.8
3807.3	1520.4
4128.9	1526.2
4667.0	1536.4

Table 8: Sound speed profile at the R/P FLIP (Source Tow).

5.3.2. Modeling with the GSM

As in the fixed station modeling, the CONGRATS ray tracing program of the Generic Sonar Model [Weinberg1985] is utilized to model the sound field. The sound speed profile in Table 8 and a Bottom Province Type 3 (Table 4) are used.

The ray-diagram in Figure 13 corresponds to the nominal source depth of 100 m. Convergence zone propagation takes place in this deep water environment with refracted surface-reflected rays. The first convergence zone reported by the GSM begins at 48 km from the source, and extends for about 8 km. Assuming a source level of 174 dB at 1 m, the power as a function of range is computed by the GSM for receiver depths of 20 m and 550 m, and plotted in Figure 13. The convergence zone, clearly, is observed for both depths with an increase in power of 10 dB above an average signal level on the order of 80 dB, beyond ranges of 20 km.

The traces of the eigenray angles at 550 m depth are plotted as a function of range between 5 and 100 km in Figure 14. The angles steeper than ±30° have been folded between -30° and +30° to make the plot look similar to the output of the FFT beam-former (recall that the array is aliased). The eigenrays with steep angles interact with the bottom and have low power levels at the ranges of interest (20 km and over). The traces of the eigenrays with range at 550 m, indicate the beginning of the first convergence zone at a range of 45 km with negative angle eigenrays (physically upgoing). They also show the trailing edge of the convergence zone at a range of 60 km with positive angle eigen-rays (physically downgoing). Also, Figure 14 shows that the second convergence should begin at about 90 km.

5.3.3. Modeling with ATLAS

As in the case of the fixed station, the ATLAS normal mode model is used to complete the acoustic modeling of the source tow. The environmental parameters are similar to the fixed station modeling ones but the sound speed profile is given in Table 8.

ATLAS is used to predict the position of the first convergence zone as well as the variations with range of the vertical arrival structure. The sound field power, corresponding to a 200 Hz source at 100 m depth with a level of 174 dB at 1 m, is contoured in Figure 15. The contour plot has contour levels from 70 to 100 dB with a 5 dB increment. The convergence zone appears at about 50 km near the surface. There is a good correspondance between the contour plot in Figure 15 and the ray-traces produced by the GSM in Figure 13.

The variations of power with range for a source at 100 m and a receiver at 20 m and at 550 m are also plotted in Figure 15. The convergence zone effect, at the deep sound axis, is not as strong as reported by the GSM.

The ATLAS model produces the complex pressure field which is processed to yield the model vertical arrival structure. The model wavefield is Fast Fourier Transformed using a Kaiser-Bessel window with α parameter of 1.5. The normalized wavenumber spectra, then, are mapped into angular spectra using a reference sound speed of 1480 m/s. The waterfall plot of the vertical arrival structure between 5 and 100 km is given in Figure 16. This plot is similar to the traces of the eigenray angles obtained with the GSM. Since the array is aliased, the angular spectra are periodic, of period $\approx 60°$, and plotted between - 30° and 30°, where 0° corresponds to the horizontal. Thus, positive angle arrivals, at small ranges, are not upgoing but, actually, are downgoing. As the range increases, the arrivals become closer to - 30° and the horizontal. Similar comments apply for arrival with negative angles with respect to the horizontal at close ranges. Figure 16 shows the first convergence zone starting between 40 and 50 km, with negative angle arrivals which correspond to physically upgoing sound. The trailing edge of the convergence zone extends up to a range of 70 km according to the ATLAS model.

5.3.4. Selection of the Tapes to Process

The data analysis described in Section 3 is performed on six data tapes recorded during the source tow. The tapes processed are given in Table 9. Also included are the GMT time at which the tapes start, and their corresponding source ranges (i.e. the radar range if available, or an estimate of the source range based on the nominal speed of 5 knts).

Tape Number	GMT Start Time	Range (km) at Start Time	Propagation Characteristics
972	02:25:50	18	Mid-range to convergence zone
980	05:33:32	47	First convergence zone
981	05:57:00	51	First convergence zone
983	06:43:55	58	Trailing edge of the convergence zone
986	07:51:12	68	Shadow zone
990	09:27:33	83	Shadow zone, second convergence zone

Table 9: Information on the source tow tapes

Tape 972 should correspond to a mid-convergence range, Tape 980 and 981 to the first convergence zone, Tape 983 to the trailing edge of the first convergence zone. Tape 986 should correspond to the shadow zone that follows the first convergence zone and, finally, Tape 990 to the end of the shadow zone and beginning of the second convergence zone. For the nominal ranges of the towing ship in Table 9, the ATLAS model angular spectra are plotted in Figures 17, 18 and 19.

5.4. Doppler Shift

The source is moving away from the VLA receivers at a speed, nominally constant, of 5 knts. The VLA array is essentially fixed since deployed from the R/P FLIP in a three point moor. The received frequency is Doppler shifted and given by [Camp1970, p 216]

$$f_r = f_t \frac{c}{c + v} \tag{2.1}$$

where f_r is the received frequency, f_t the transmitted frequency (i.e. 200 Hz), c the sound speed and v the tow ship speed. Assuming a constant sound speed of 1500 m/s and a tow speed of 5 knts, the received frequency is 199.657 Hz. It is different from 200 Hz by 5 to 6 times the bin width of the Fast Fourier Trasnform, where the bin width is 61 mHz (a 8192 point FFT is used for a -250 Hz to 250 Hz frequency band). The 200 Hz signals from the towed source should lay in bins 7368 and 7369 since in the fixed station case the 200 Hz signals were found in bins 7373 and 7374 (Section 4.1).

5.5. Analysis Results

The data analysis results are given in Appendix 2. The power spectra of selected array channels indicate the good quality of the data. The 200 Hz line component, clearly, is observed in all six tapes.

The signal is slightly more spread in frequency (more bins actually contain signal) than in the fixed station case, but lays mostly in two frequency bins. The vertical distribution of power is plotted for those two signal bins and for the bins 7360 and 7375 which correspond to noise. Table 10 gives the start time of the data segment (long of 4 minutes and 22 seconds) used to produce the vertical power distribution plots. As in the fixed station case, one observes for the noise bins, variations in self noise from channel to channel. For Tapes 972, 980, 981 and 983 the signal is observed in bins 7368 and 7369, the predicted bins. For Tapes 986 and 990, the signal is observed in the bins 7367 and 7368. This additional frequency shift of one FFT bin corresponds to a faster ship speed, slightly above 6 knts.

The distribution of power across the vertical array shows that 3 channels are malfunctionning (channels 55, 71 and 100). The power is almost equally distributed in the vertical for the data segments selected from Tapes 972 and 990. For Tapes 980, 981, 983 and 986, one observes an interference pattern and variations of power in the vertical on the order of 10 dB. The power levels for Tape 972 are on the order of 90 dB. This is

consistent with a signal with a source level of 174 dB at 1 m suffering spherical spreading up to a range equal to a water depth and, then, experiencing cylindrical spreading (174 dB - 10 log 5000 - 10 log 18000 = 94 dB). The power is mainly distributed in the top portion of the array for Tape 980 while, for Tape 983, it is mainly distributed in the bottom portion of the array. Tape 980 matches the convergence zone with sound focussing in the upper part of the VLA, while Tape 983 matches the trailing edge of the first convergence zone (with sound focussing in the lower part of the VLA).

Tape number	GMT start time
972	02:25:50
980	05:33:32
981	05:57:00
983	06:43:55
986	07:51:16
990	09:27:33

Table 10: GMT time reference for the vertical distribution of power plots.

The FFT beamformer processes the four FFT bins considered for each tape (the two noise bins 7360 and 7375, and either the signal bin pair 7367 and 7368, or 7368 and 7369). The angular spectra are plotted between ±30° with respect to the horizontal (the array is aliased). For each tape, the arrival structure is displayed in a waterfall plot referenced in GMT time. The number of incoherent averages used to produce a particular angular spectrum is given in Table 11. This table also contains the corresponding 90 % confidence interval associated to each angular spectrum. The arrival structure of Tape 972 varies with time with steep arrivals between -30° and -20°. The strongest arrivals move closer to the horizontal, between -10° and 0°, for Tape 980. Negative angles of arrival indicate upgoing sound. The waterfall plot of the angular spectra of Tape 983, shows the transfert of the strongest arrivals from negative angle (upgoing sound) to positive angle (downgoing sound). The vertical arrival structure for Tape 980, 981 and 983 are consistent with the source moving through the first convergence zone. The power lev-

els of the arrivals of Tape 986 are significantly lower than the ones of the previous tapes. This follows the modeling prediction that the 200 Hz source is in the shadow zone. Finally, the arrivals in the waterfall plot of Tape 990 have power levels higher than in Tape 986. Once again this is consistent with the fact that the 200 Hz source is at the very beginning of the second convergence zone.

Tape 972			Tape 980			Tape 981		
GMT Time	Number of Averages	Confidence Interval (dB)	GMT Time	Number of Averages	Confidence Interval (dB)	GMT Time	Number of Averages	Confidence Interval (dB)
02:25:50	15	+2.0/-1.6	05:33:32	15	+2.0/-1.6	05:57:00	15	+2.0/-1.6
02:28:01	15	+2.0/-1.6	05:35:43	15	+2.0/-1.6	05:59:11	15	+2.0/-1.6
02:30:12	15	+2.0/-1.6	05:37:54	15	+2.0/-1.4	06:01:22	15	+2.0/-1.6
02:32:23	15	+2.0/-1.6	05:40:05	15	+2.0/-1.9	06:03:33	15	+2.0/-1.6
02:34:34	15	+2.0/-1.6	05:42:16	15	+2.0/-1.6	06:05:44	15	+2.0/-1.6
02:36:45	15	+2.0/-1.6	05:44:27	15	+2.0/-1.6	06:07:55	15	+2.0/-1.6
02:38:56	15	+2.0/-1.6	05:46:38	15	+2.0/-1.6	06:10:06	15	+2.0/-1.6
02:41:07	15	+2.0/-1.6	05:48:49	15	+2.0/-1.6	06:12:17	15	+2.0/-1.6
02:43:18	15	+2.0/-1.6	05:51:00	15	+2.0/-1.6	06:14:28	15	+2.0/-1.6
02:45:29	15	+2.0/-1.6	05:53:11	15	+2.0/-1.6	06:16:39	15	+2.0/-1.6
02:47:40	10	+2.6/-2.0	05:55:15	10	+2.6/-2.0	06:18:50	10	+2.6/-12.0

Tape 983			Tape 986			Tape 990		
GMT Time	Number of Averages	Confidence Interval (dB)	GMT Time	Number of Averages	Confidence Interval (dB)	GMT Time	Number of Averages	Confidence Interval (dB)
06:43:55	7	+3.3/-2.3	07:51:12	15	+2.0/-1.6	09:27:33	11	+2.5/-1.9
06:46:06	7	+3.3/-2.3	07:53:23	15	+2.0/-1.6	09:29:11	15	+2.0/-1.6
06:48:17	15	+2.0/-1.6	07:55:34	15	+2.0/-1.4	09:31:23	15	+2.0/-1.6
06:50:28	15	+2.0/-1.6	07:57:45	15	+2.0/-1.9	09:33:34	15	+2.0/-1.6
06:52:39	15	+2.0/-1.6	07:59:56	12	+2.5/-1.8	09:35:45	15	+2.0/-1.6
06:54:50	15	+2.0/-1.6	08:02:07	15	+2.0/-1.6	09:37:45	15	+2.0/-1.6
06:57:01	15	+2.0/-1.6	08:04:18	15	+2.0/-1.6	09:40:07	15	+2.0/-1.6
06:59:12	15	+2.0/-1.6	08:06:29	13	+2.3/-1.8	09:42:18	15	+2.0/-1.6
07:01:23	15	+2.0/-1.6	08:08:40	15	+2.0/-1.6	09:44:29	15	+2.0/-1.6
07:03:34	15	+2.0/-1.6	08:10:51	13	+2.3/-1.8	09:46:29	5	+4.0/-2.6
07:05:45	10	+2.6/-2.0	08:13:02	10	+2.6/-2.0			

Table 11: Source tow waterfall plots information.

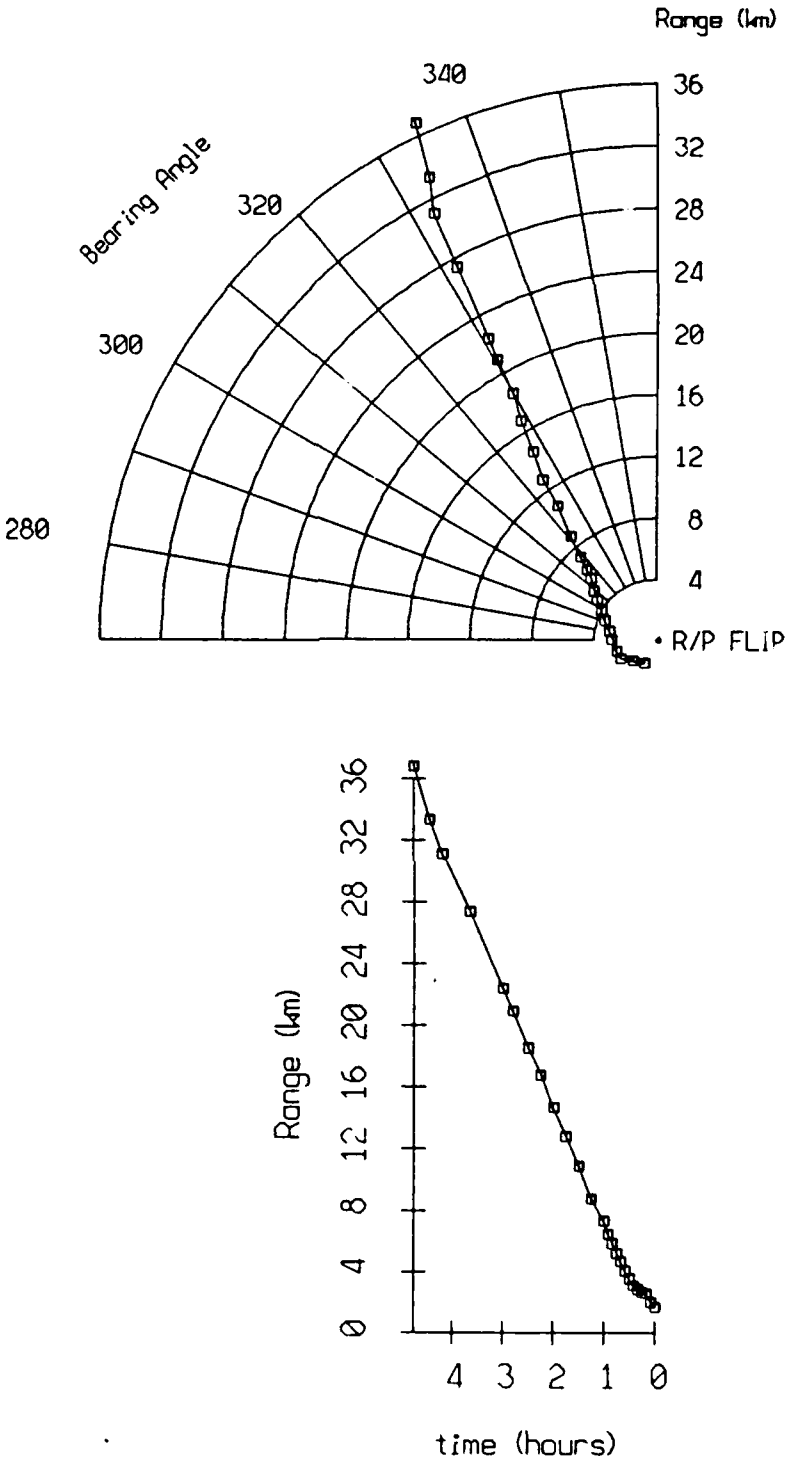

Figure 11: Tow ship radar tracking.

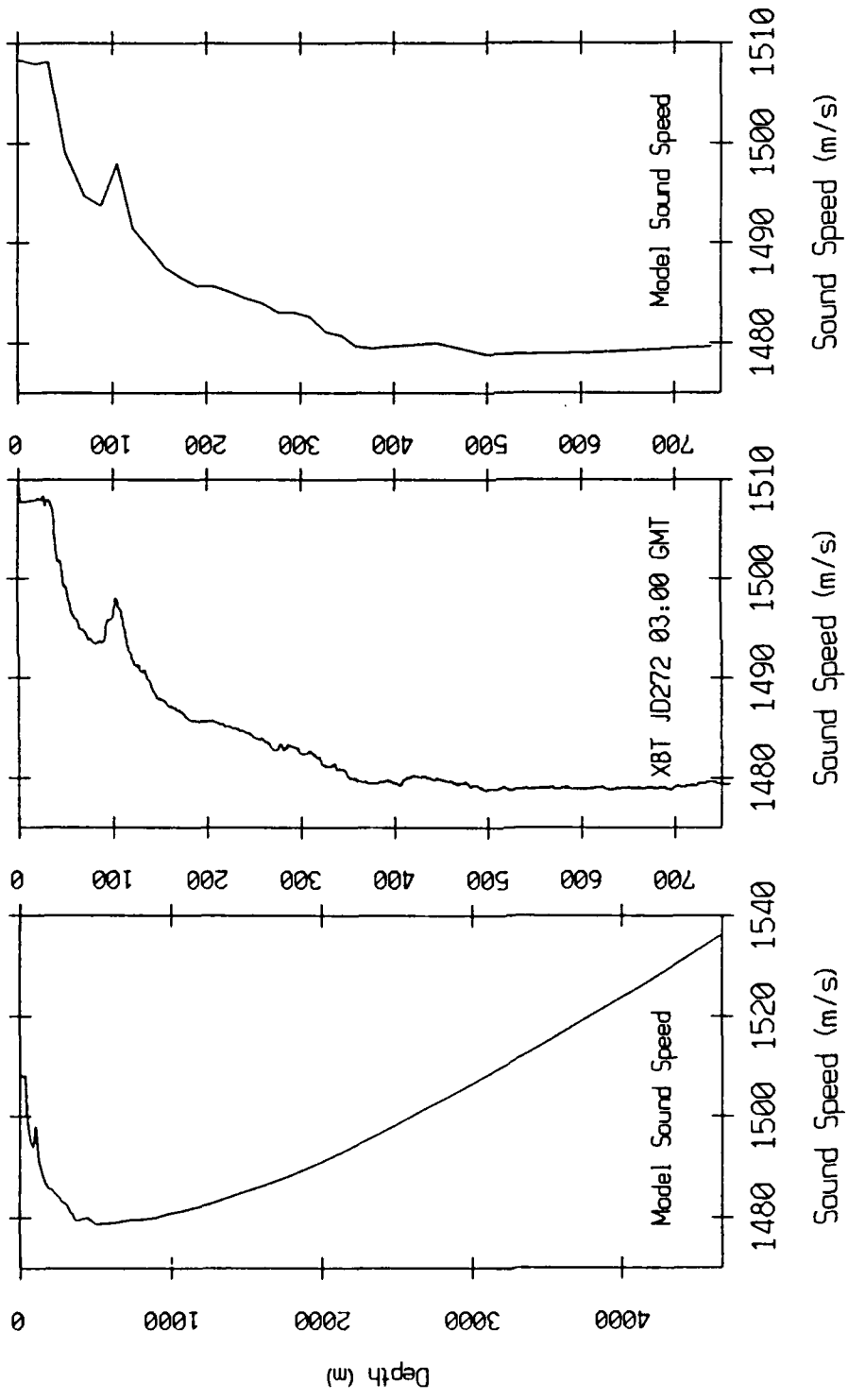

Figure 12: Source tow sound speed profiles.

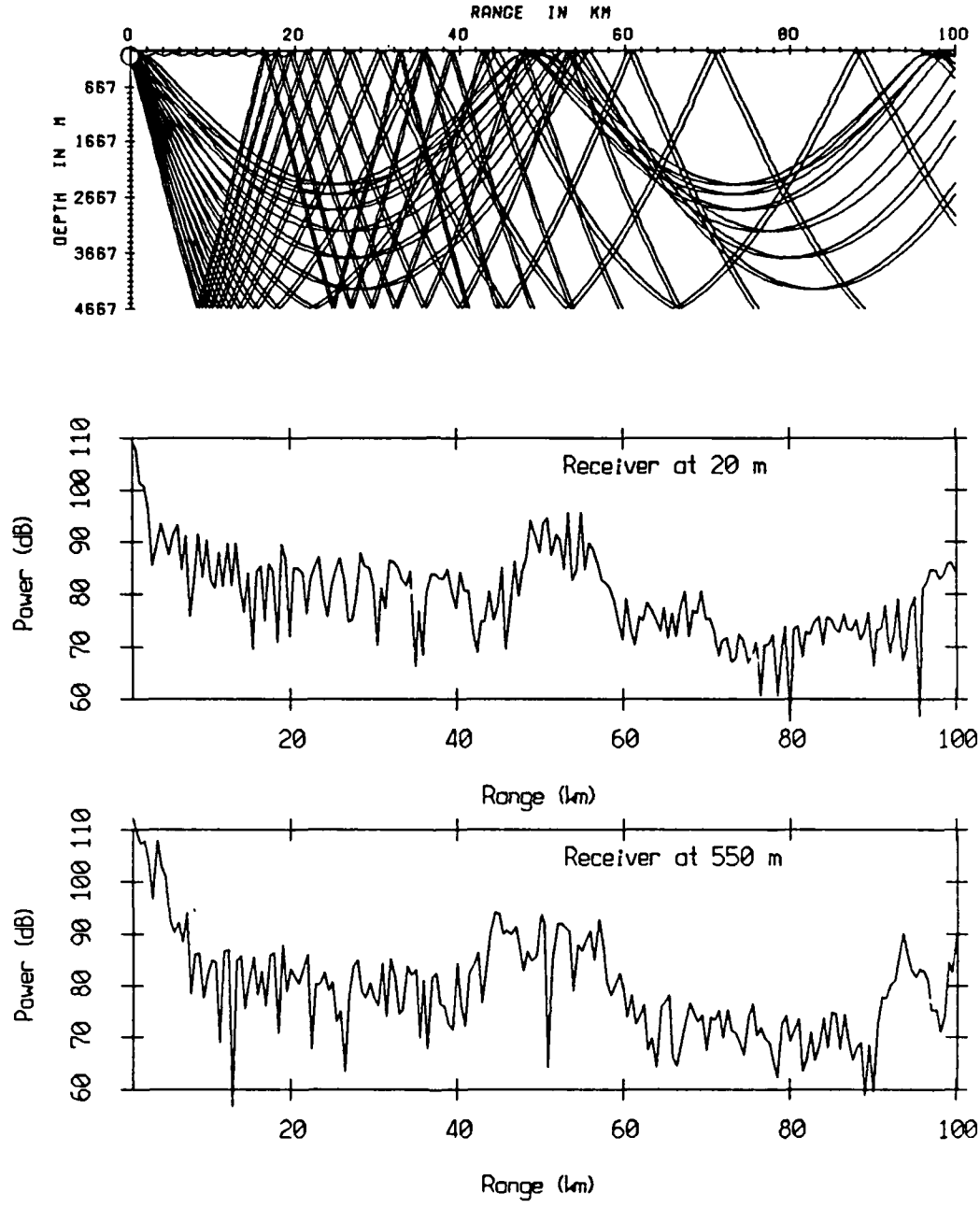

Figure 13: GSM ray traces and power versus range.

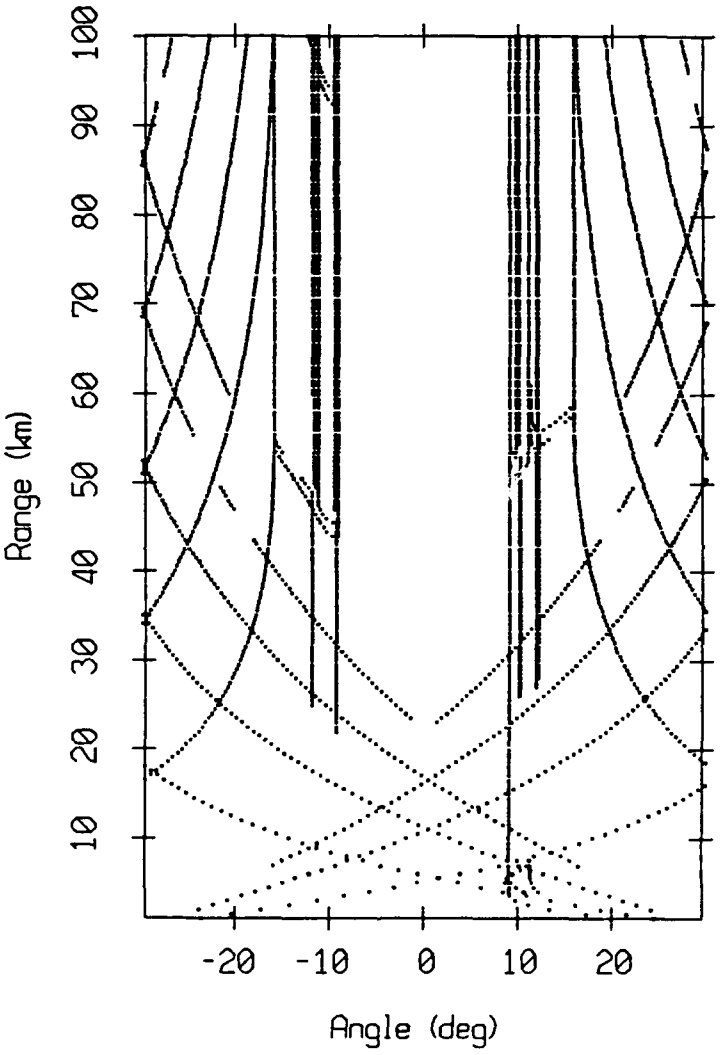

Figure 14: GSM eigenray angles with range.

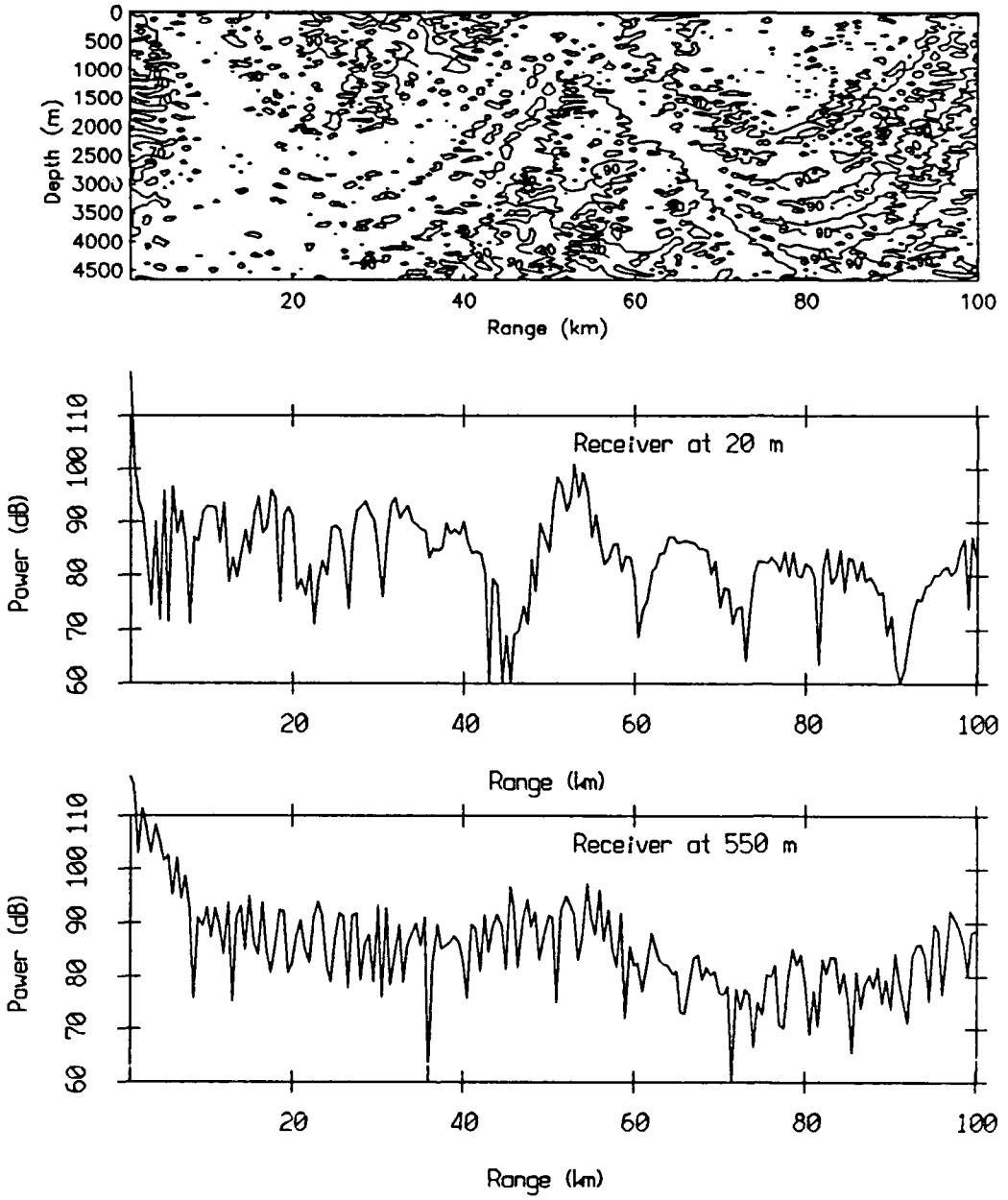

Figure 15: ATLAS transmission loss contour plot and power versus range.

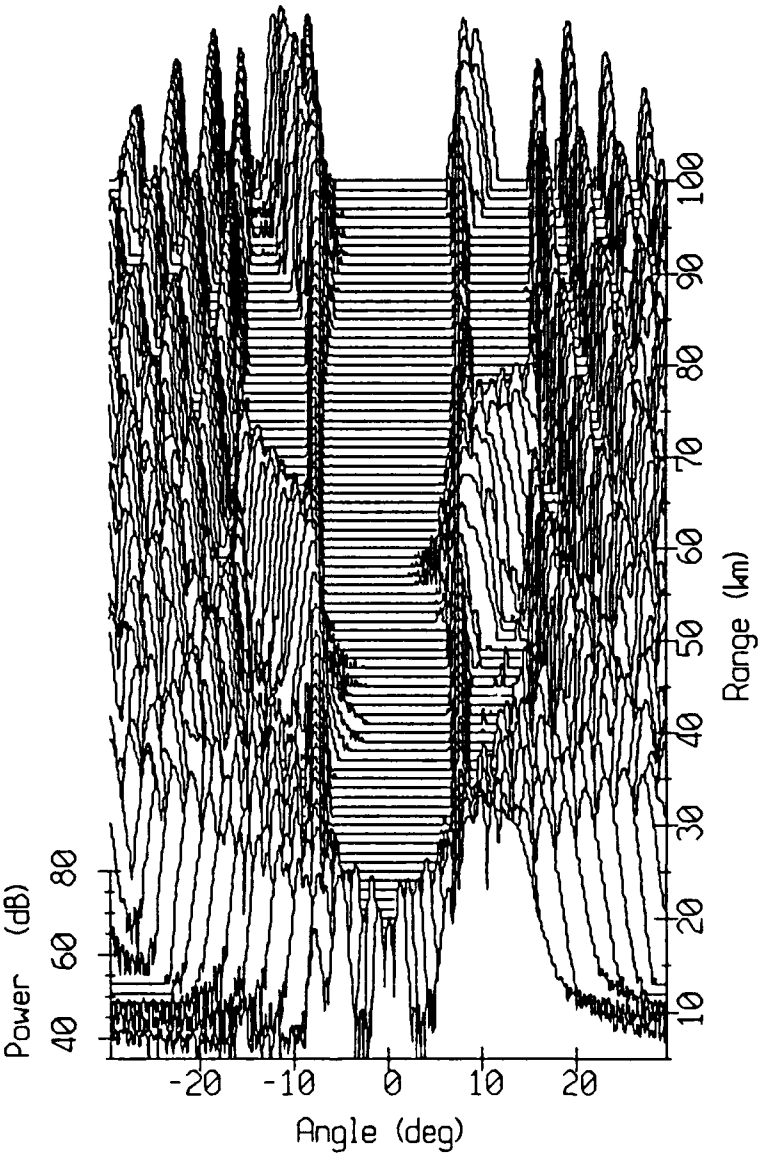

Figure 16: ATLAS angular spectra as a funtion of range.

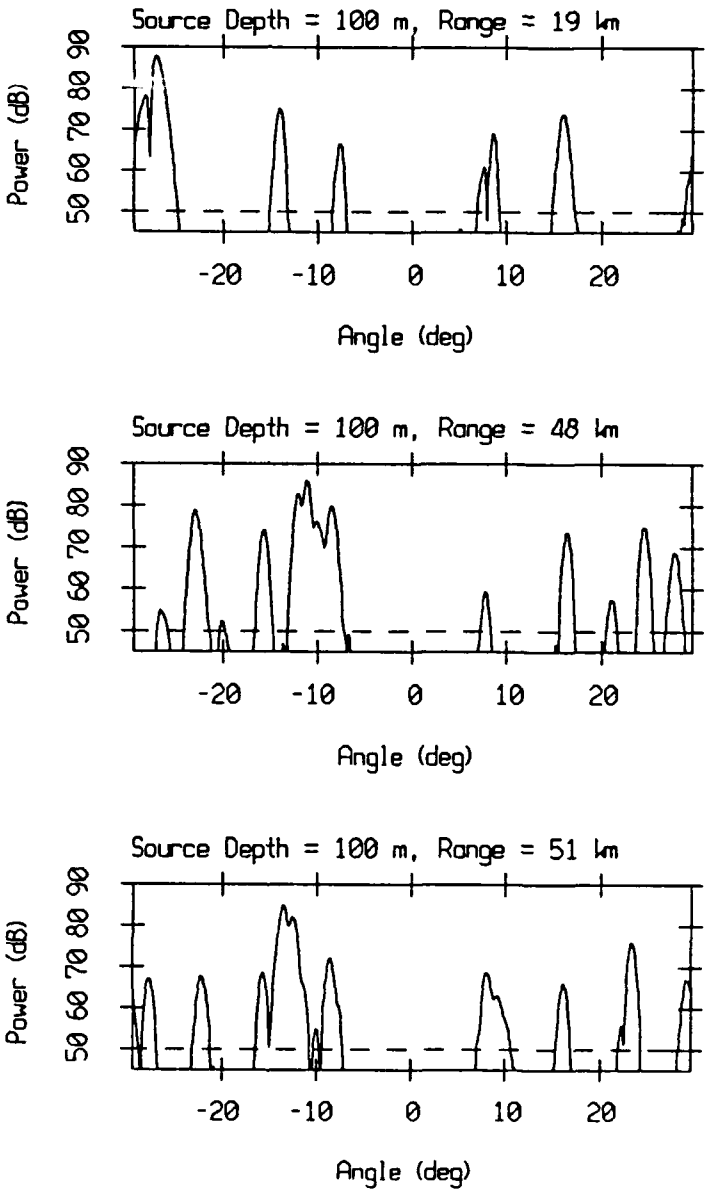

Figure 17: ATLAS angular spectra at 19, 48 and 51 km ranges.

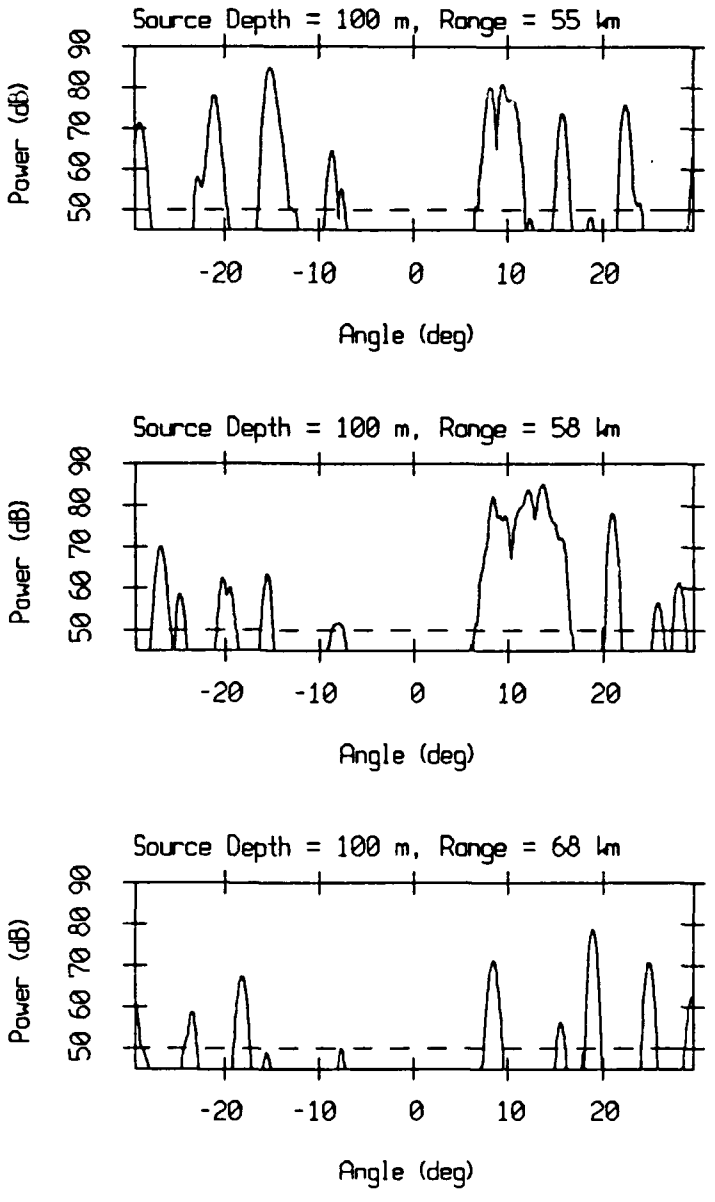

Figure 18: ATLAS angular spectra at 55, 58 and 68 km ranges.

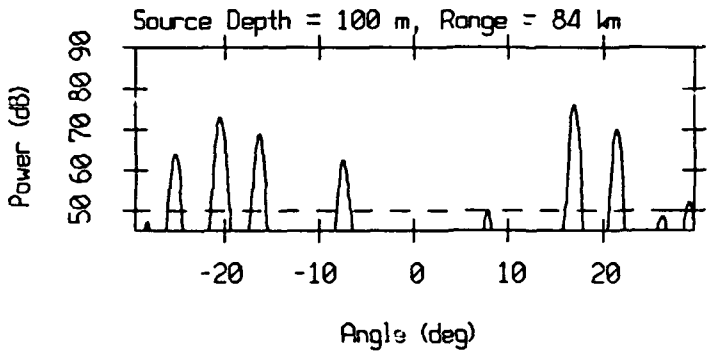

Figure 19: ATLAS angular spectrum at 84 km range.

6. Conclusion

This technical report presents the conventional processing of the 200 Hz CW tone propagation data recorded on Julian Day 270 and 272, during the the September 1987 VLA experiment. Two power spectra between 0 and 250 Hz are computed and plotted for each array section. Vertical distribution of power, across the VLA, is obtained for the signal and the noise at 200 Hz. Finally, conventional beamforming was performed on the data to obtain the vertical arrival structure of the projected 200 Hz signal and noise at 200 Hz.

The available environmental information allows a successful acoustic modeling in both the fixed station case, where source depth is varied, and the source tow case, where range varies from 0 to 100 km. Acoustic modeling with the CONGRATS ray-theory model of the GSM and the ATLAS normal mode model, agrees with the experimental data. It provides some insight to interpret the data set and understand the propagation physics.

BIBLIOGRAPHY

Camp, L., *Underwater Acoustics,* Wiley, N.Y. , 1970.

Fofonoff, N. P., *Algoritms for the Computation of Fundamental Properties of Seawater,* Technical Paper 44, Unesco Division of Marine Sciences, Paris, France , 1983.

Gordon, D. F. and H. P. Bucker, *Arctic Acoustic Propagation Model with Ice Scattering,* NOSC Technical Report 985, 30 September 1984.

Harris, F. J., "On the Use of Windows for Harmonic Analysis with the Discrete Fourier Transform," *IEEE Proc.*, vol. 66, no. 1, pp. 51-83, January 1978.

Mackenzie, K. V., "Nine-term Equation for Sound Speed in the Oceans," *J. Acoust. Soc. Am.*, vol. 70, no. 3, p. 808, September 1981.

Sotirin, B. J. and J. A. Hildebrand, "Large Aperture Digital Acoustic Array," *IEEE J. Oceanic Eng.*, vol. 13, no. 4, pp. 271-281, October 1988.

Sotirin, B. J., *Large Aperture Acoustic Array, MPL-U-47/89, SIO Reference 89-10,* Marine Physical Laboratory, Scripps Institution of Oceanography, July 1989.

Urick, R. J., *Ambient Noise in the Sea,* Peninsula, Los Altos, CA, 1986.

Weinberg, H., *Generic Sonar Model.* NUSC Technical Document 5971-D, 6 June 1985.

Appendix 1

VLA Tape 915, Sept, 1987 - Time 20:52:26 GMT Cal. Pressure Spectra
Data dur.: 2 min 11 sec. FFT Length: 16.38 sec. Samp Freq: 500 Hz

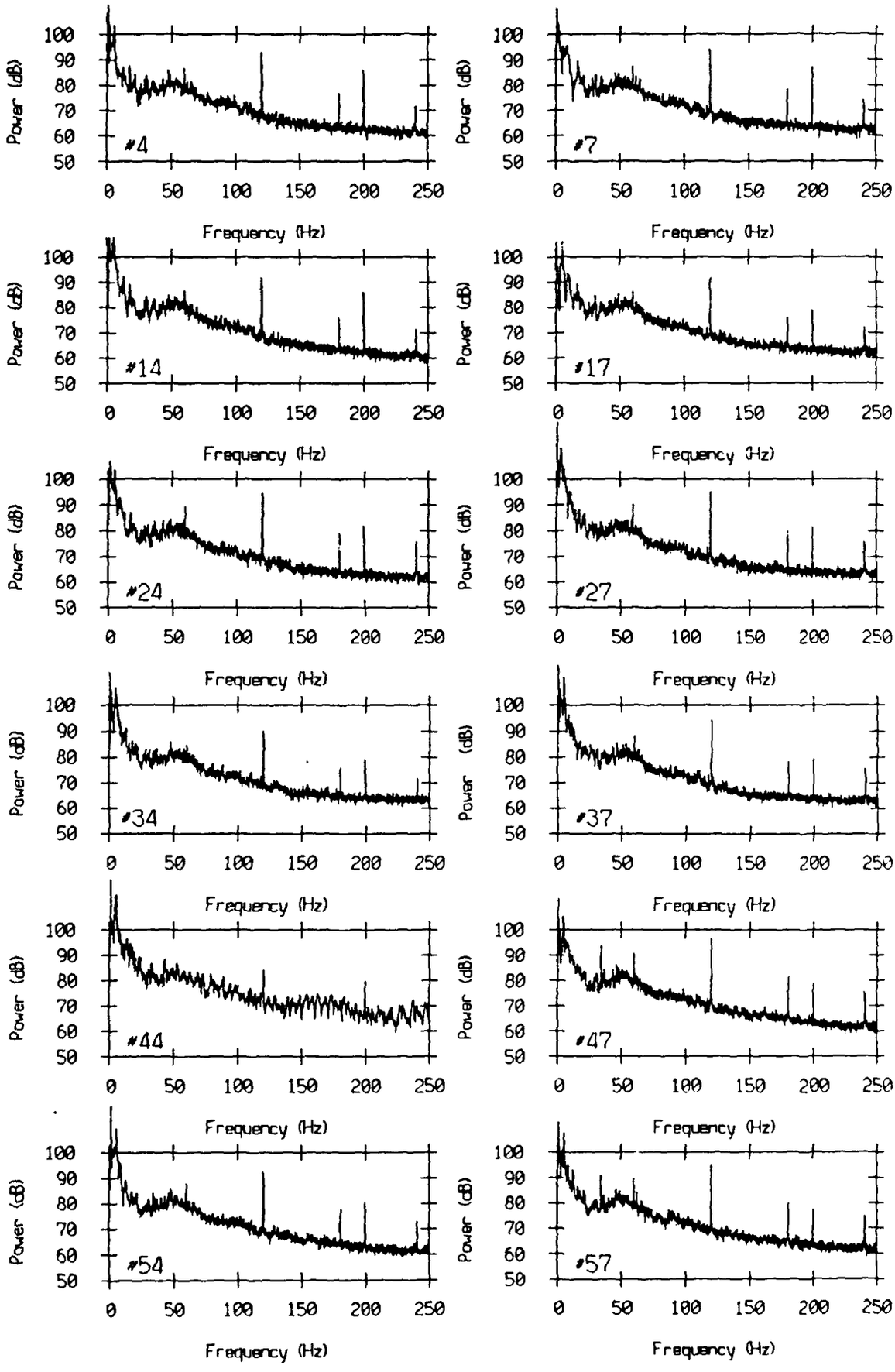

VLA Tape 915, Sept, 1987 - Time 20:52:26 GMT Cal. Pressure Spectra
Data dur.: 2 min 11 sec. FFT Length: 16.38 sec. Samp Freq: 500 Hz

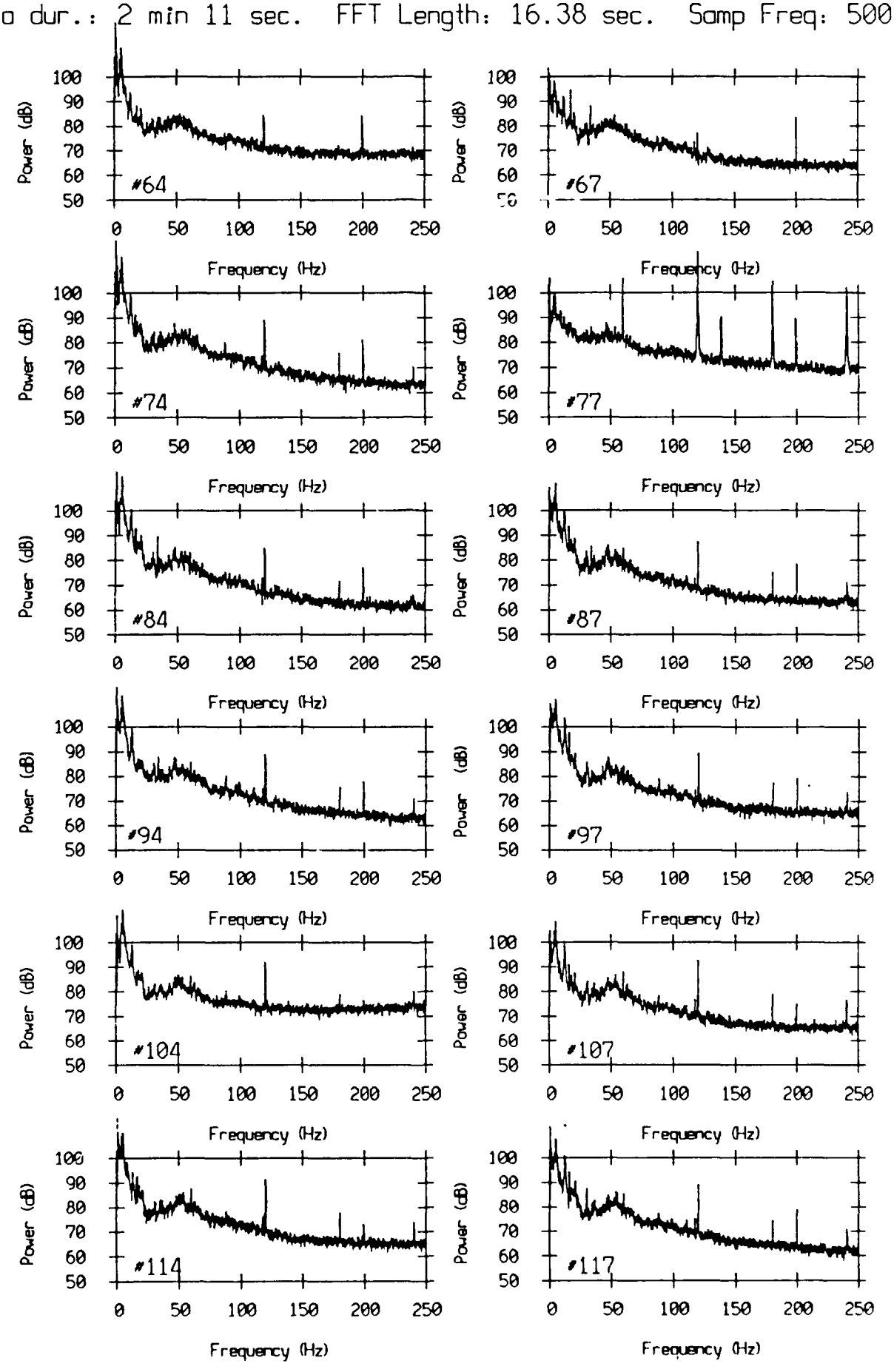

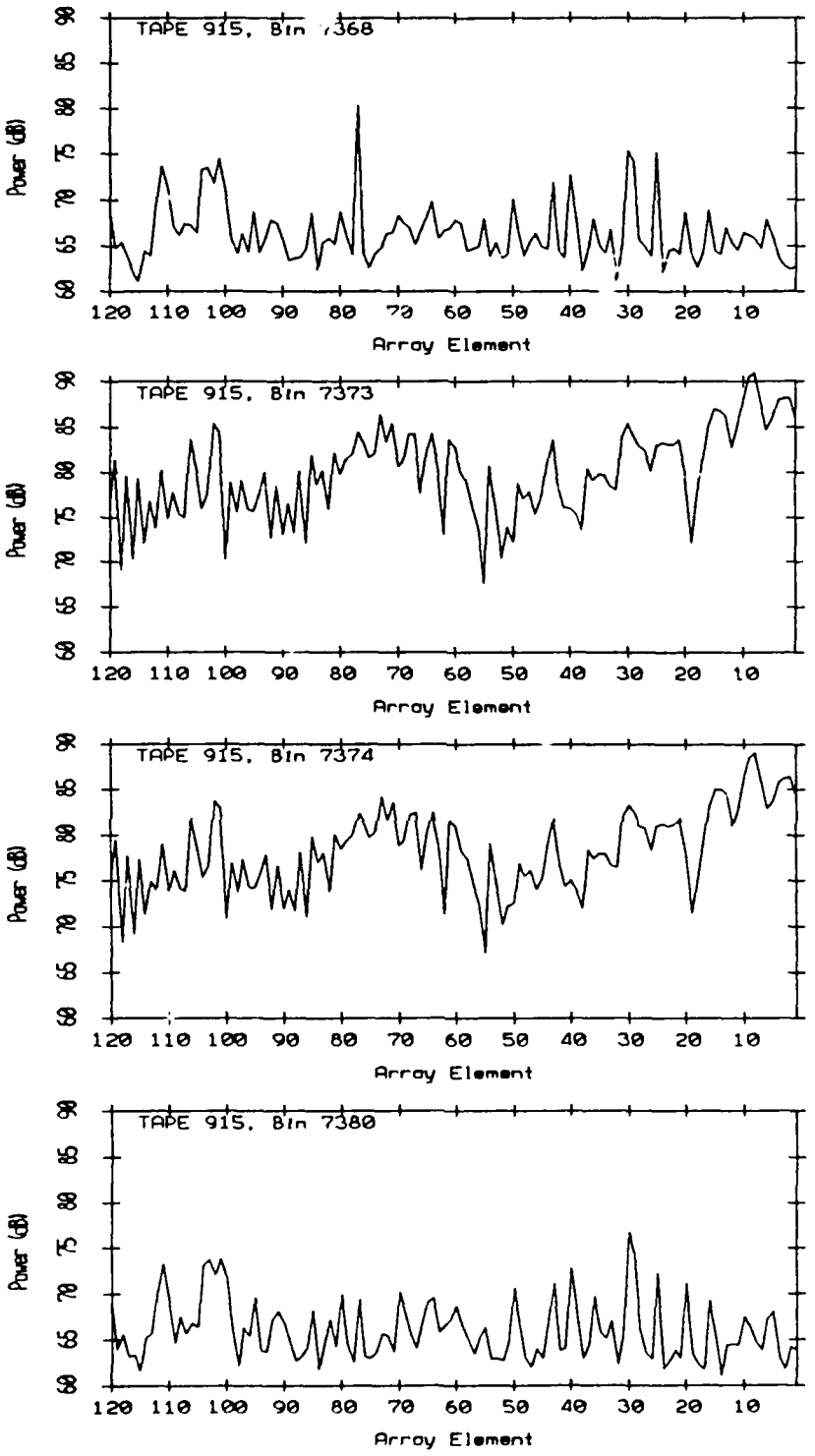
TAPE 915, Bin 7368
TAPE 915, Bin 7373
TAPE 915, Bin 7374
TAPE 915, Bin 7380
Power (dB)
90
85
80
75
70
65
60
120 110 100 90 80 70 60 50 40 30 20 10
Array Element

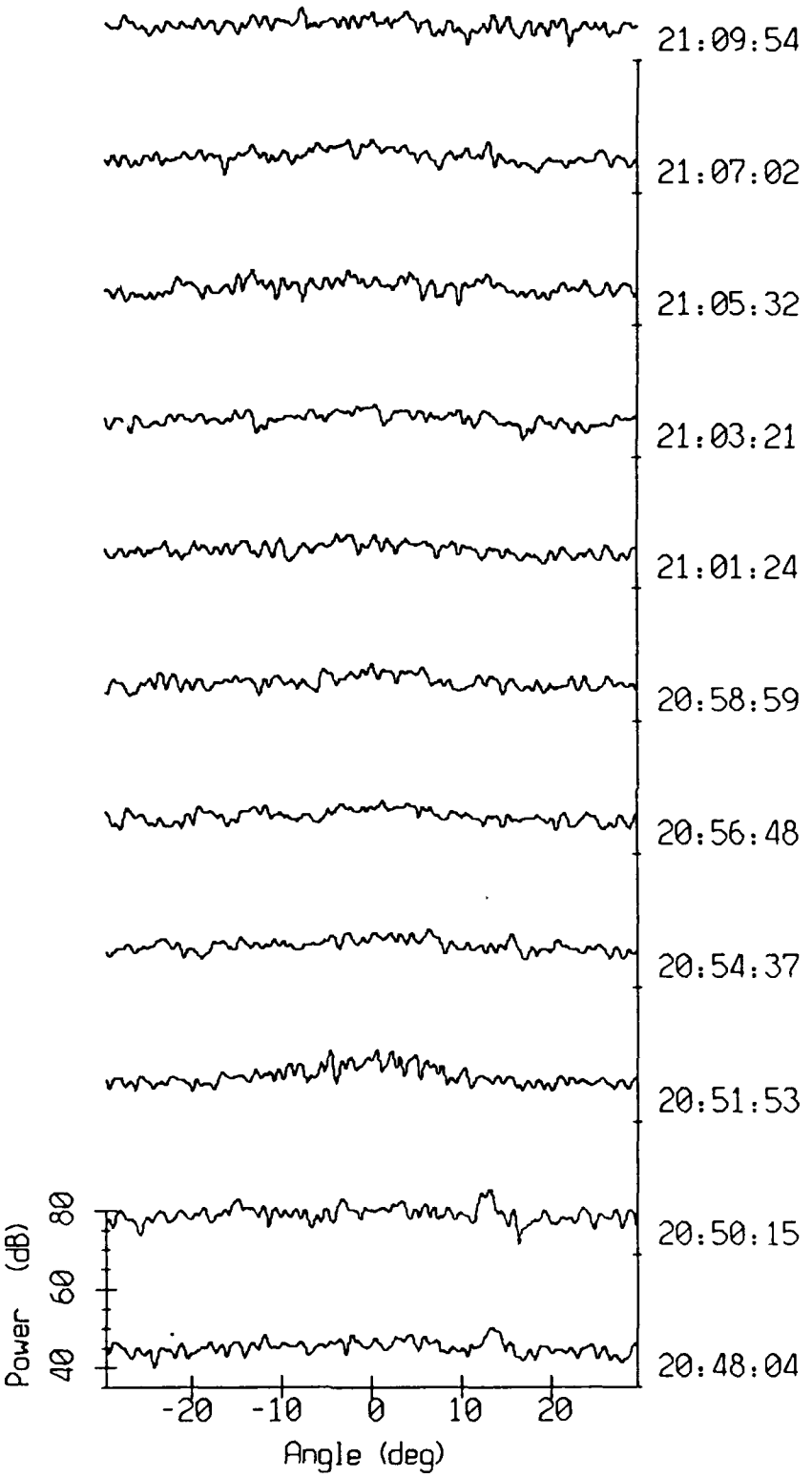
21:09:54
21:07:02
21:05:32
21:03:21
21:01:24
20:58:59
20:56:48
20:54:37
20:51:53
20:50:15
20:48:04
Power (dB)
40
60
80
-20
-10
0
10
20
Angle (deg)

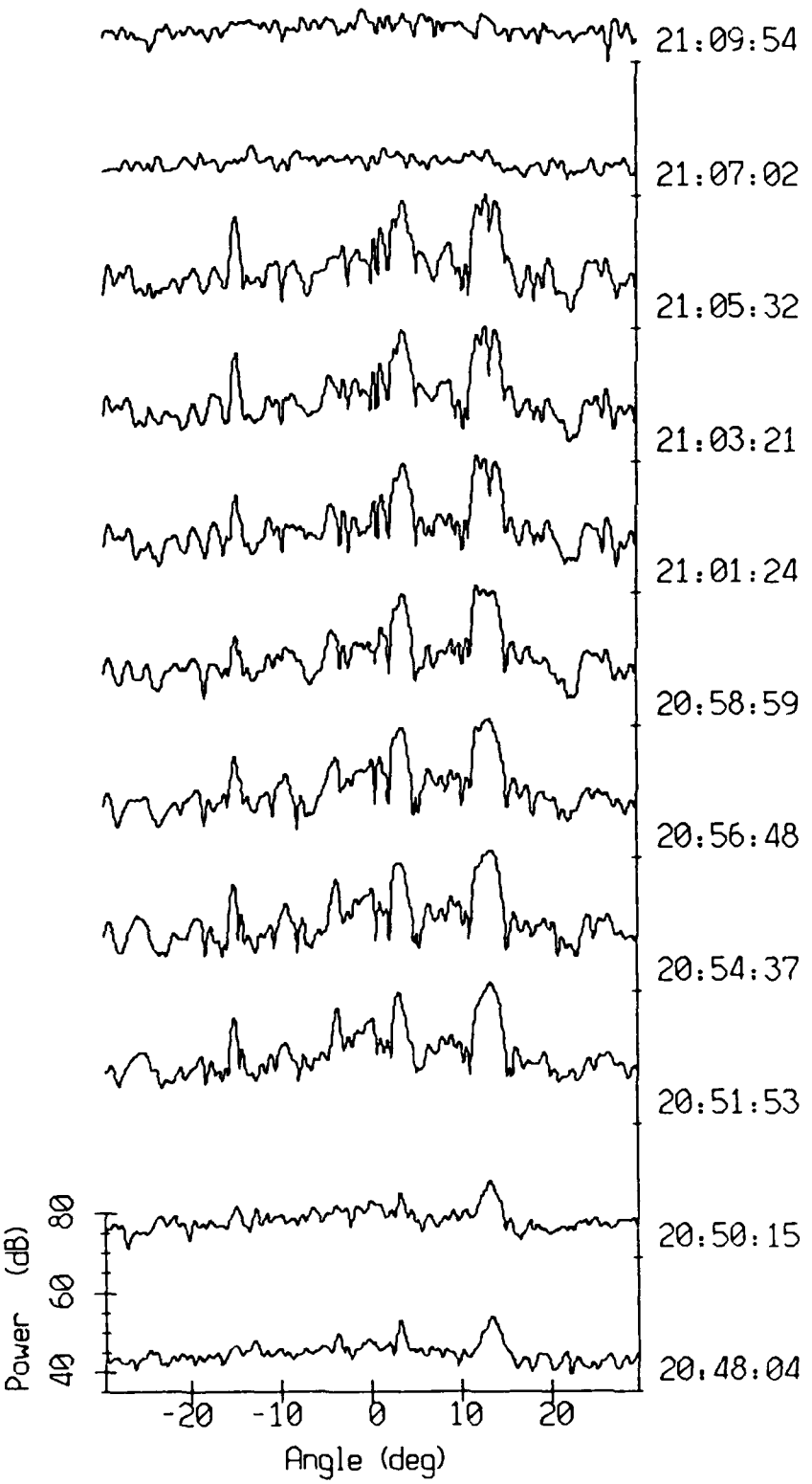
21:09:54
21:07:02
21:05:32
21:03:21
21:01:24
20:58:59
20:56:48
20:54:37
20:51:53
20:50:15
20:48:04
Power (dB)
40
60
80
-20
-10
0
10
20
Angle (deg)

Tape 915 : Bin 7374

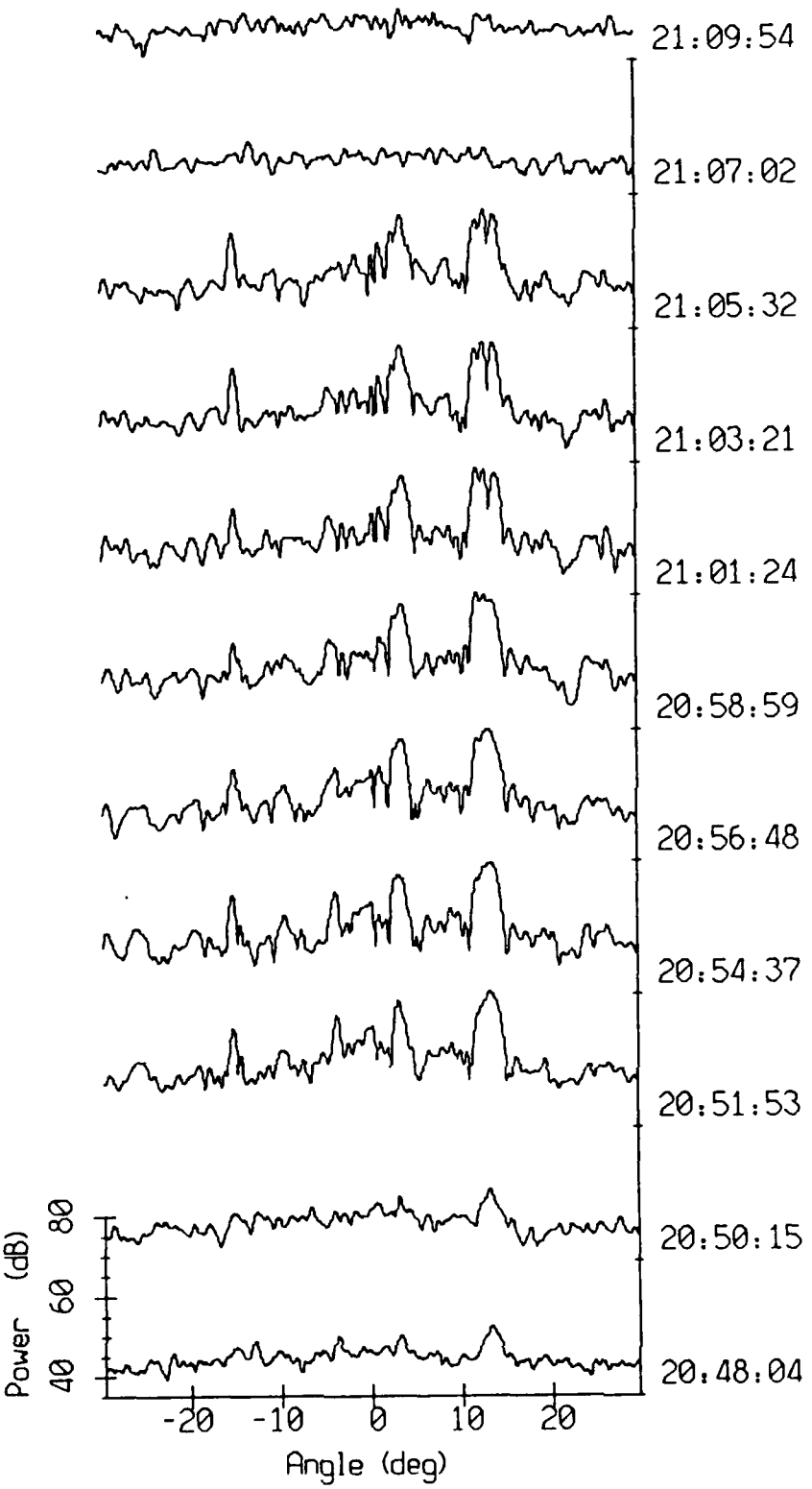

Tape 915 : Bin 7380

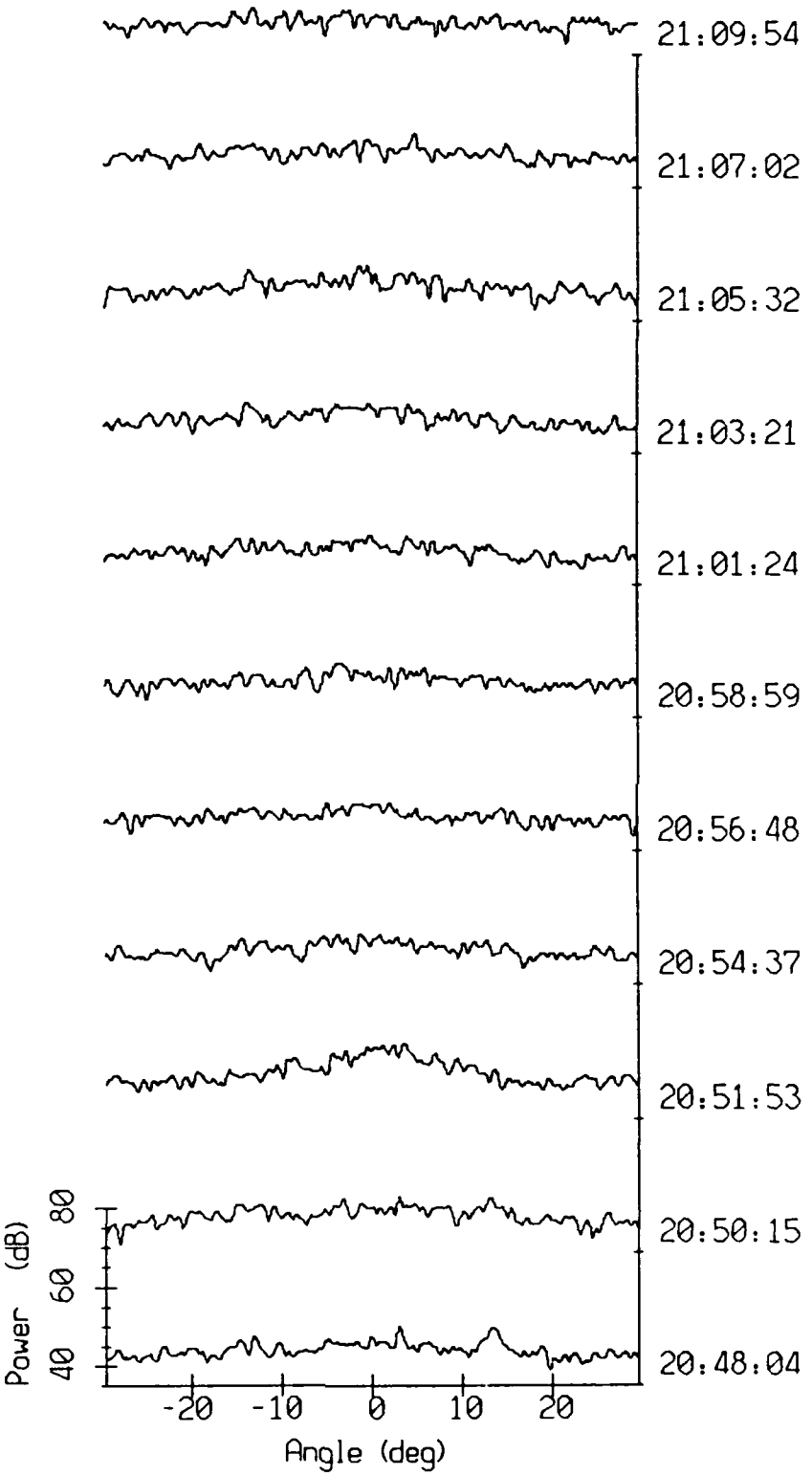

VLA Tape 917, Sept, 1987 - Time 21:34:59 GMT Cal. Pressure Spectra
Data dur.: 2 min 11 sec. FFT Length: 16.38 sec. Samp Freq: 500 Hz

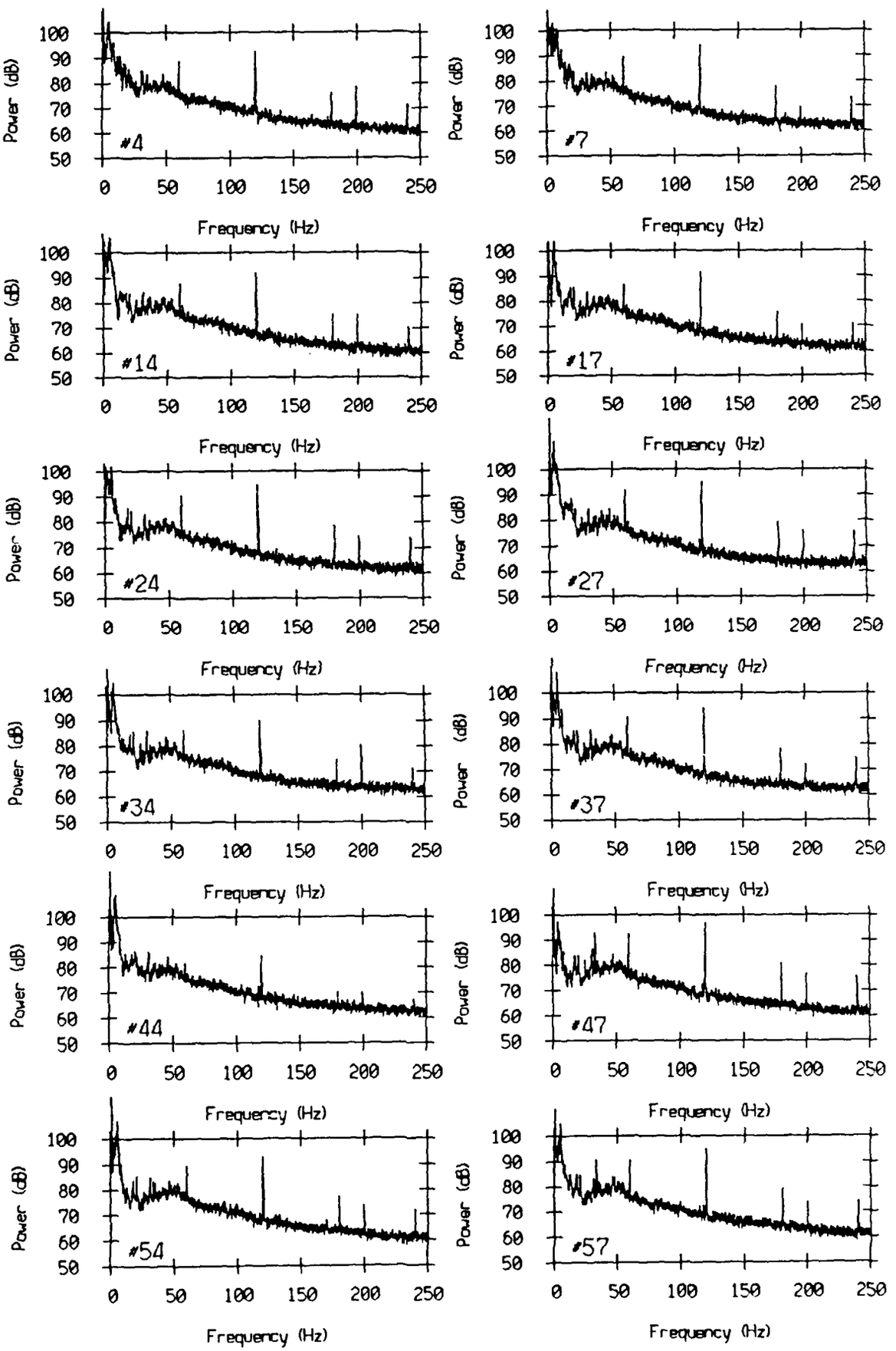

VLA Tape 917, Sept, 1987 - Time 21:34:59 GMT Cal. Pressure Spectra
Data dur.: 2 min 11 sec. FFT Length: 16.38 sec. Samp Freq: 500 Hz

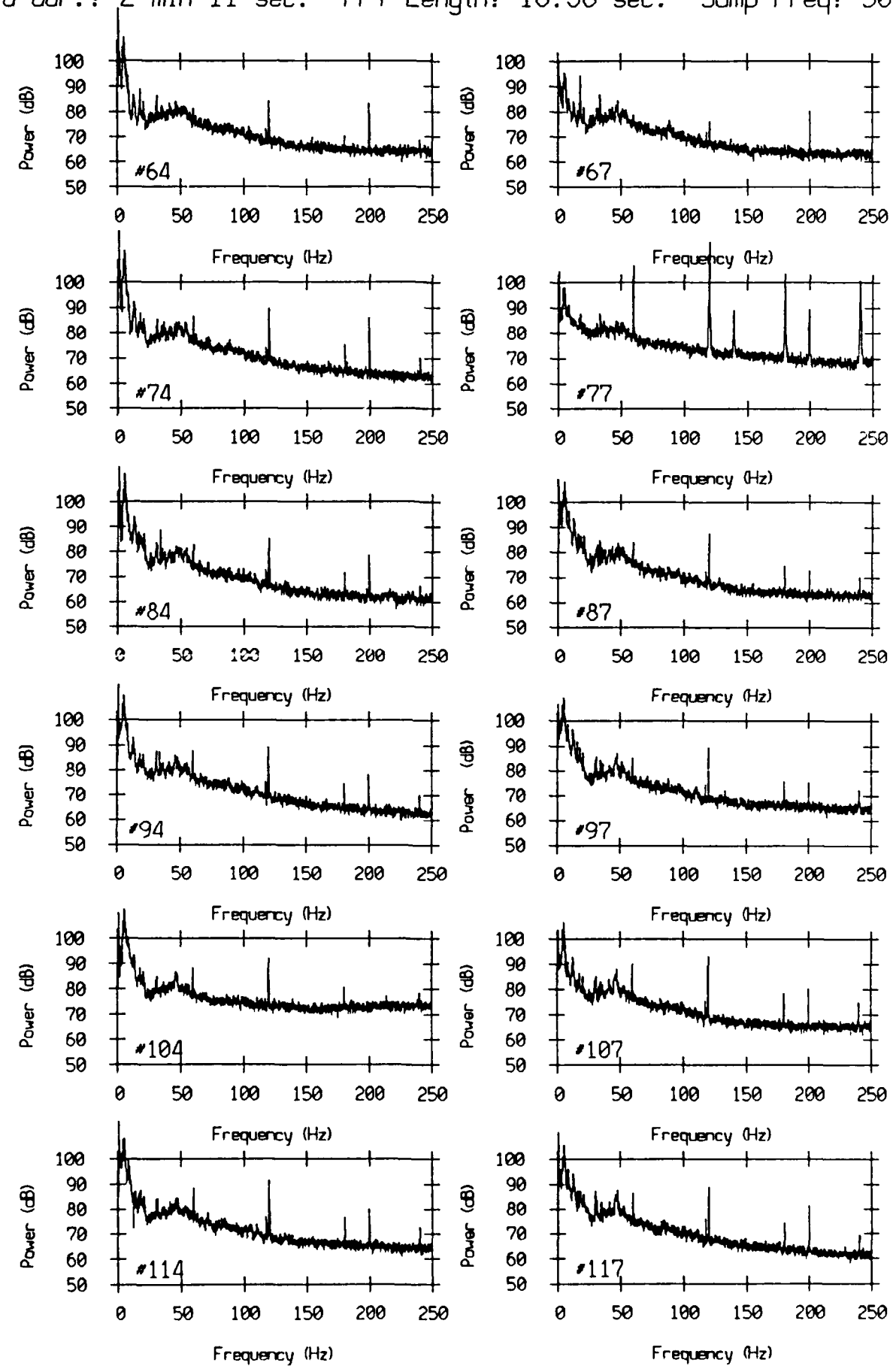

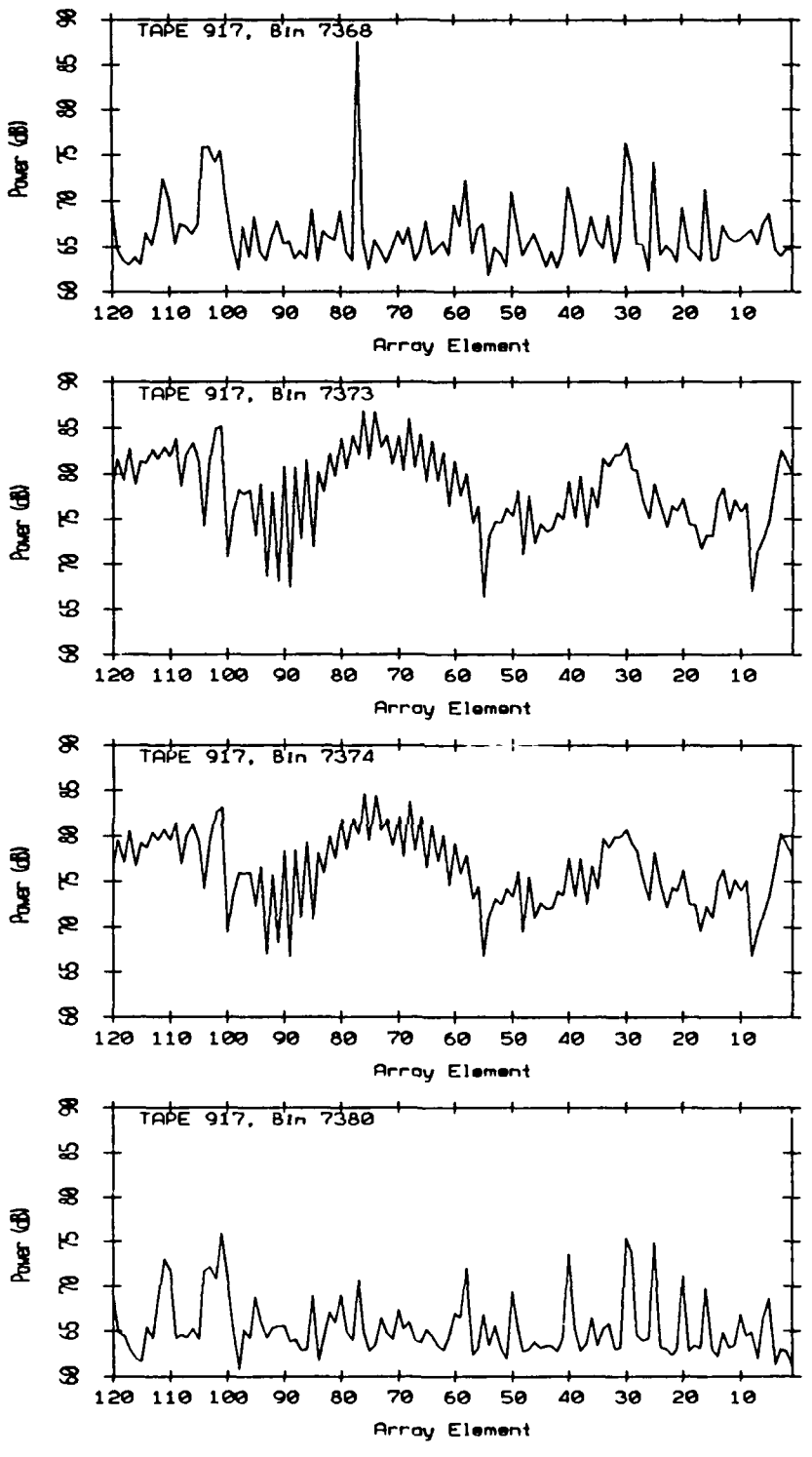
TAPE 917, Bin 7368
TAPE 917, Bin 7373
TAPE 917, Bin 7374
TAPE 917, Bin 7380
Power (dB)
90
85
80
75
70
65
60
120 110 100 90 80 70 60 50 40 30 20 10
Array Element

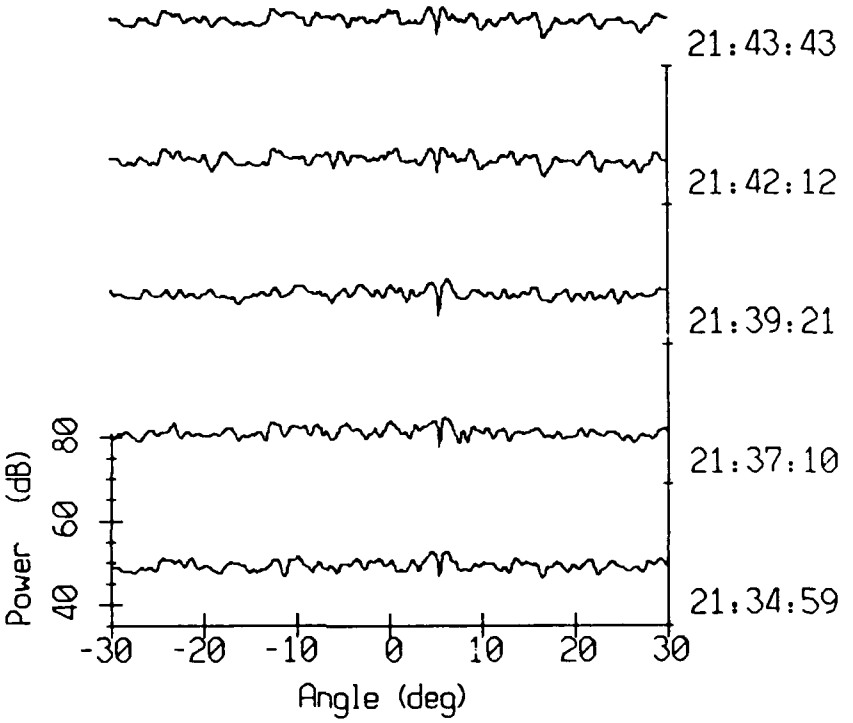
21:43:43
21:42:12
21:39:21
21:37:10
21:34:59
Power (dB)
40
60
80
-30
-20
-10
0
10
20
30
Angle (deg)

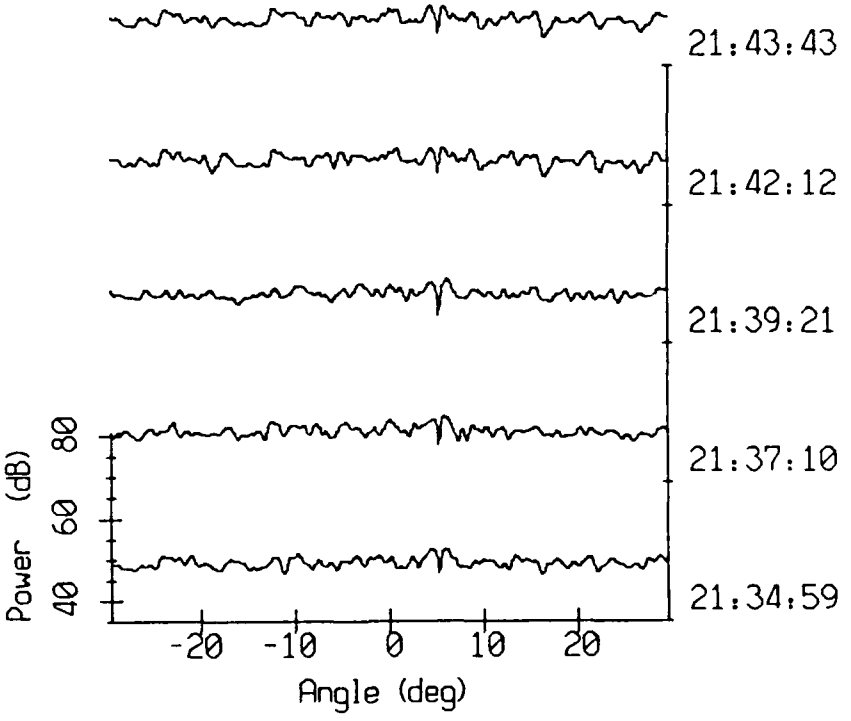
21:43:43
21:42:12
21:39:21
21:37:10
21:34:59
Power (dB)
40
60
80
-20
-10
0
10
20
Angle (deg)

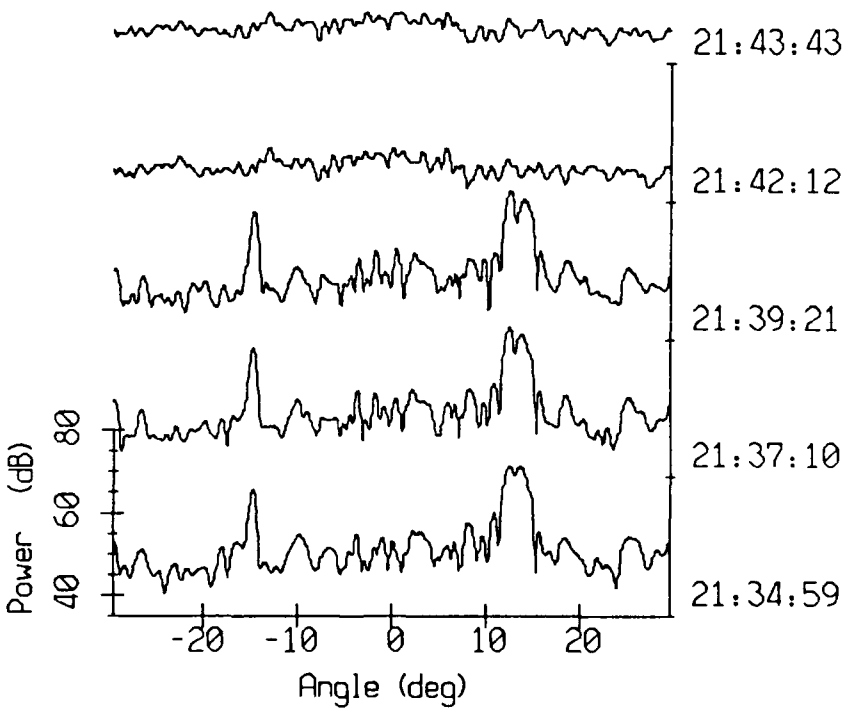
21:43:43
21:42:12
21:39:21
21:37:10
21:34:59
Power (dB)
40
60
80
-20
-10
0
10
20
Angle (deg)

Tape 917 : Bin 7374

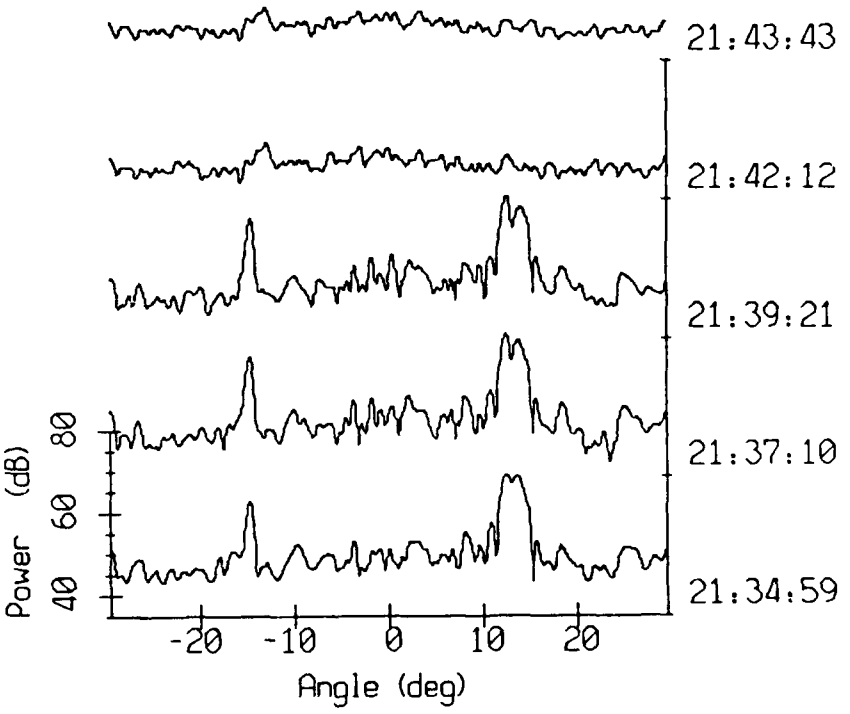

Tape 917 : Bin 7380

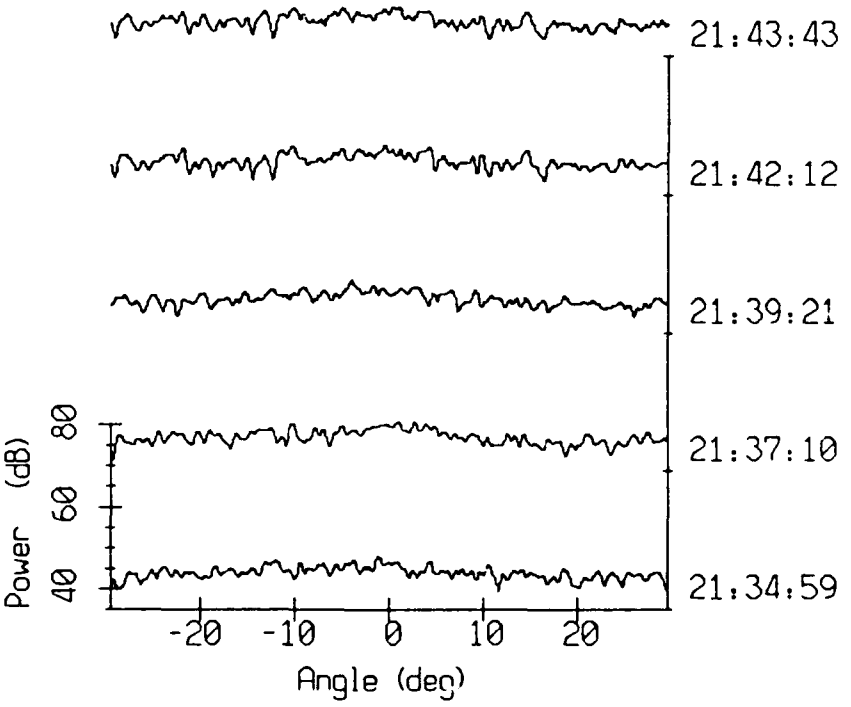

VLA Tape 918, Sept, 1987 - Time 22:09:22 GMT Cal. Pressure Spectra
Data dur.: 2 min 11 sec. FFT Length: 16.38 sec. Samp Freq: 500 Hz

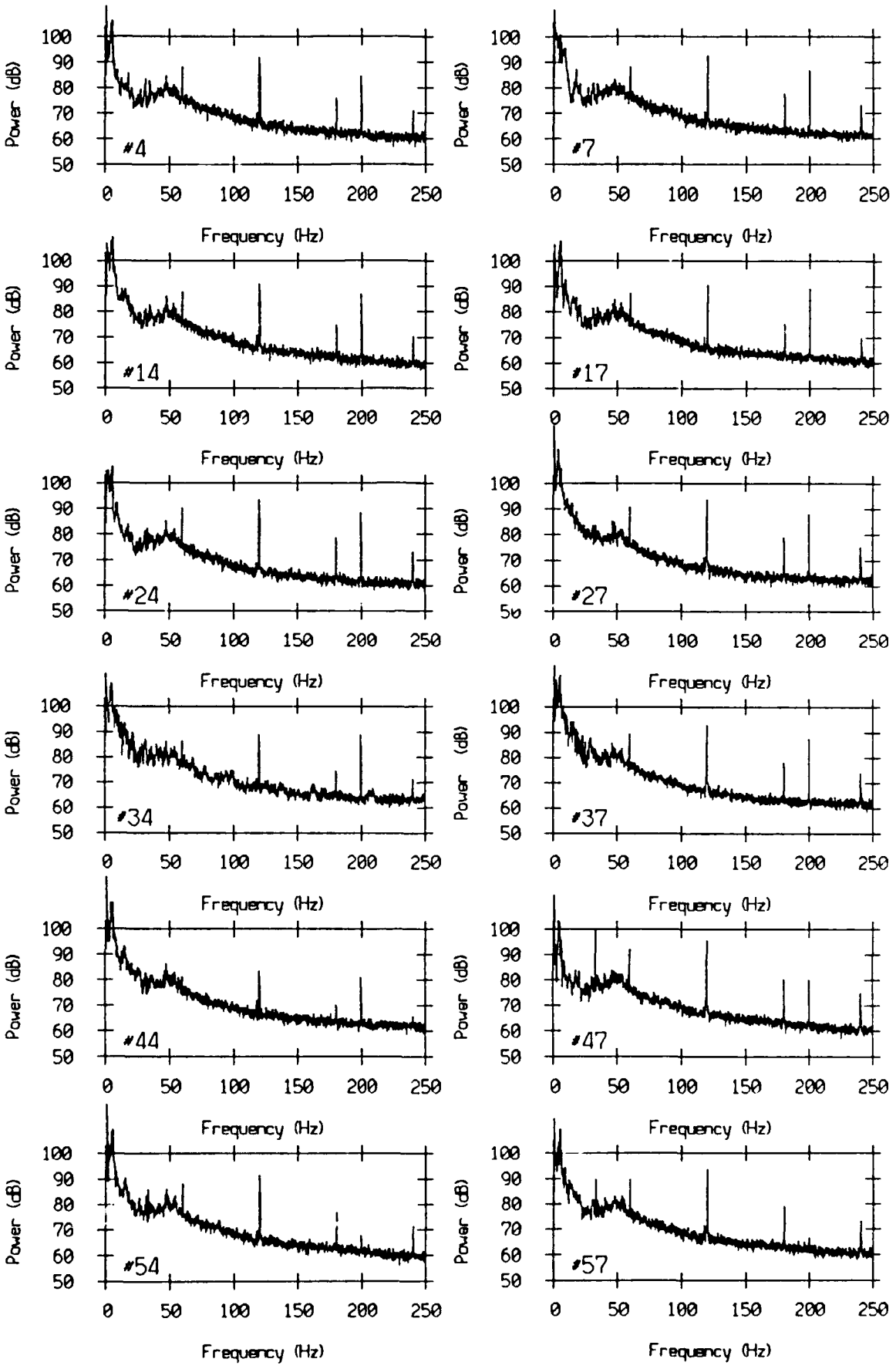

VLA Tape 918, Sept, 1987 - Time 22:09:22 GMT Cal. Pressure Spectra
Data dur.: 2 min 11 sec. FFT Length: 16.38 sec. Samp Freq: 500 Hz

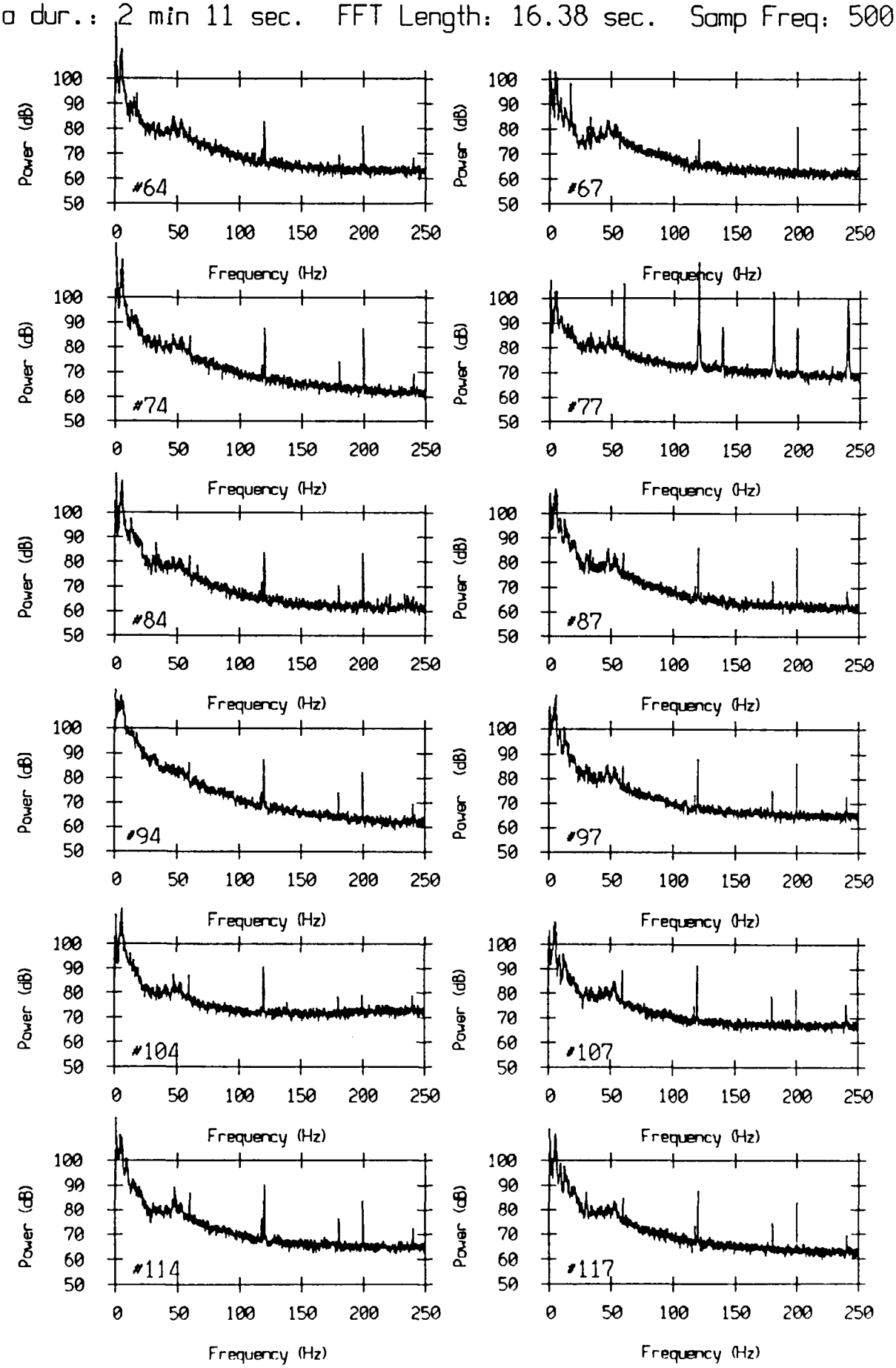

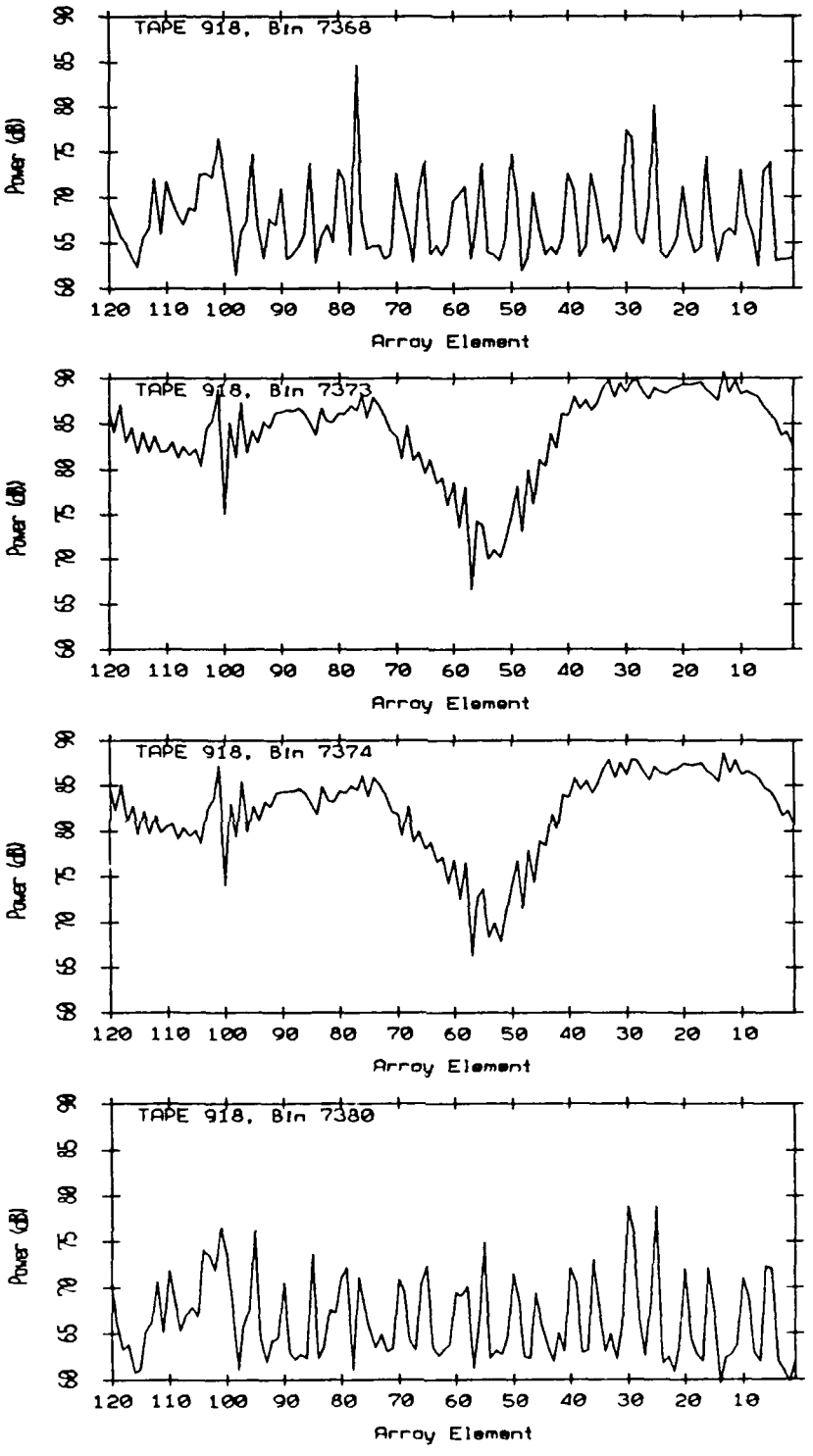
TAPE 918, Bin 7368
TAPE 918, Bin 7373
TAPE 918, Bin 7374
TAPE 918, Bin 7380
Power (dB)
60 65 70 75 80 85 90
120 110 100 90 80 70 60 50 40 30 20 10
Array Element

Tape 918 : Bin 7368

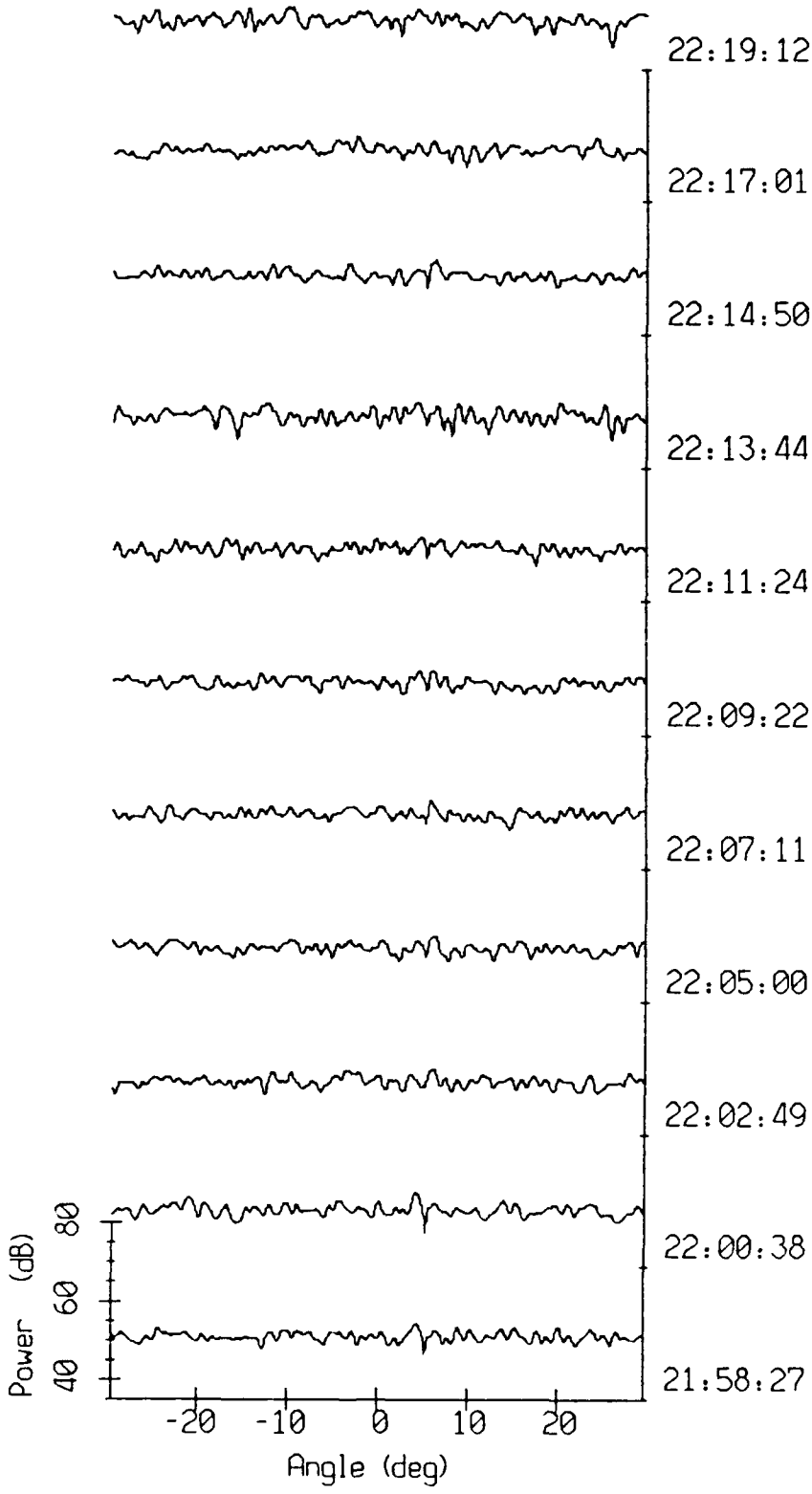

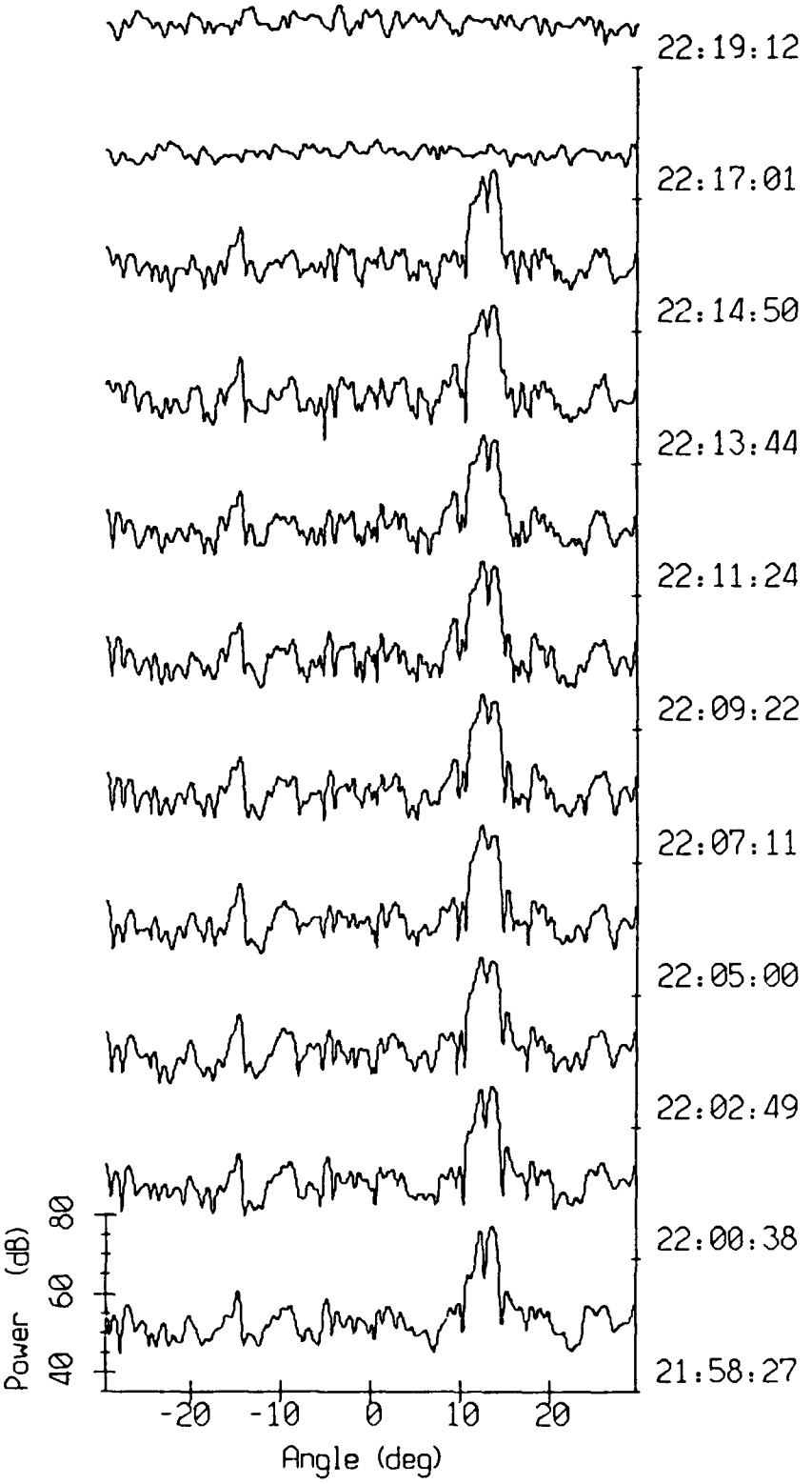
22:19:12
22:17:01
22:14:50
22:13:44
22:11:24
22:09:22
22:07:11
22:05:00
22:02:49
22:00:38
21:58:27
Power (dB)
40
60
80
-20
-10
0
10
20
Angle (deg)

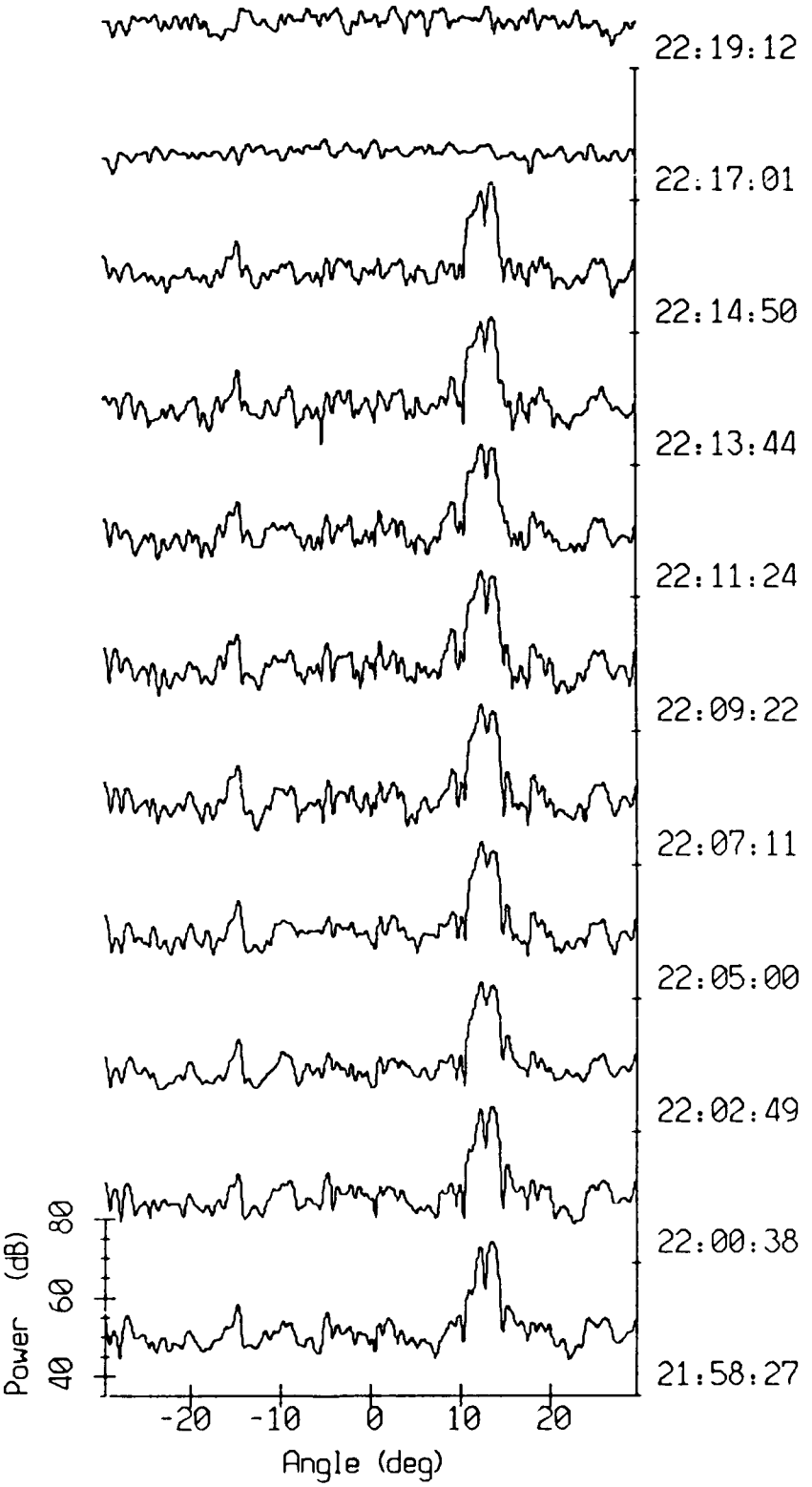
22:19:12
22:17:01
22:14:50
22:13:44
22:11:24
22:09:22
22:07:11
22:05:00
22:02:49
22:00:38
21:58:27
Power (dB)
40
60
80
-20
-10
0
10
20
Angle (deg)

Tape 918 : Bin 7380

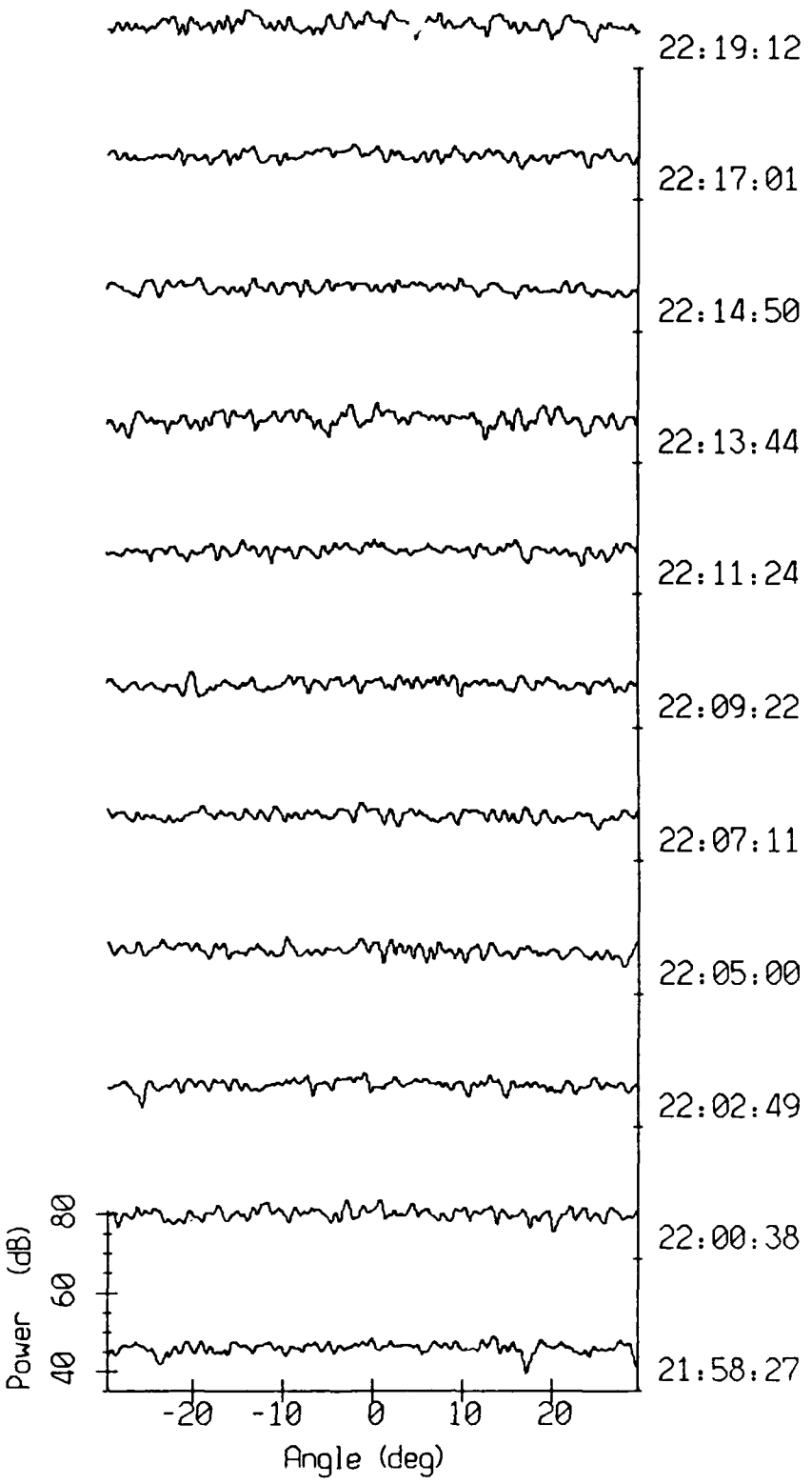

Appendix 2

VLA Tape 972, Sept, 1987 - Time 02:25:50 GMT Cal. Pressure Spectra 72
Data dur.: 2 min 11 sec. FFT Length: 16.38 sec. Samp Freq: 500 Hz

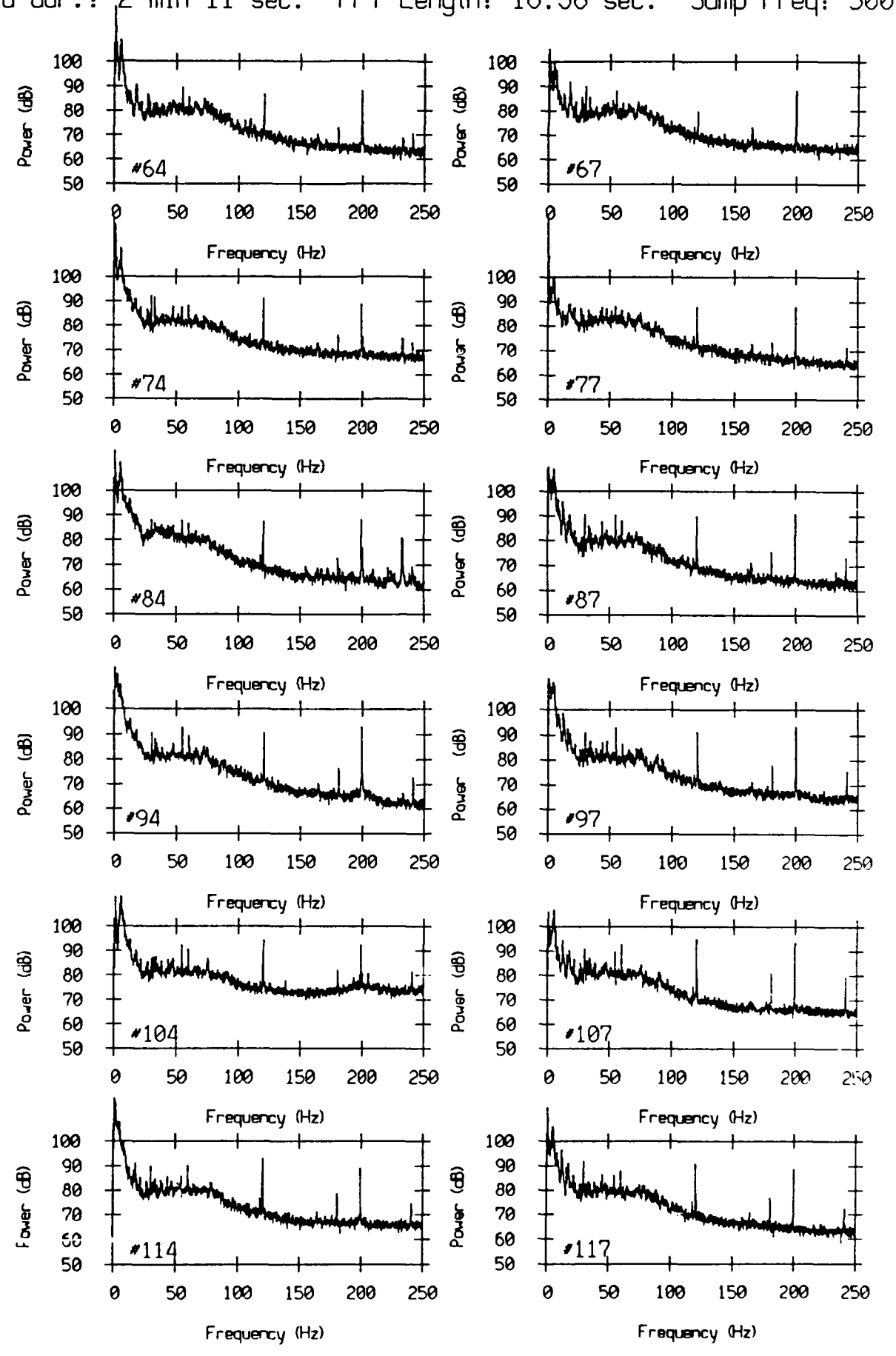

VLA Tape 972, Sept, 1987 - Time 02:25:50 GMT Cal. Pressure Spectra 73
Data dur.: 2 min 11 sec. FFT Length: 16.38 sec. Samp Freq: 500 Hz

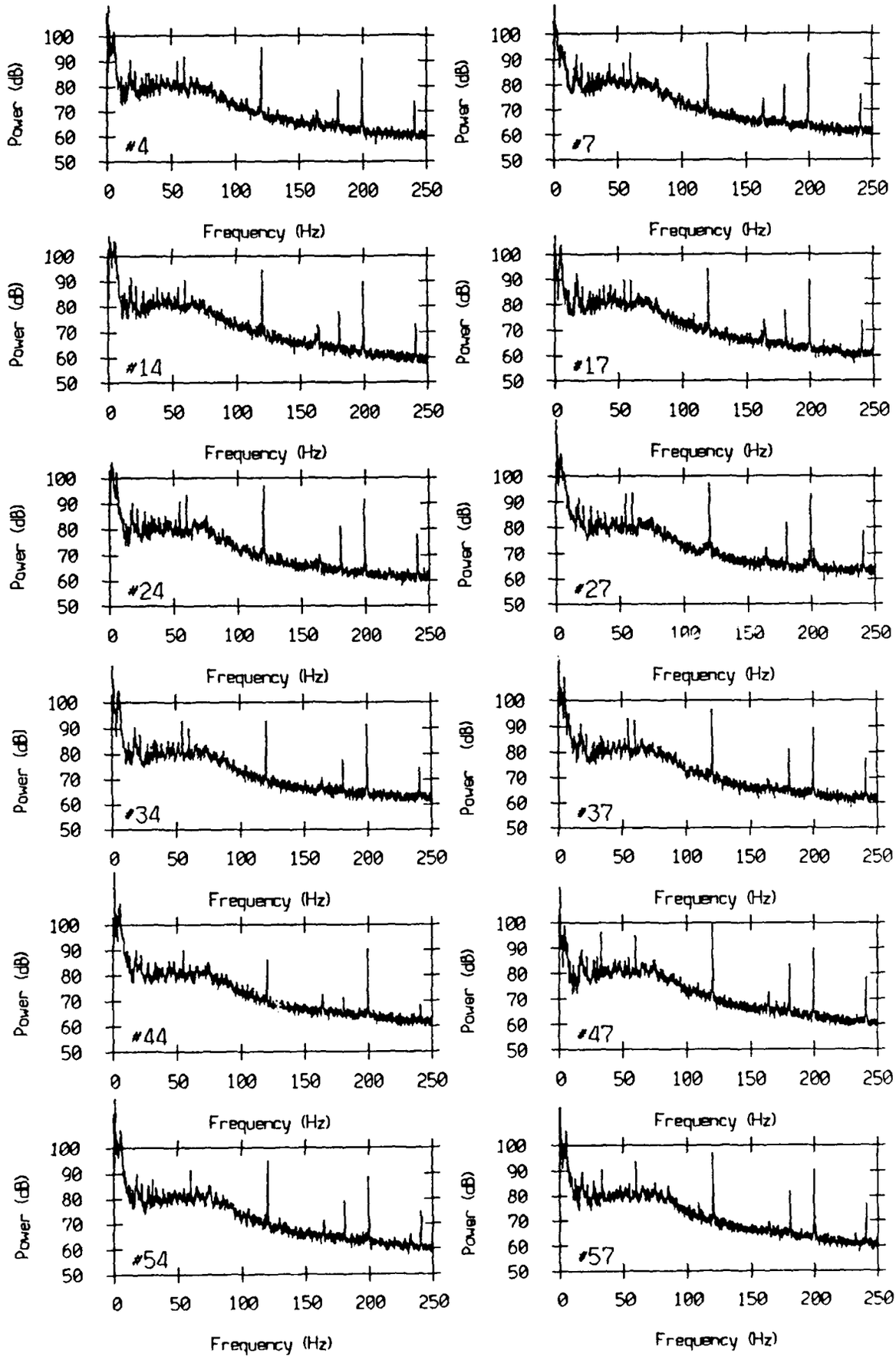

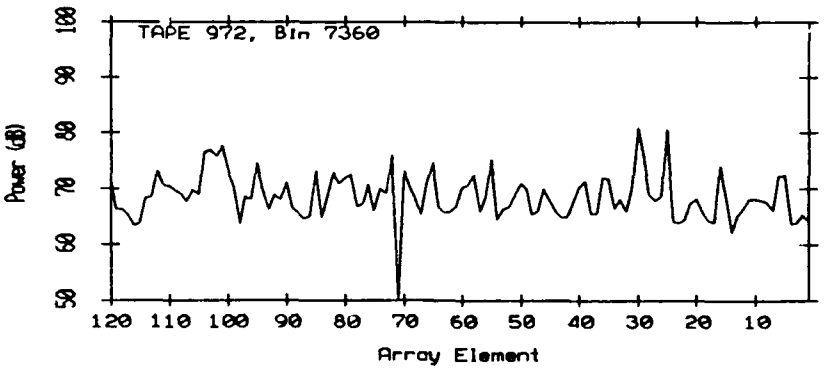
TAPE 972, Bin 7360
Power (dB)
100
90
80
70
60
50
120 110 100 90 80 70 60 50 40 30 20 10
Array Element

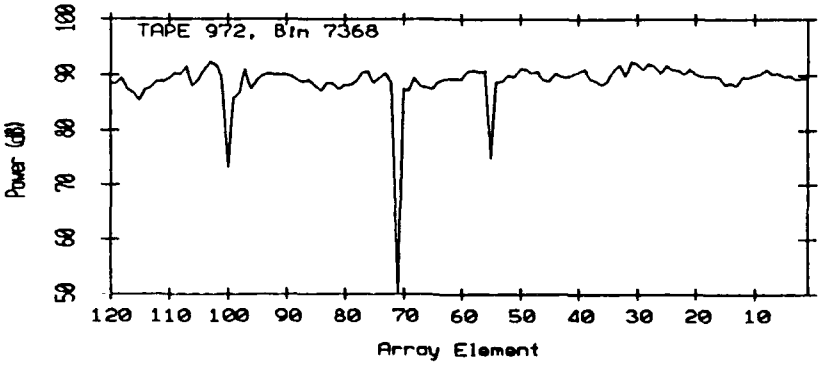
TAPE 972, Bin 7368
Power (dB)
100
90
80
70
60
50
120 110 100 90 80 70 60 50 40 30 20 10
Array Element


TAPE 972, Bin 7369
Power (dB)
100
90
80
70
60
50
120 110 100 90 80 70 60 50 40 30 20 10
Array Element

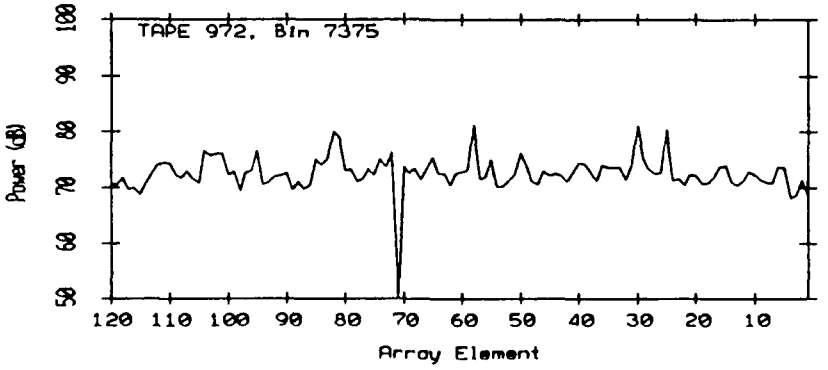
TAPE 972, Bin 7375
Power (dB)
100
90
80
70
60
50
120 110 100 90 80 70 60 50 40 30 20 10
Array Element

Tape 972 : Bin 7360

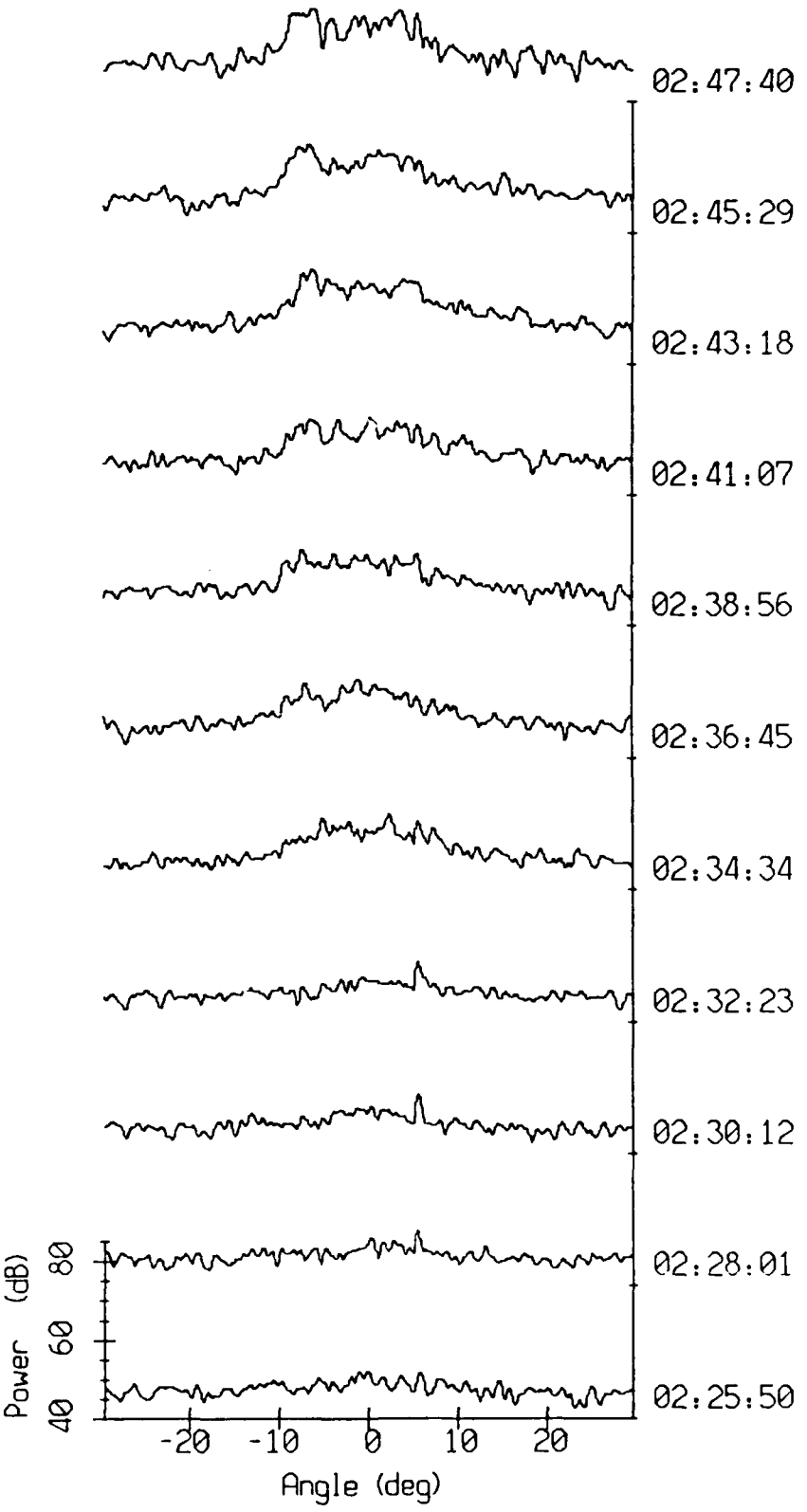

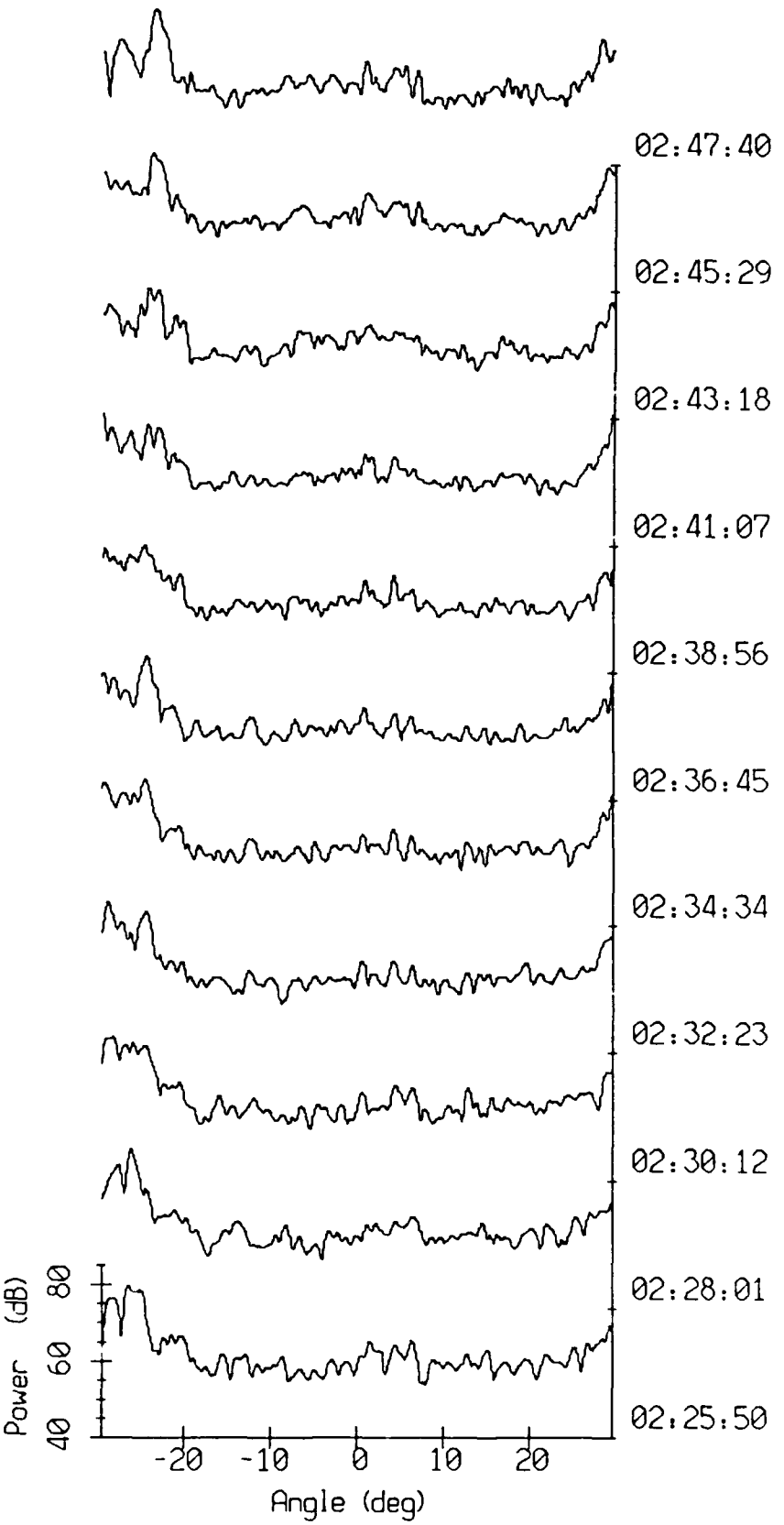
Tape 972 : Bin 7368
02:47:40
02:45:29
02:43:18
02:41:07
02:38:56
02:36:45
02:34:34
02:32:23
02:30:12
02:28:01
02:25:50
Power (dB)
40
60
80
-20
-10
0
10
20
Angle (deg)

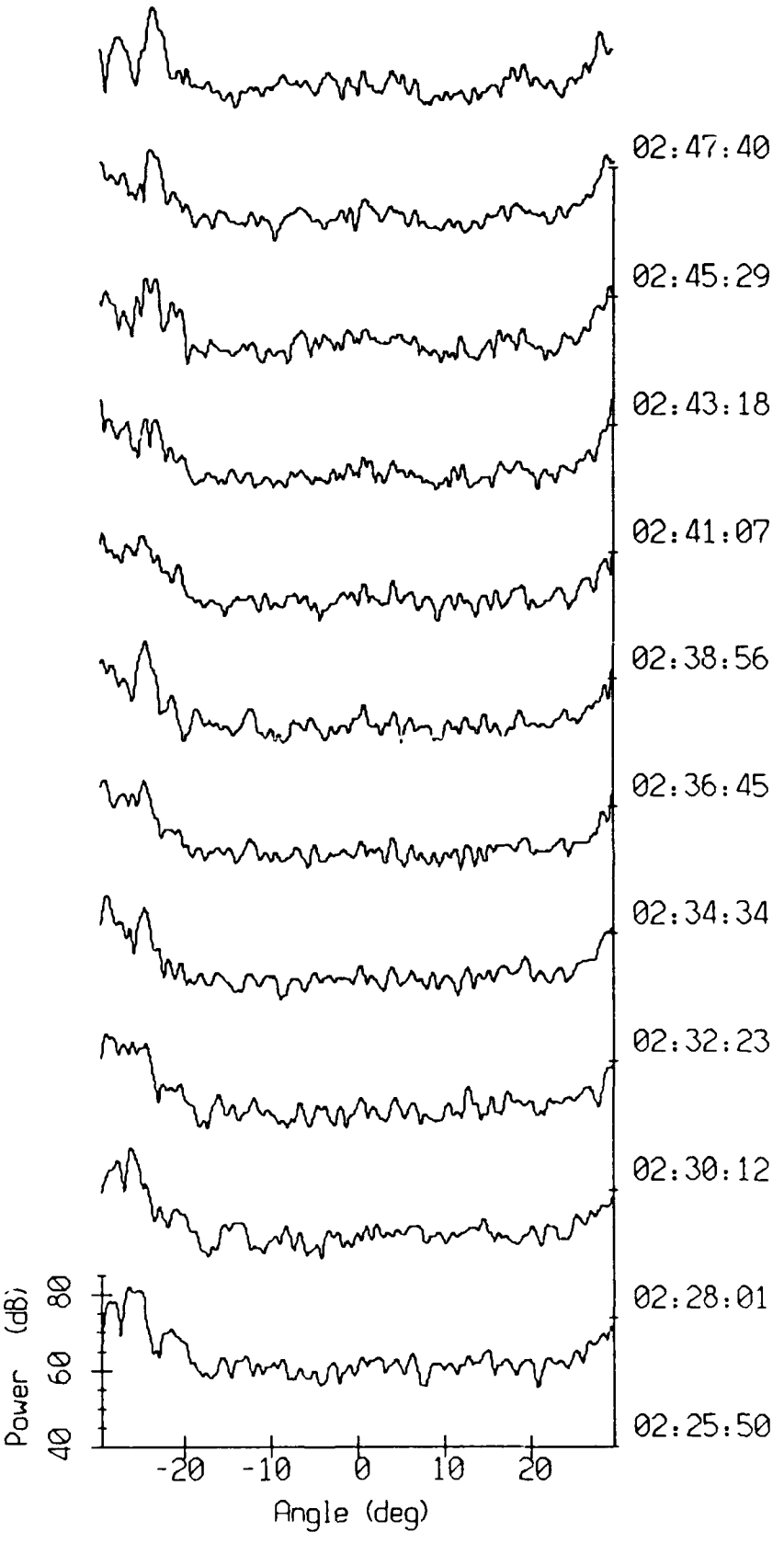
Tape 972 : Bin 7369
02:47:40
02:45:29
02:43:18
02:41:07
02:38:56
02:36:45
02:34:34
02:32:23
02:30:12
02:28:01
02:25:50
Power (dB)
40
60
80
-20
-10
0
10
20
Angle (deg)

Tape 972 : Bin 7375

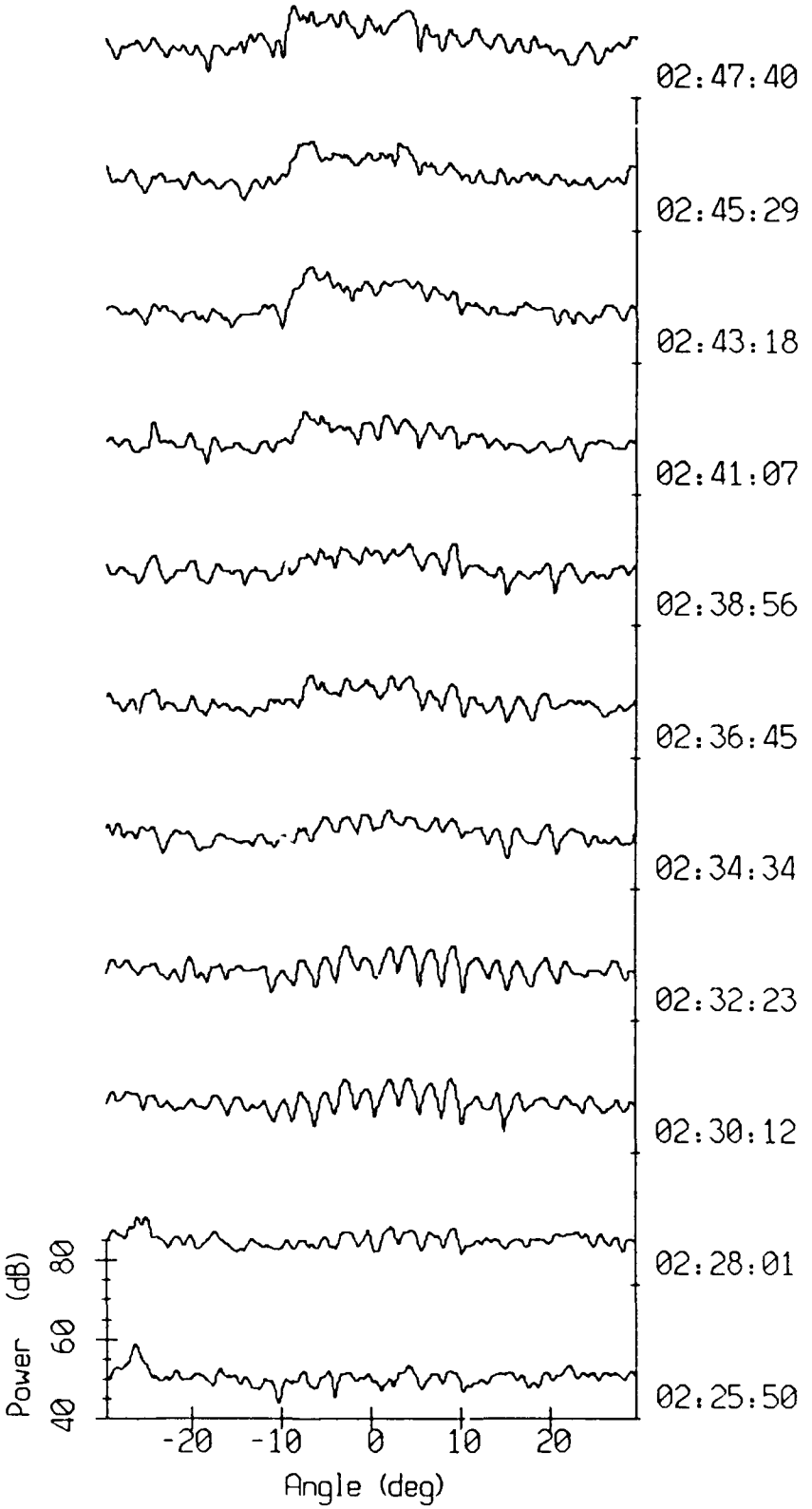

VLA Tape 980, Sept, 1987 - Time 05:33:32 GMT Cal. Pressure Spectra 79
Data dur.: 2 min 11 sec. FFT Length: 16.38 sec. Samp Freq: 500 Hz

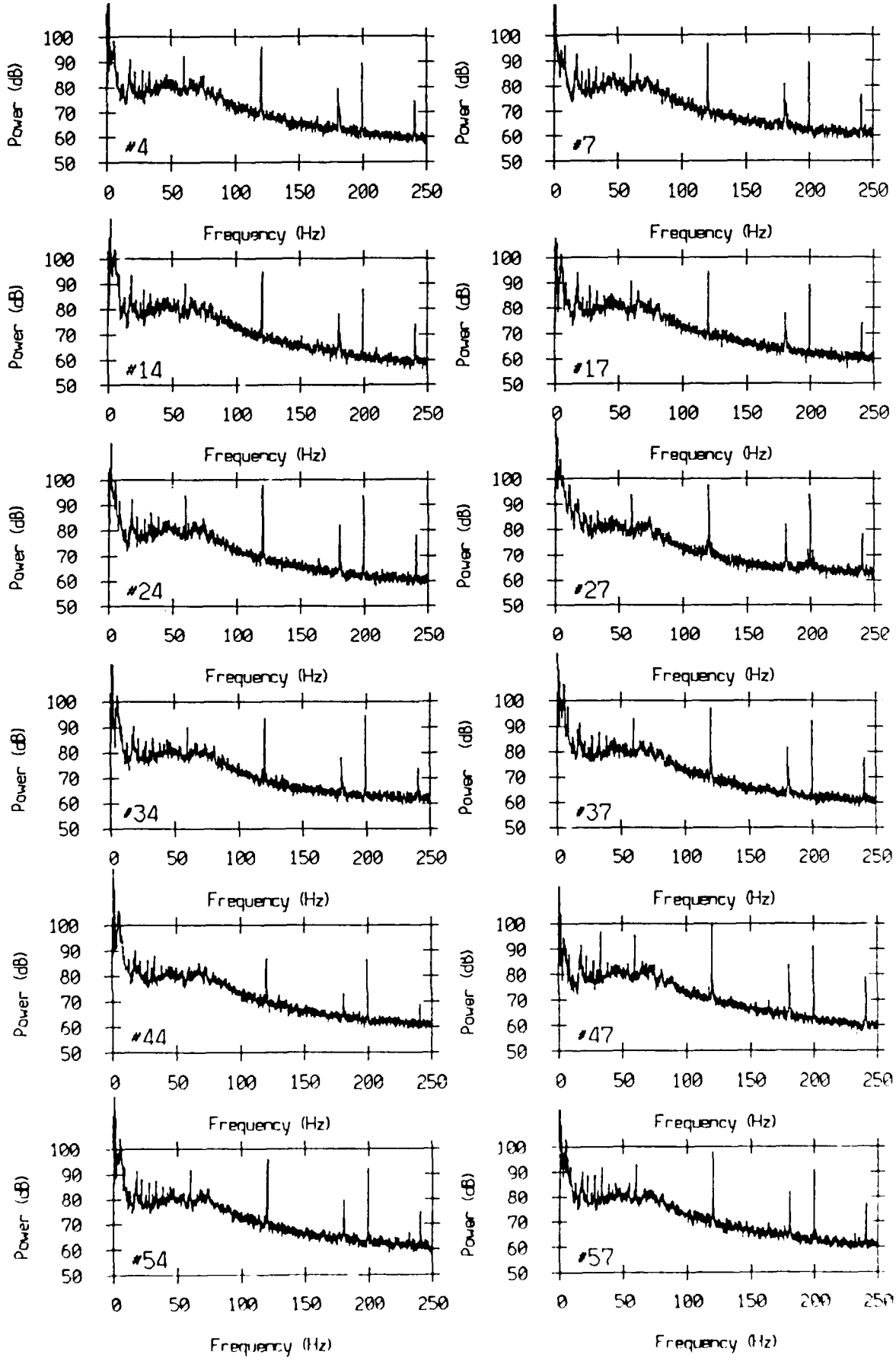

VLA Tape 980, Sept, 1987 - Time 05:33:32 GMT Cal. Pressure Spectra 8(
Data dur.: 2 min 11 sec. FFT Length: 16.38 sec. Samp Freq: 500 Hz

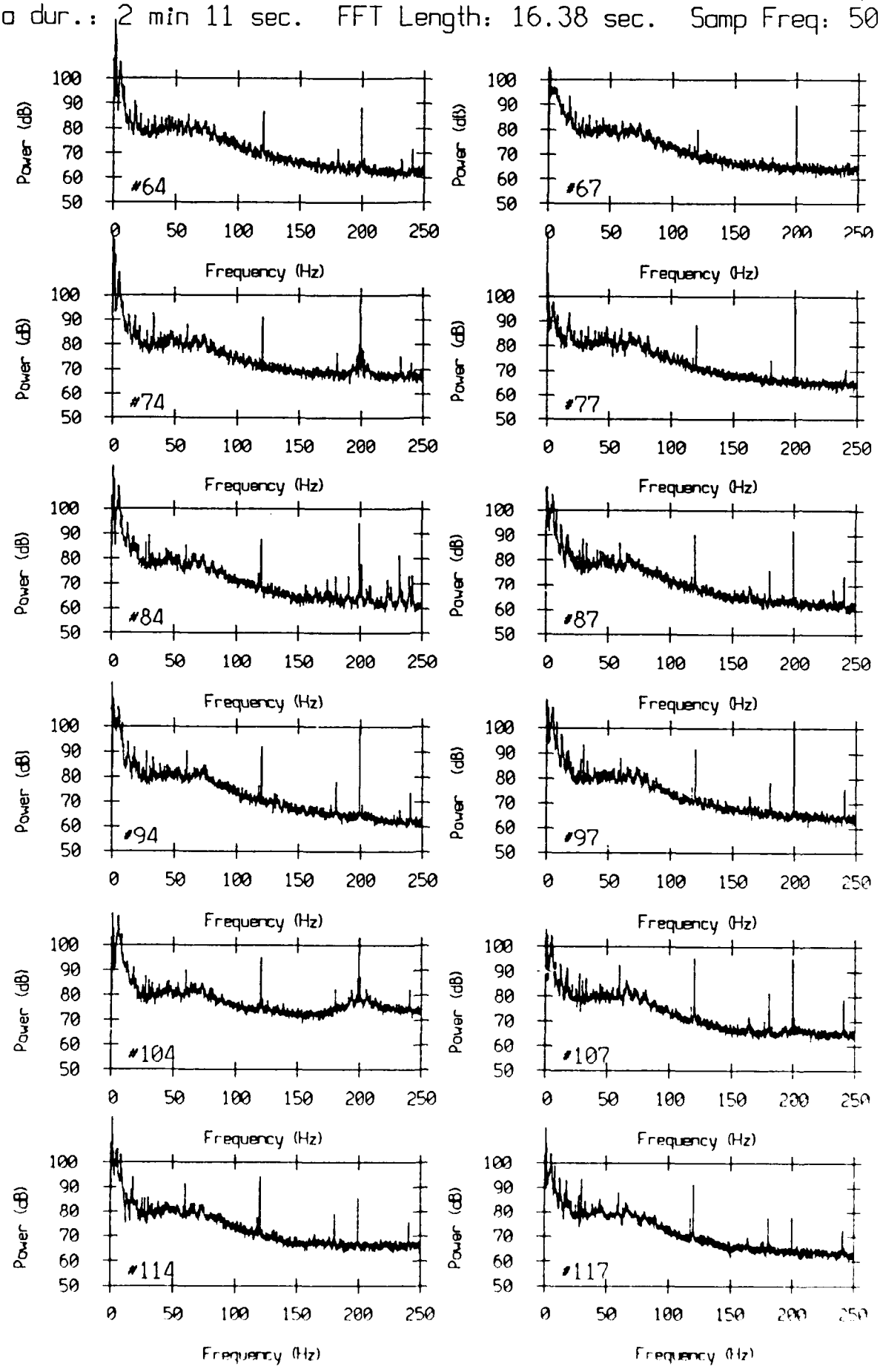

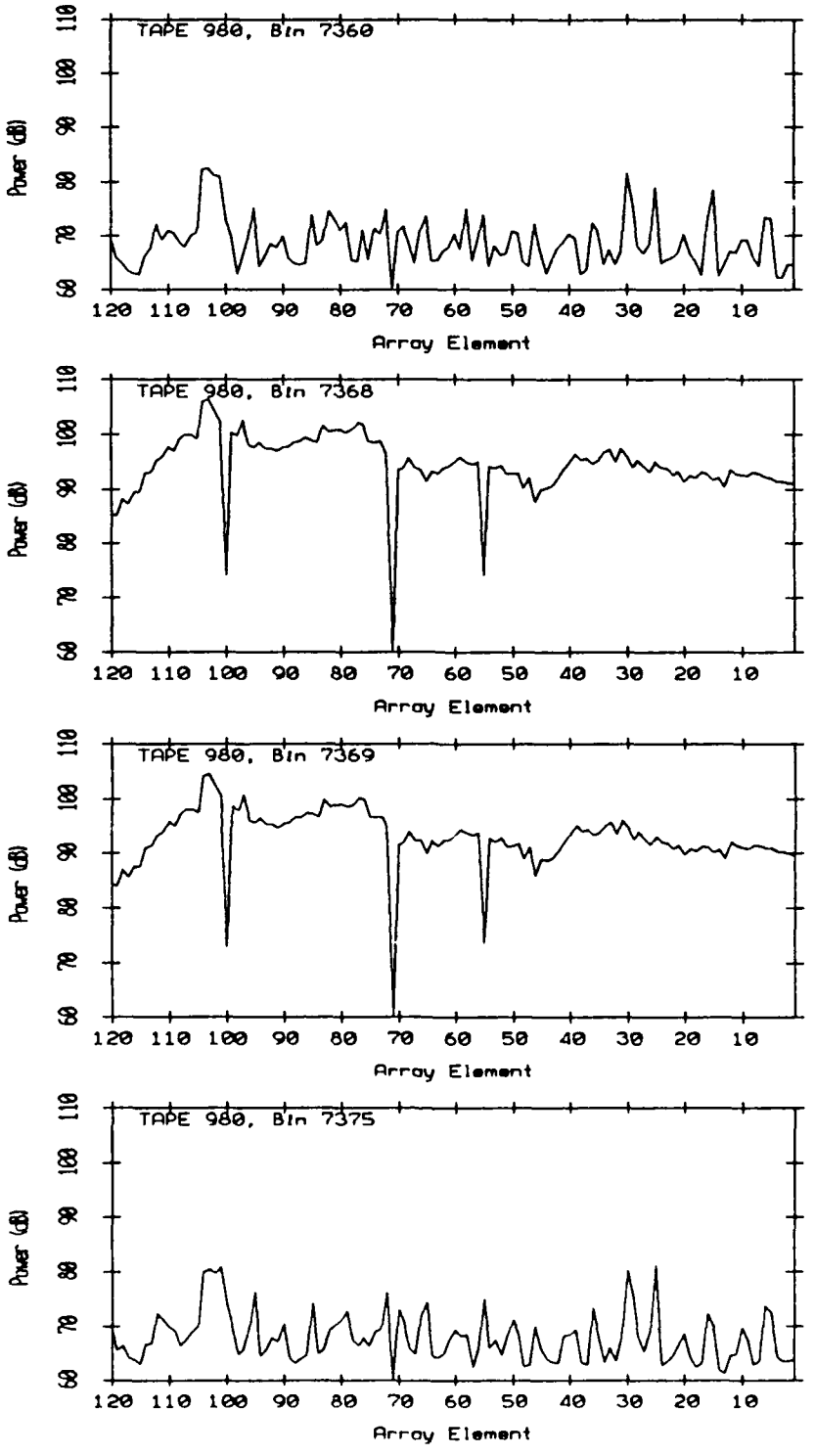
TAPE 980, Bin 7360
TAPE 980, Bin 7368
TAPE 980, Bin 7369
TAPE 980, Bin 7375
Power (dB)
Array Element
120 110 100 90 80 70 60 50 40 30 20 10
60 70 80 90 100 110

Tape 980 : Bin 7360

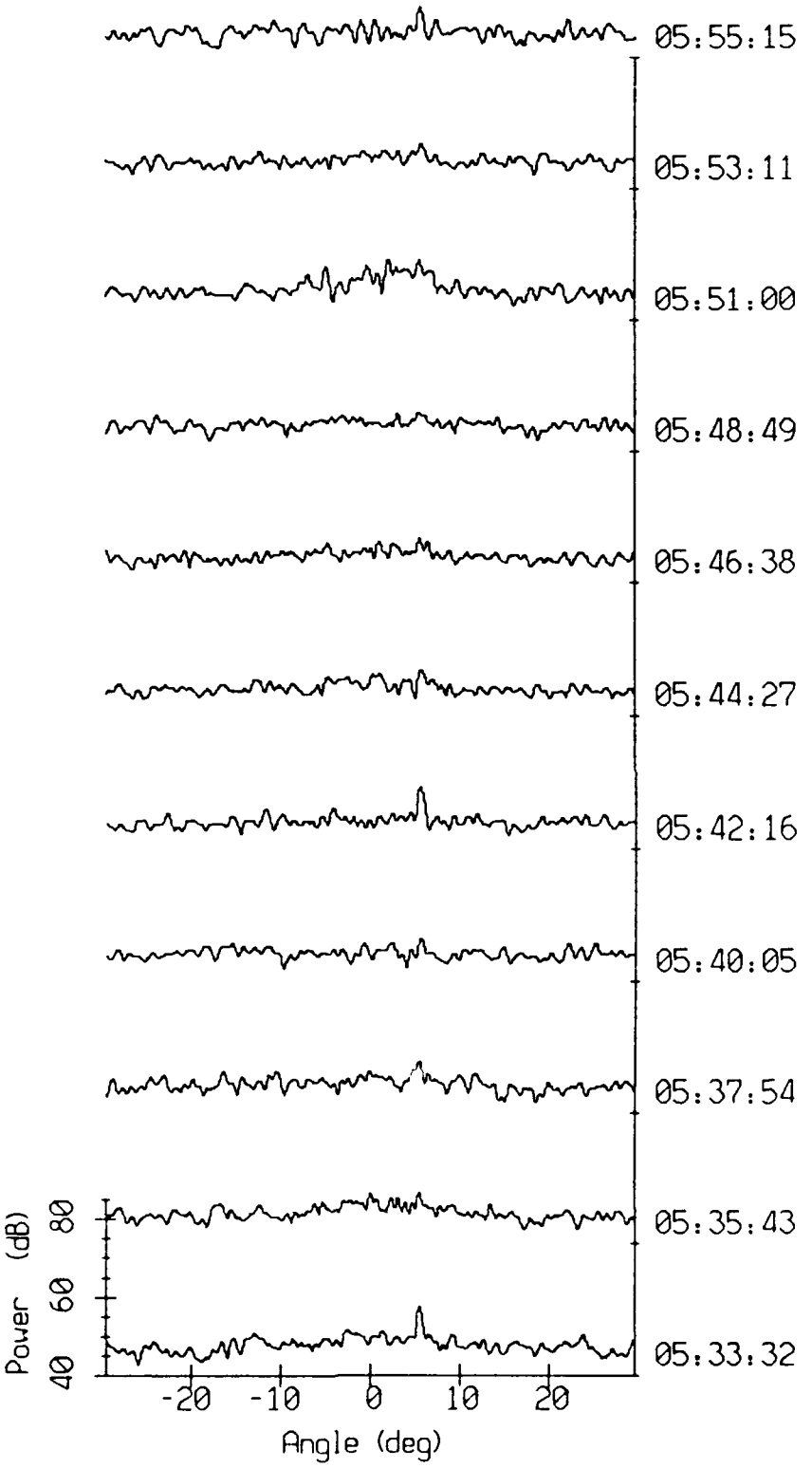

Tape 980 : Bin 7368

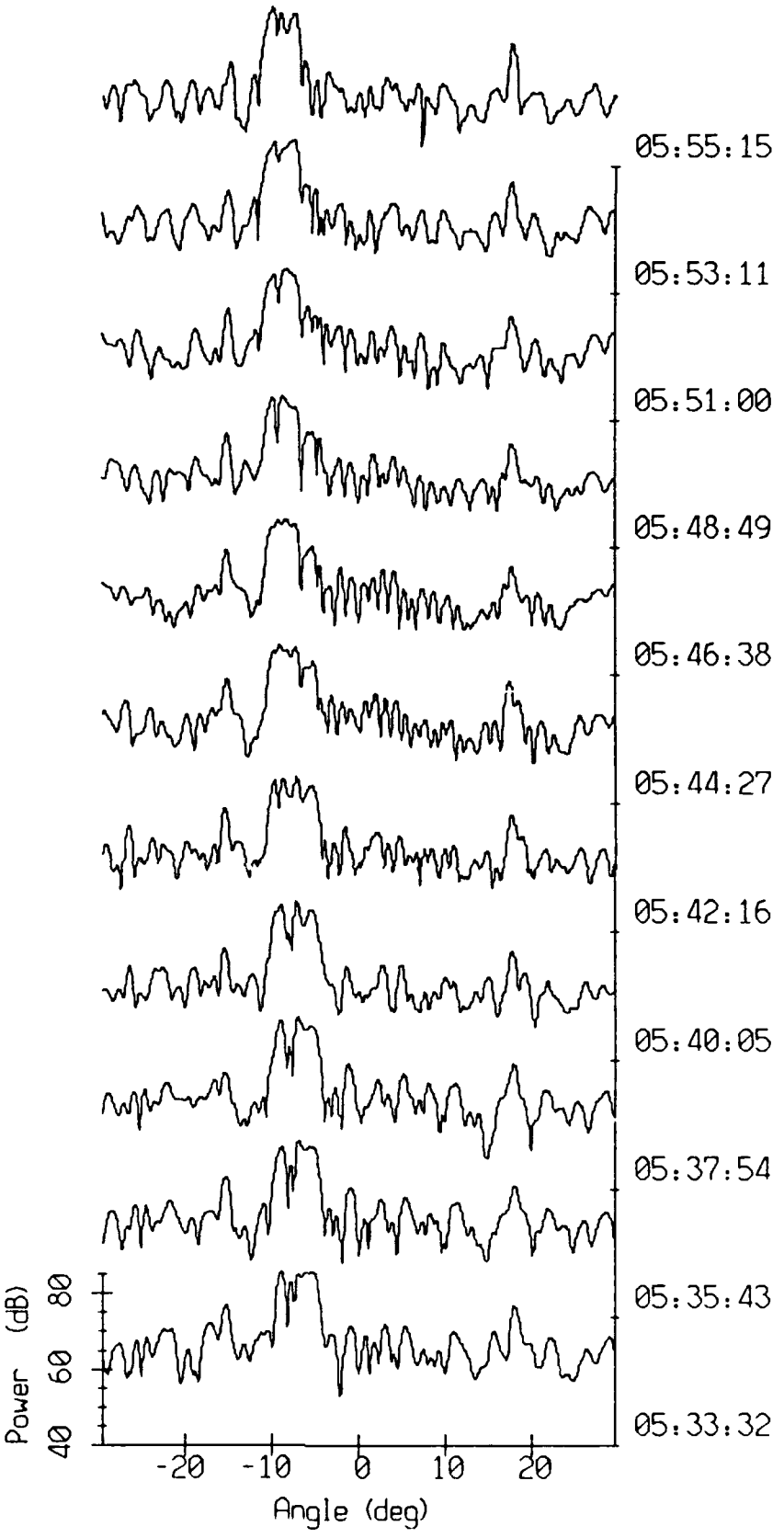

Tape 980 : Bin 7369

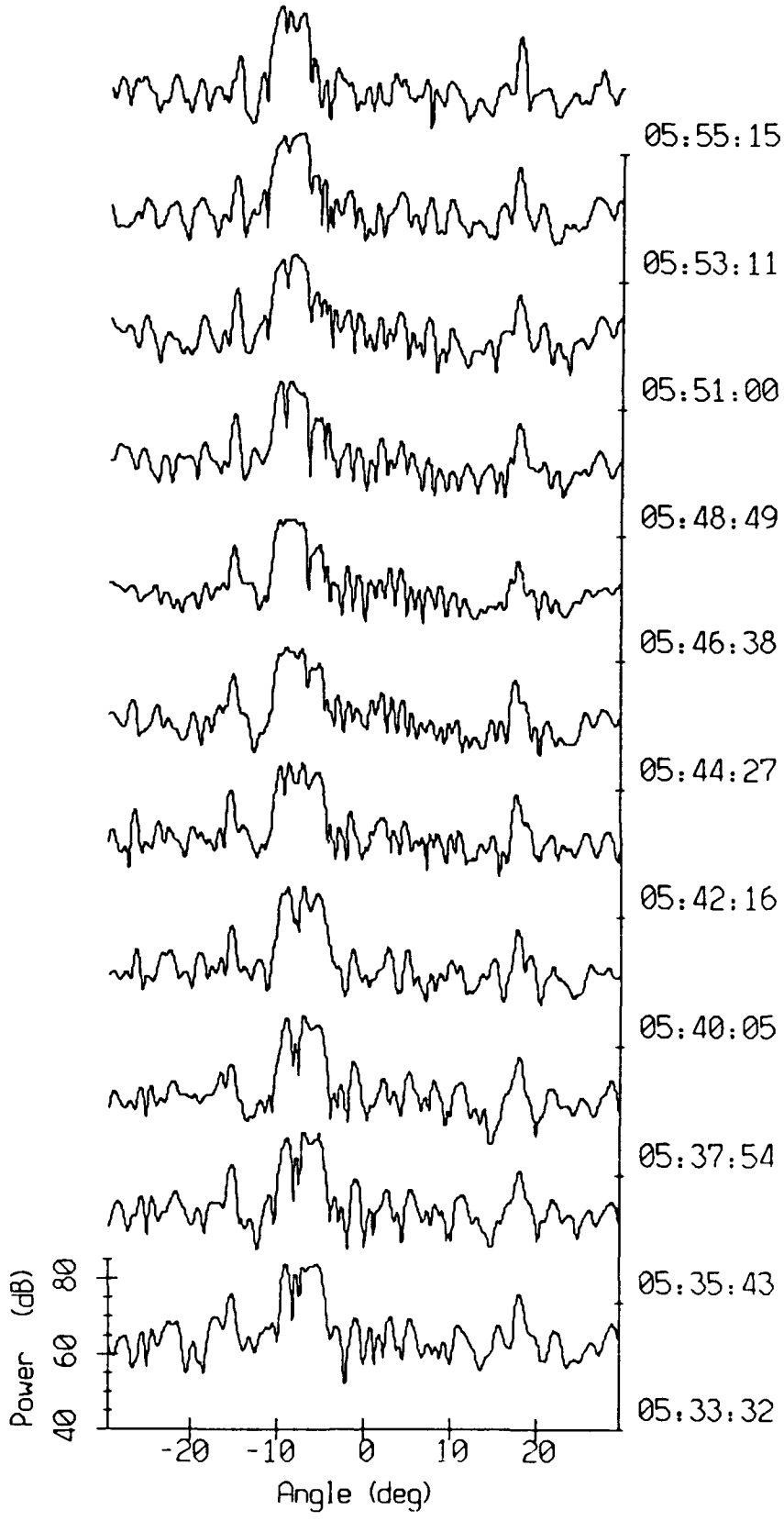

Tape 980 : Bin 7375

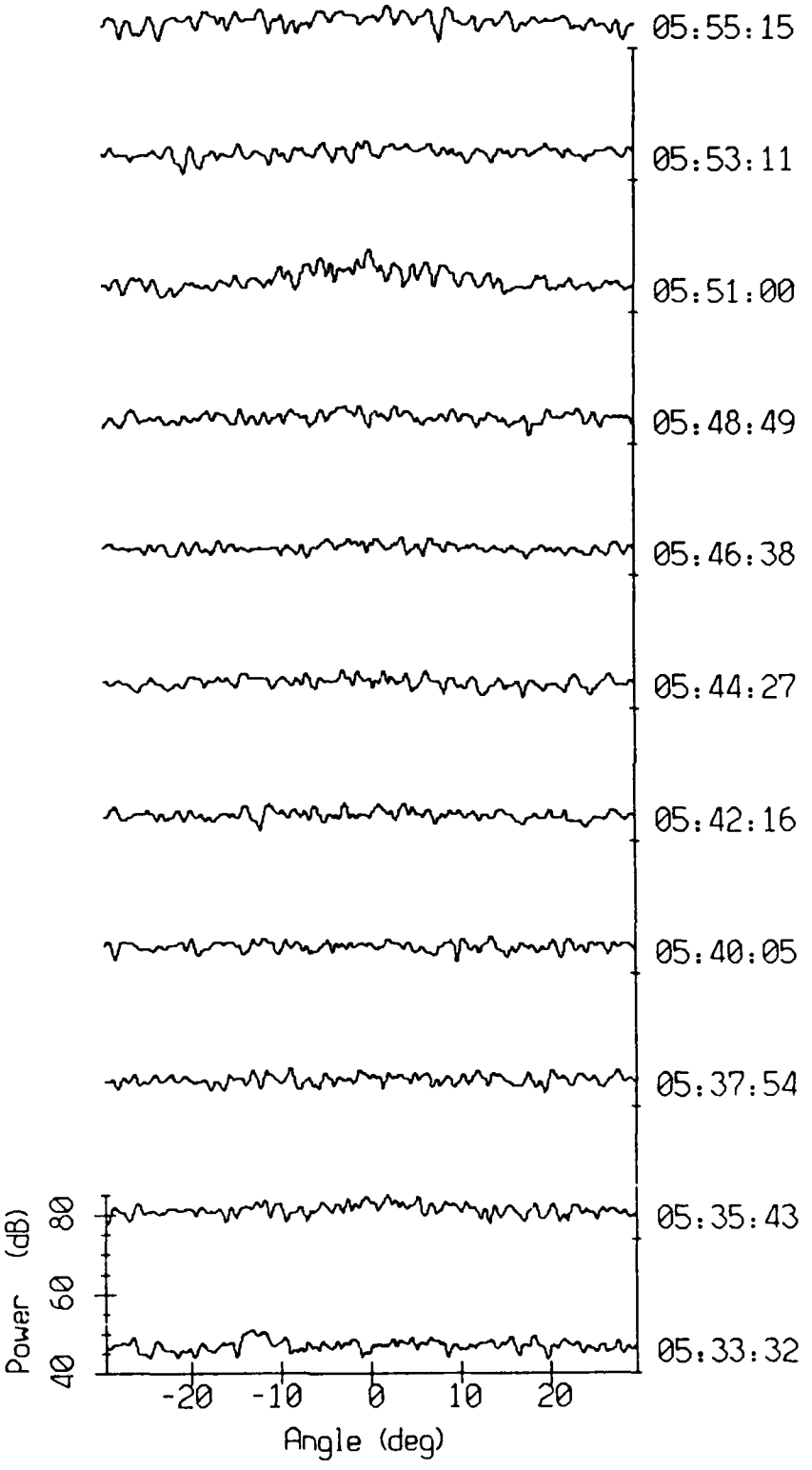

VLA Tape 981, Sept, 1987 - Time 06:16:39 GMT Cal. Pressure Spectra
Data dur.: 2 min 11 sec. FFT Length: 16.38 sec. Samp Freq: 500 Hz

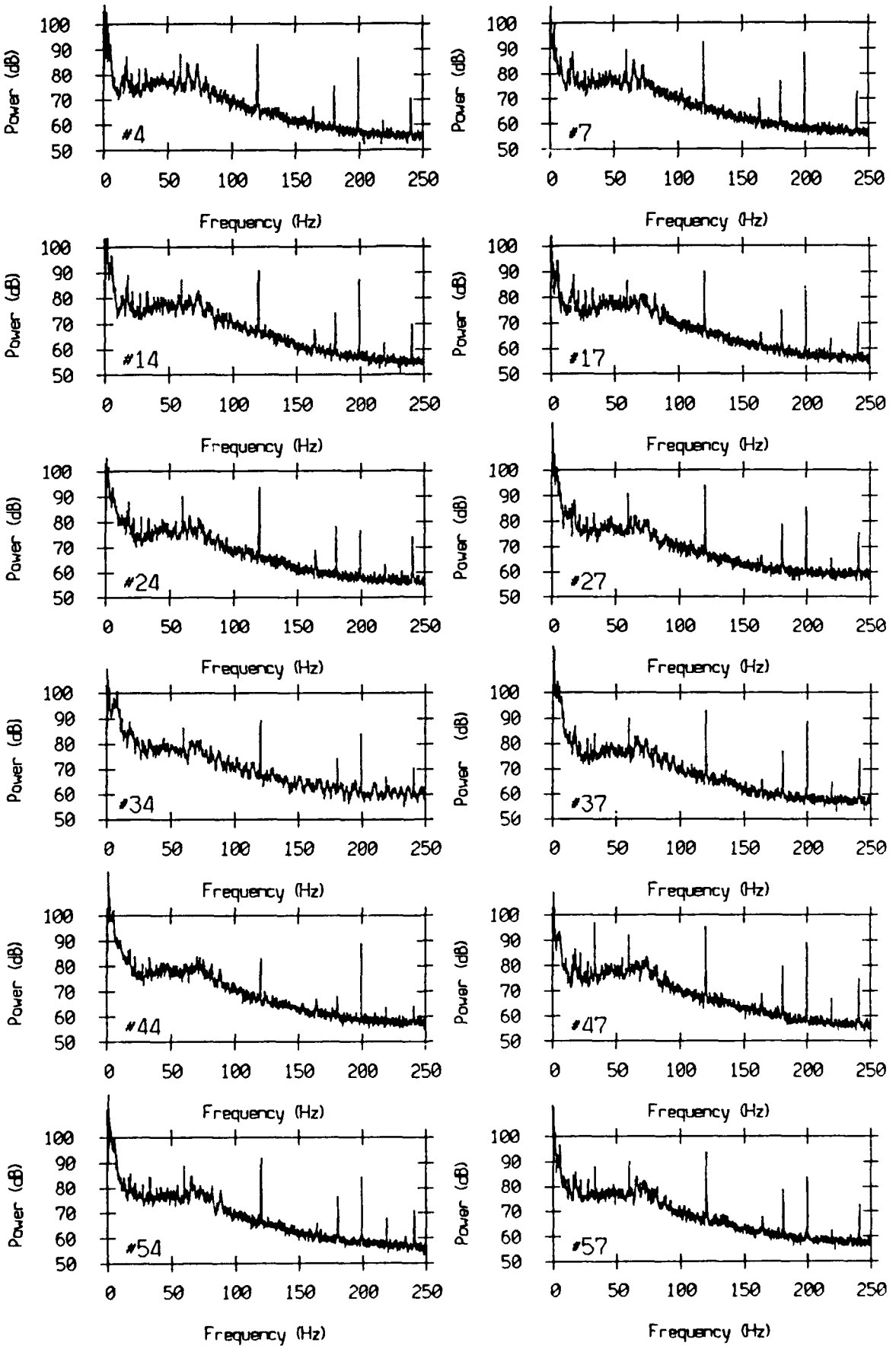

VLA Tape 981, Sept, 1987 - Time 06:16:39 GMT Cal. Pressure Spectra
Data dur.: 2 min 11 sec. FFT Length: 16.38 sec. Samp Freq: 500 Hz

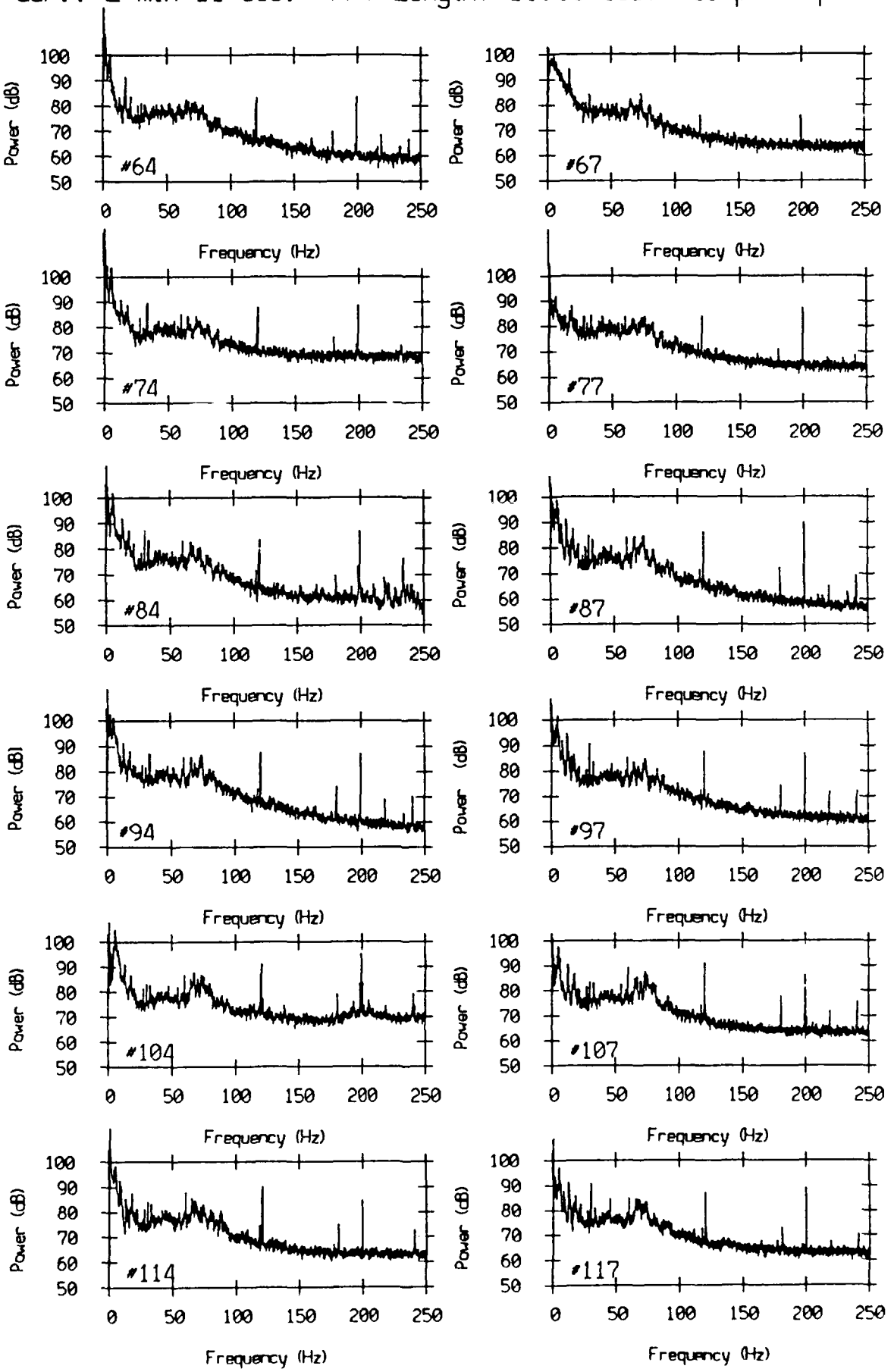


TAPE 981, Bin 7360
Power (dB)
100
90
80
70
60
50
120 110 100 90 80 70 60 50 40 30 20 10
Array Element


TAPE 981, Bin 7368
Power (dB)
100
90
80
70
60
50
120 110 100 90 80 70 60 50 40 30 20 10
Array Element


TAPE 981, Bin 7369
Power (dB)
100
90
80
70
60
50
120 110 100 90 80 70 60 50 40 30 20 10
Array Element

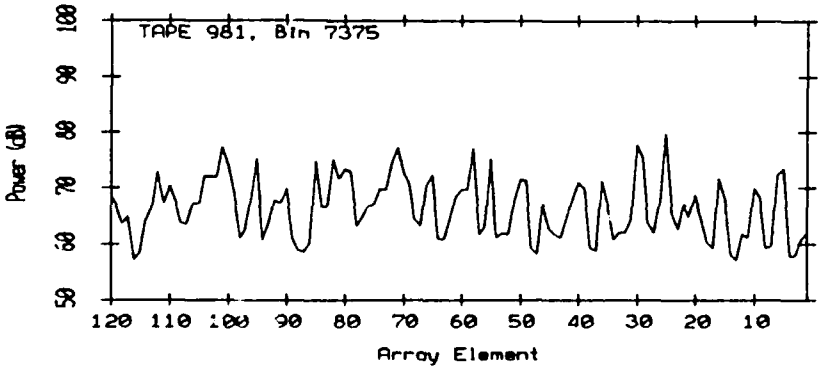
TAPE 981, Bin 7375
Power (dB)
100
90
80
70
60
50
120 110 100 90 80 70 60 50 40 30 20 10
Array Element

Tape 981 : Bin 7360

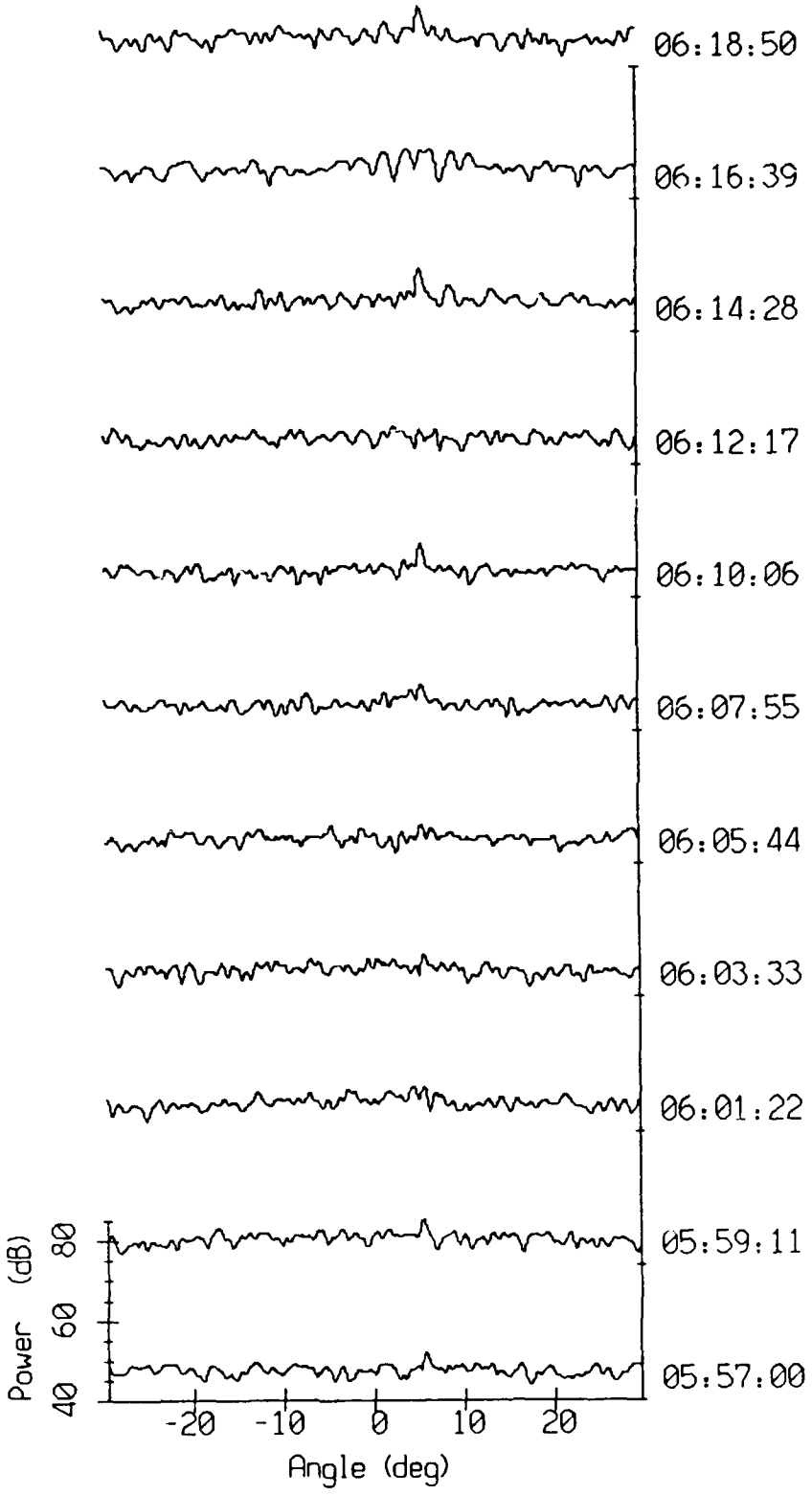

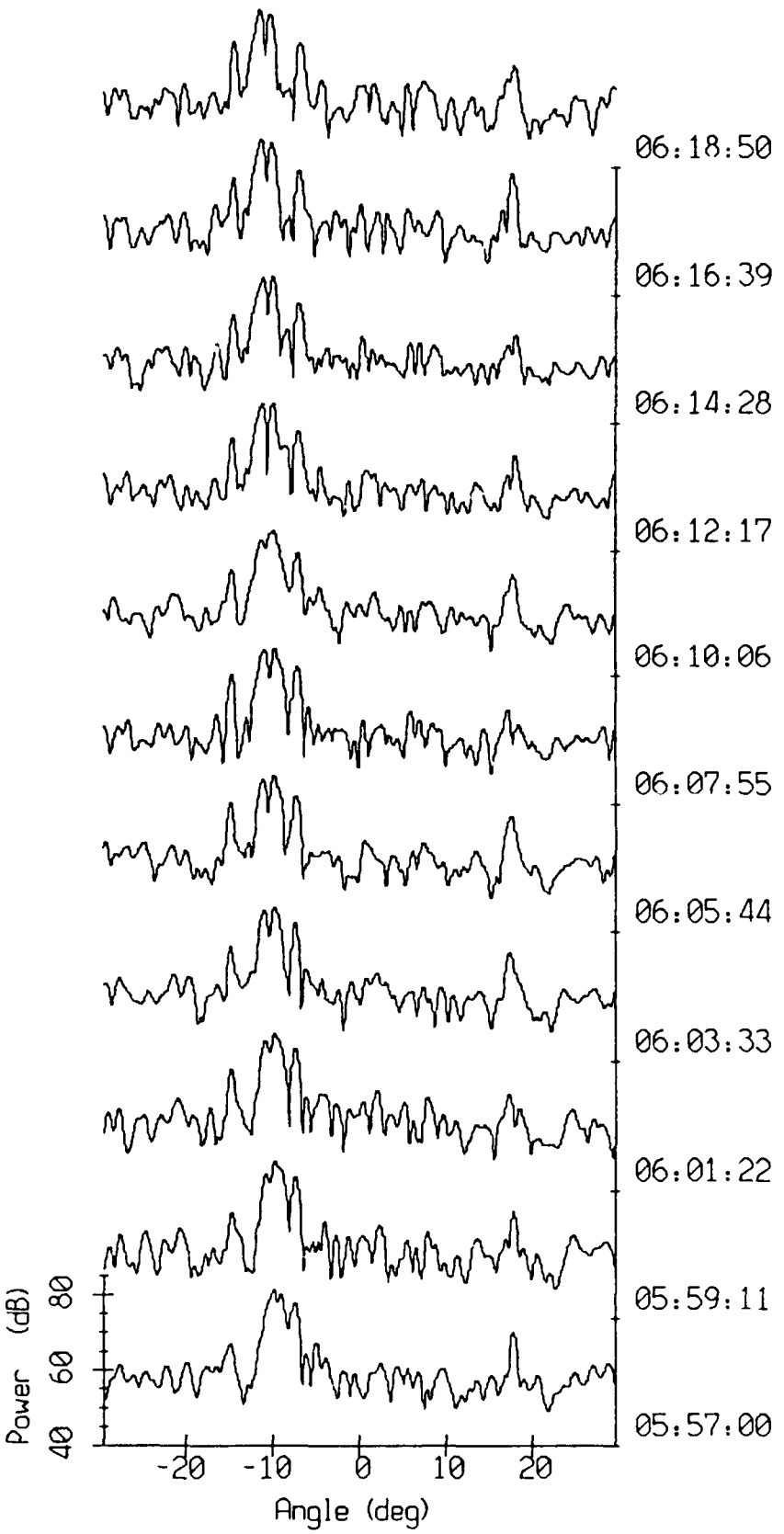
Tape 981 : Bin 7368
06:18:50
06:16:39
06:14:28
06:12:17
06:10:06
06:07:55
06:05:44
06:03:33
06:01:22
05:59:11
05:57:00
Power (dB)
40
60
80
-20
-10
0
10
20
Angle (deg)

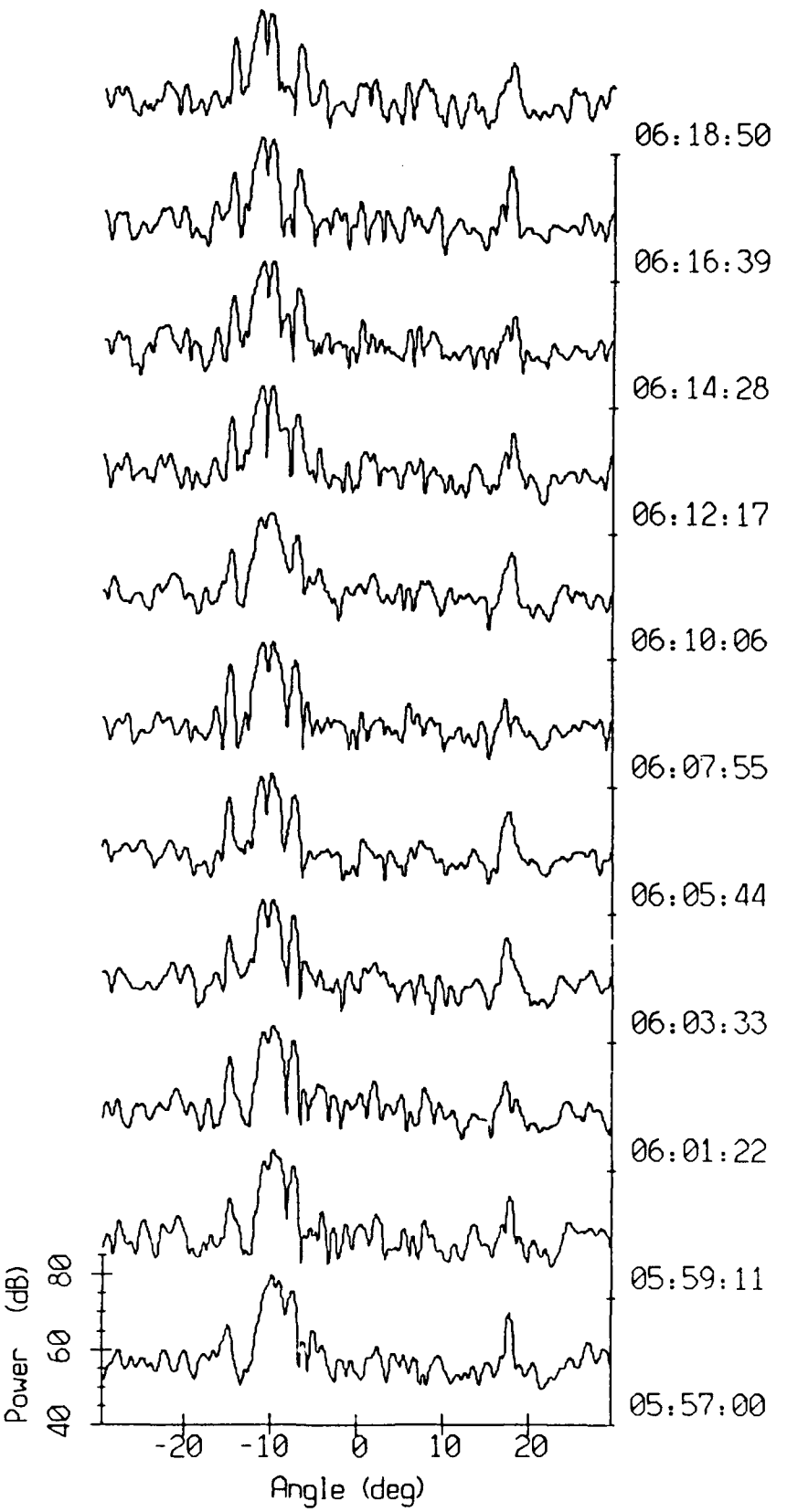
Tape 981 : Bin 7369
06:18:50
06:16:39
06:14:28
06:12:17
06:10:06
06:07:55
06:05:44
06:03:33
06:01:22
05:59:11
05:57:00
Power (dB)
40
60
80
-20
-10
0
10
20
Angle (deg)

Tape 981 : Bin 7375

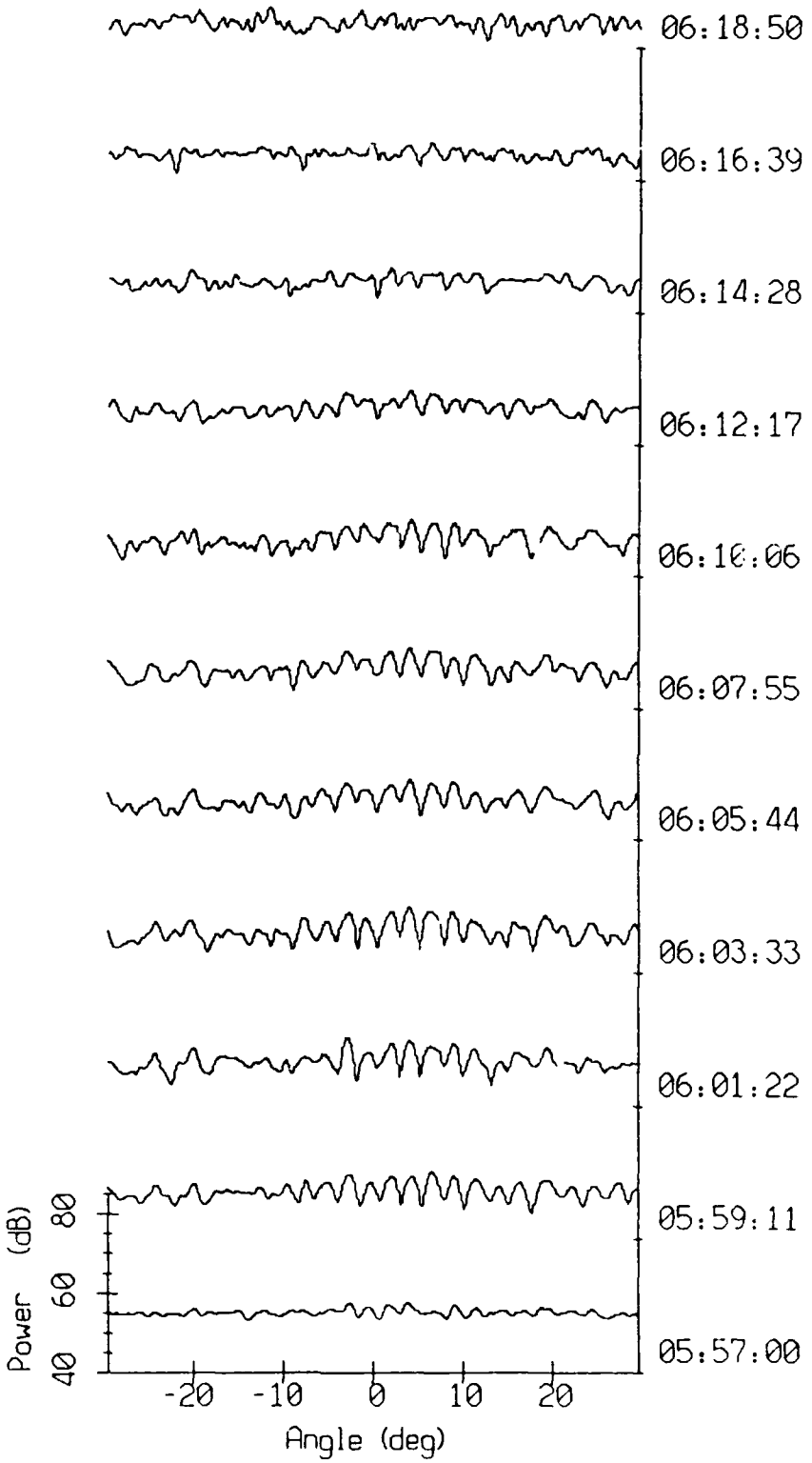

VLA Tape 983, Sept, 1987 - Time 06:48:17 GMT Cal. Pressure Spectra
Data dur.: 2 min 11 sec. FFT Length: 16.38 sec. Samp Freq: 500 Hz

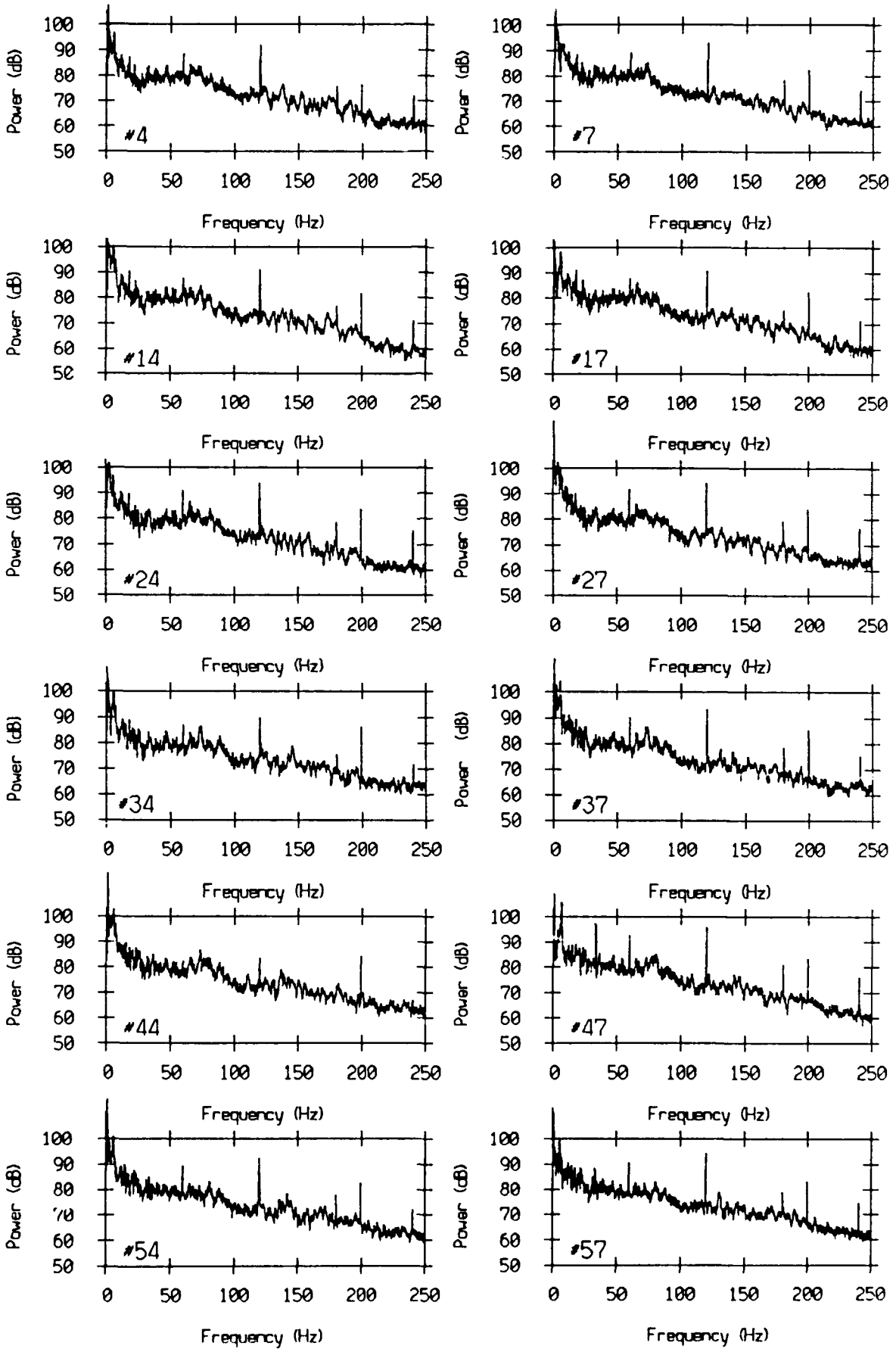

VLA Tape 983, Sept, 1987 - Time 06:48:17 GMT Cal. Pressure Spectra
Data dur.: 2 min 11 sec. FFT Length: 16.38 sec. Samp Freq: 500 Hz

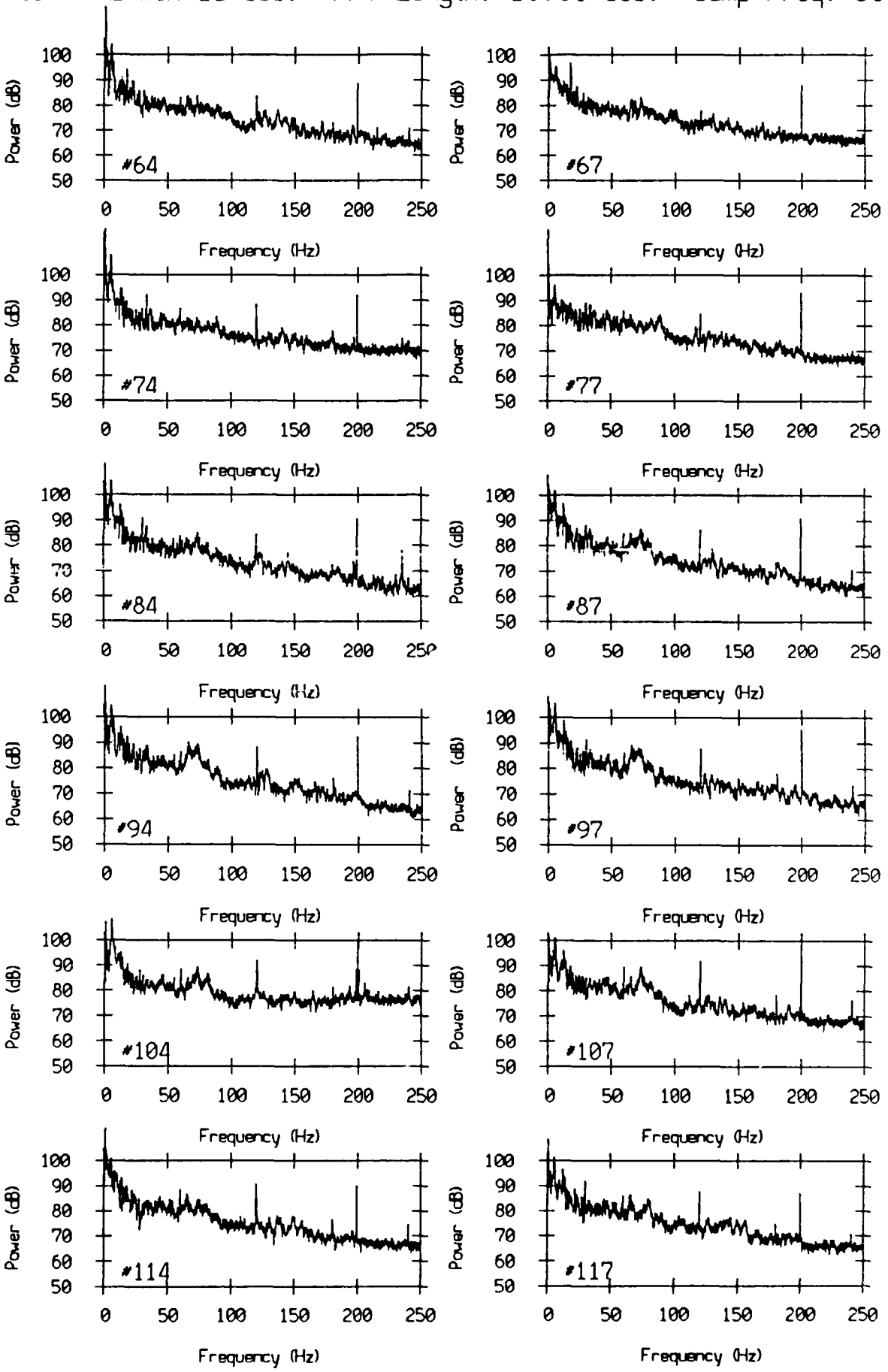

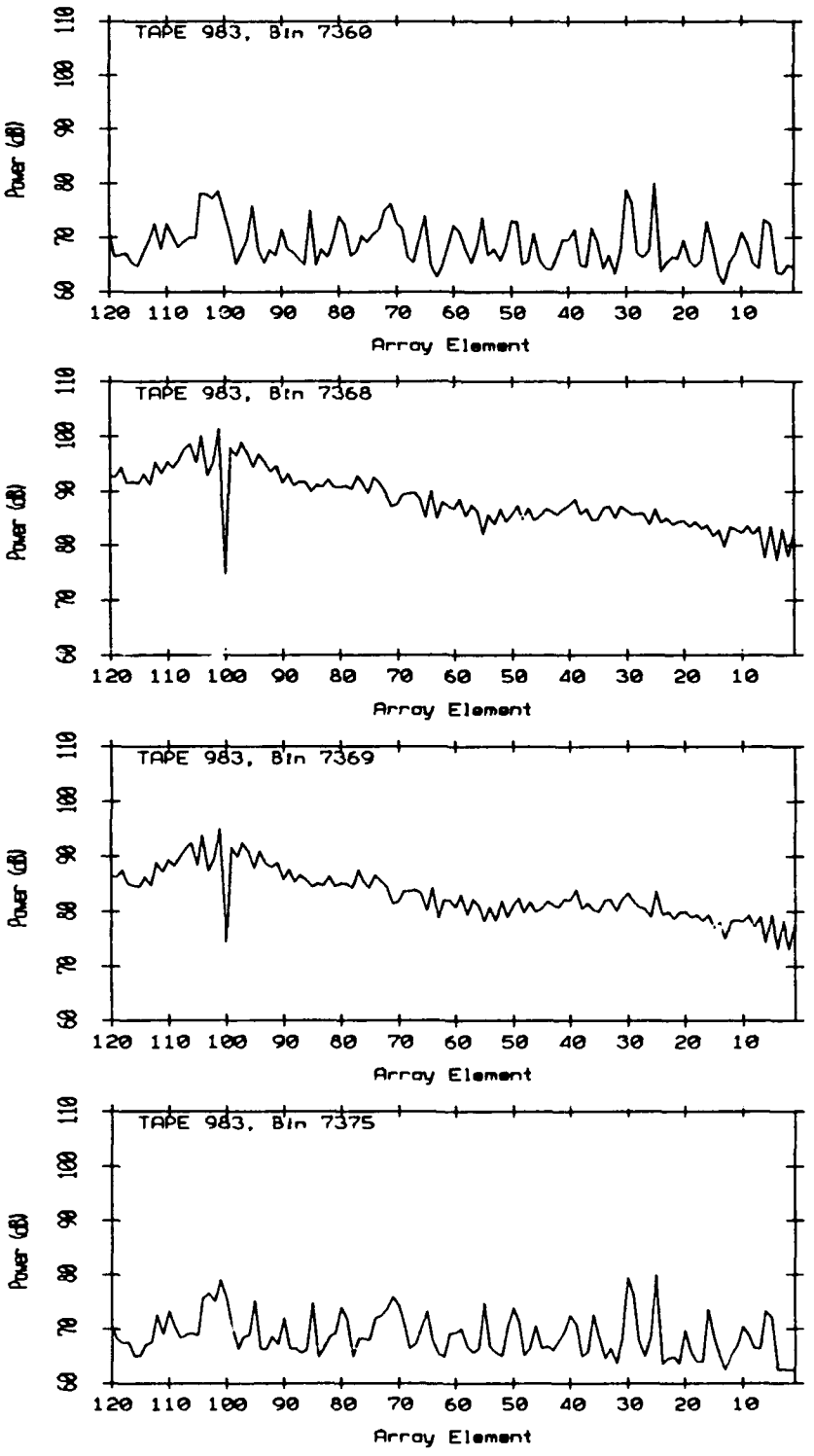
TAPE 983, Bin 7360
TAPE 983, Bin 7368
TAPE 983, Bin 7369
TAPE 983, Bin 7375
Power (dB)
Array Element
110
100
90
80
70
60
120 110 100 90 80 70 60 50 40 30 20 10

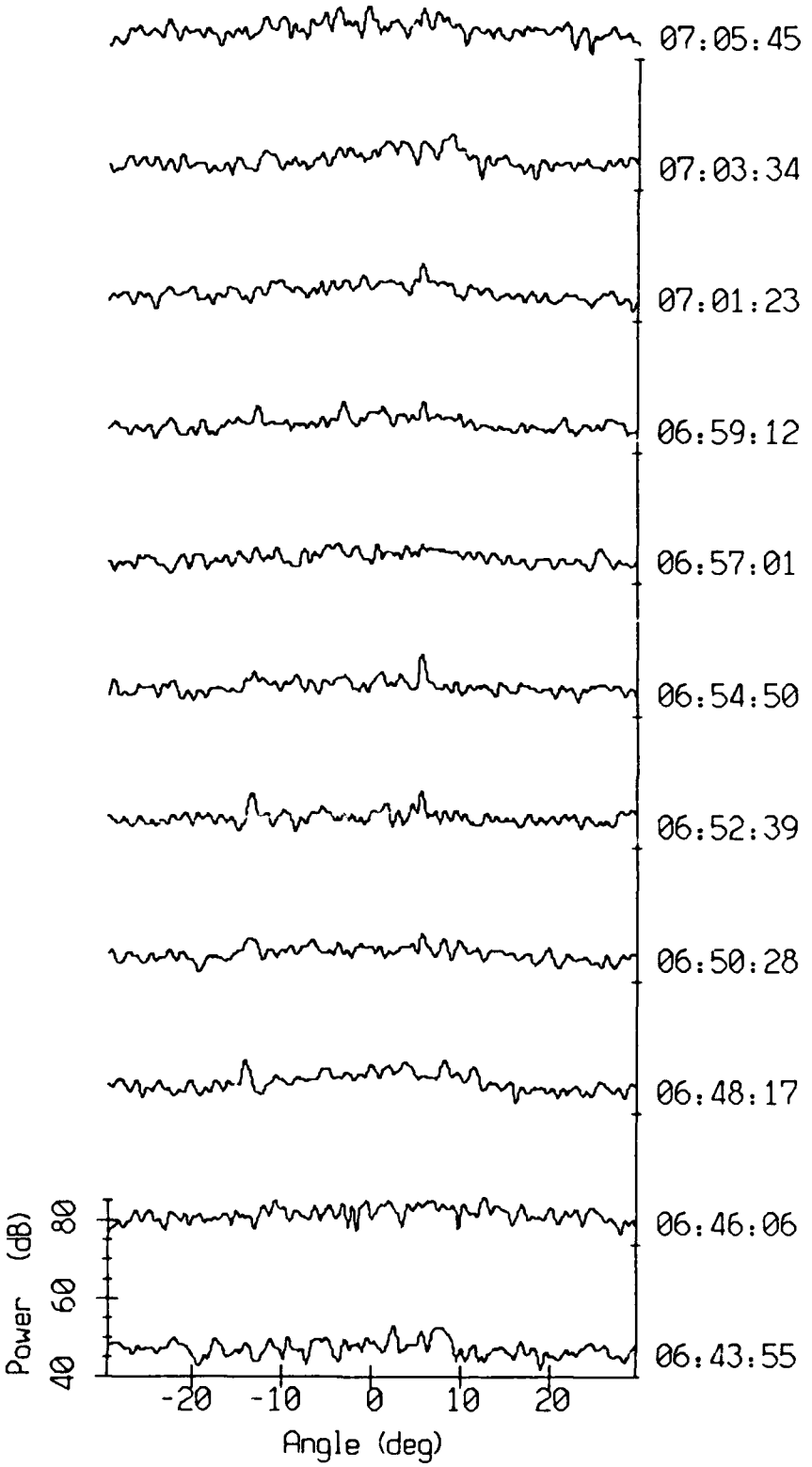
07:05:45
07:03:34
07:01:23
06:59:12
06:57:01
06:54:50
06:52:39
06:50:28
06:48:17
06:46:06
06:43:55
Power (dB)
40
60
80
-20
-10
0
10
20
Angle (deg)

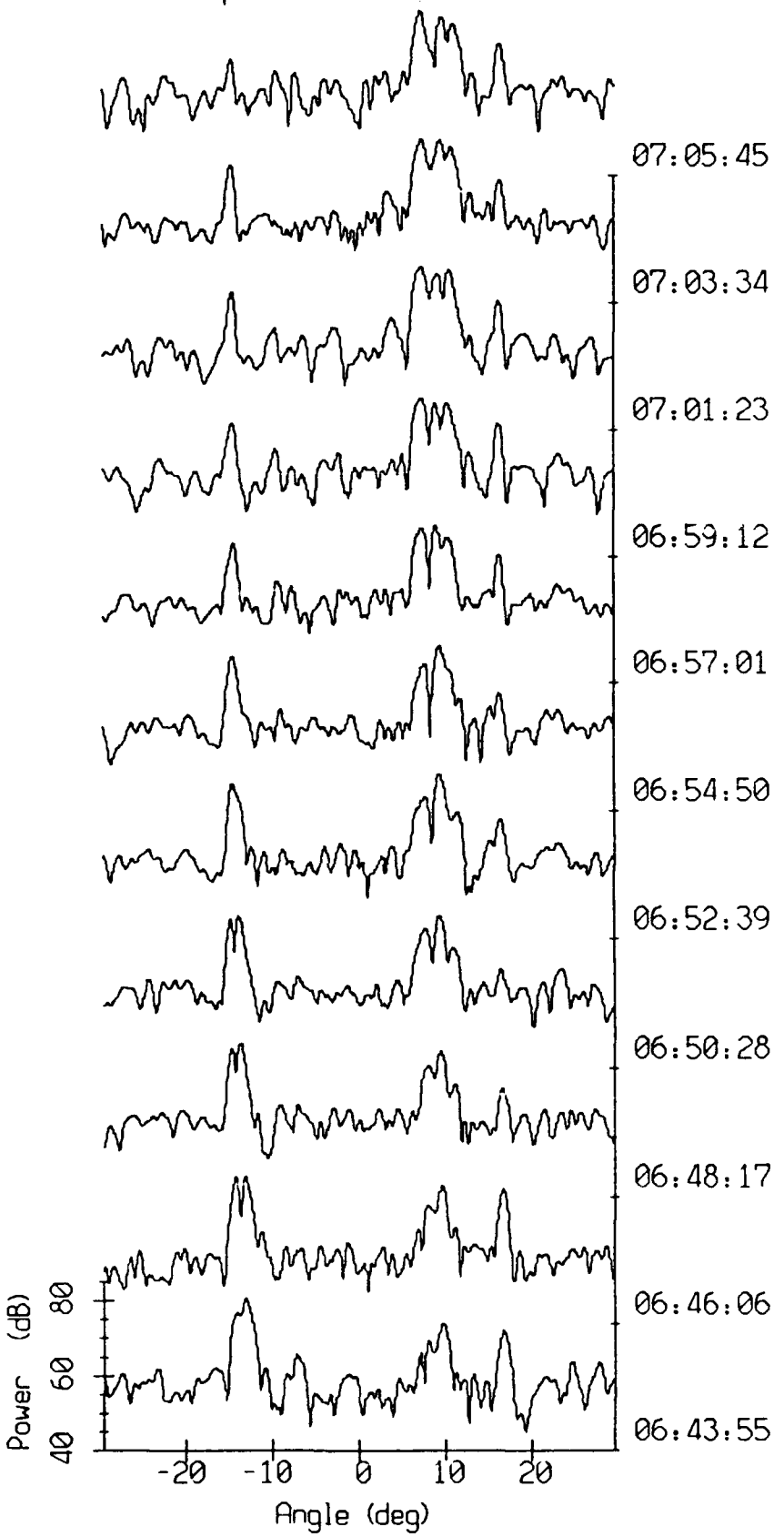
Tape 983 : Bin 7368
07:05:45
07:03:34
07:01:23
06:59:12
06:57:01
06:54:50
06:52:39
06:50:28
06:48:17
06:46:06
06:43:55
Power (dB)
40
60
80
-20
-10
0
10
20
Angle (deg)

Tape 983 : Bin 7369

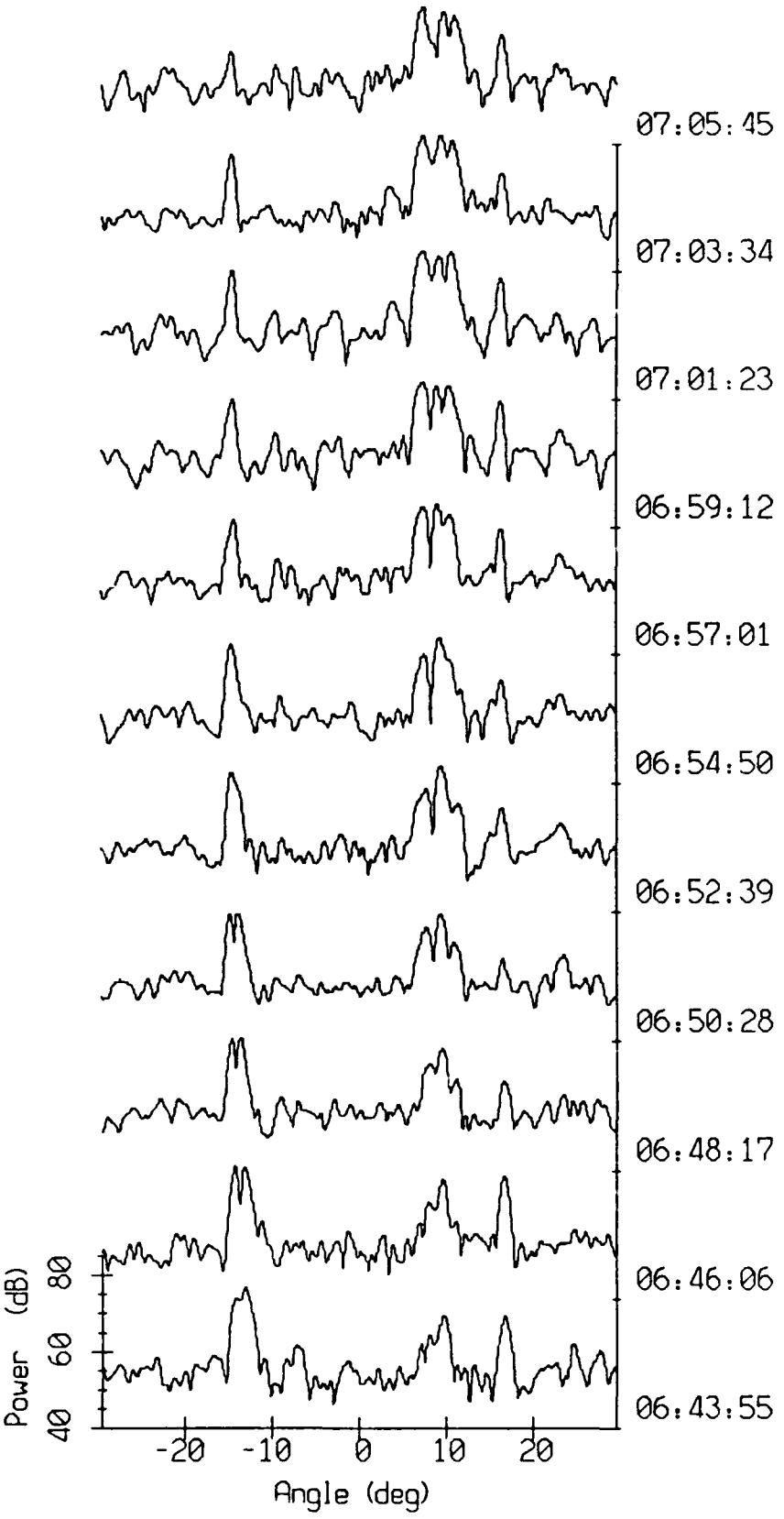

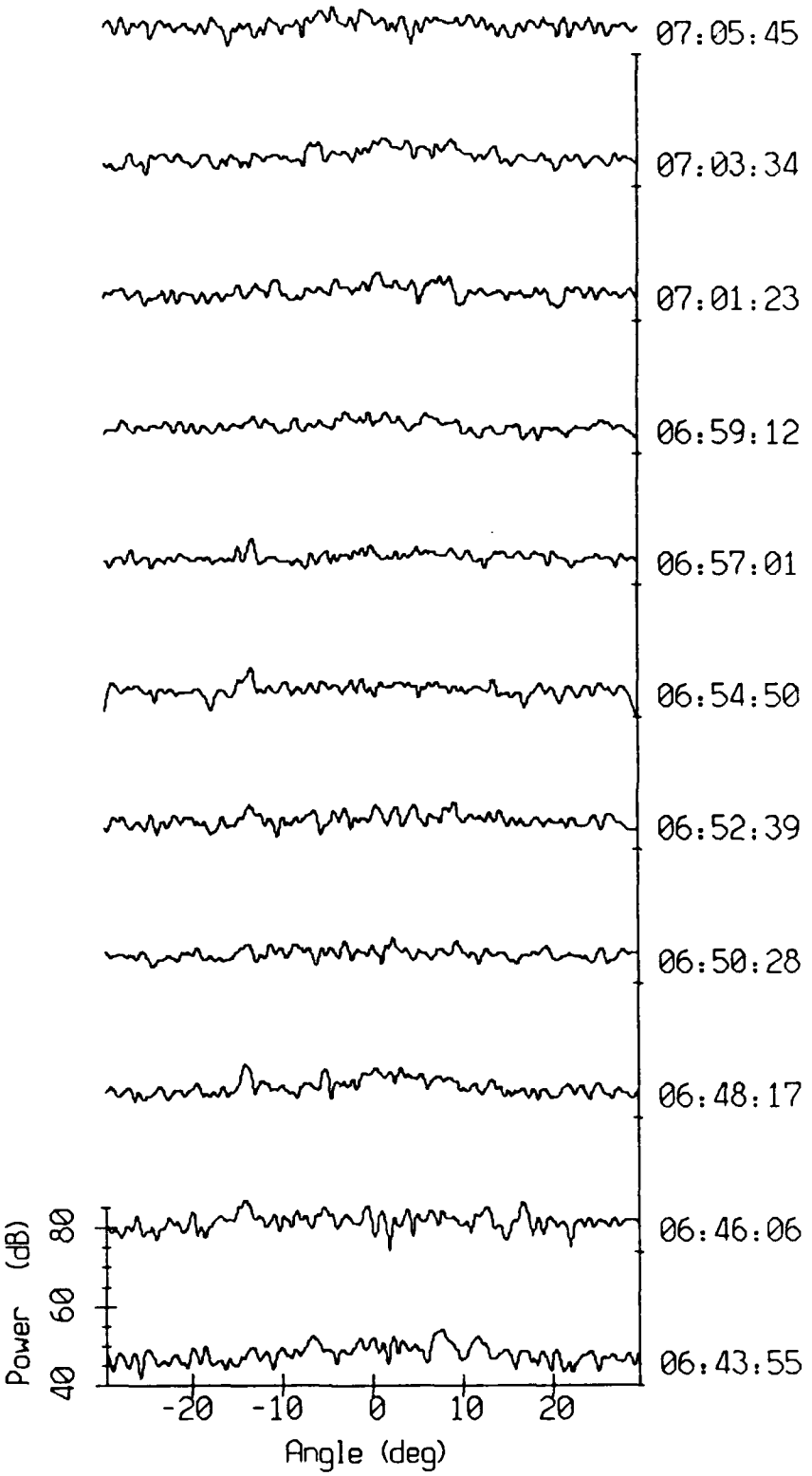
07:05:45
07:03:34
07:01:23
06:59:12
06:57:01
06:54:50
06:52:39
06:50:28
06:48:17
06:46:06
06:43:55
Power (dB)
40
60
80
-20
-10
0
10
20
Angle (deg)

VLA Tape 986, Sept, 1987 - Time 07:51:12 GMT Cal. Pressure Spectra 10(

Data dur.: 2 min 11 sec. FFT Length: 16.38 sec. Samp Freq: 500 Hz

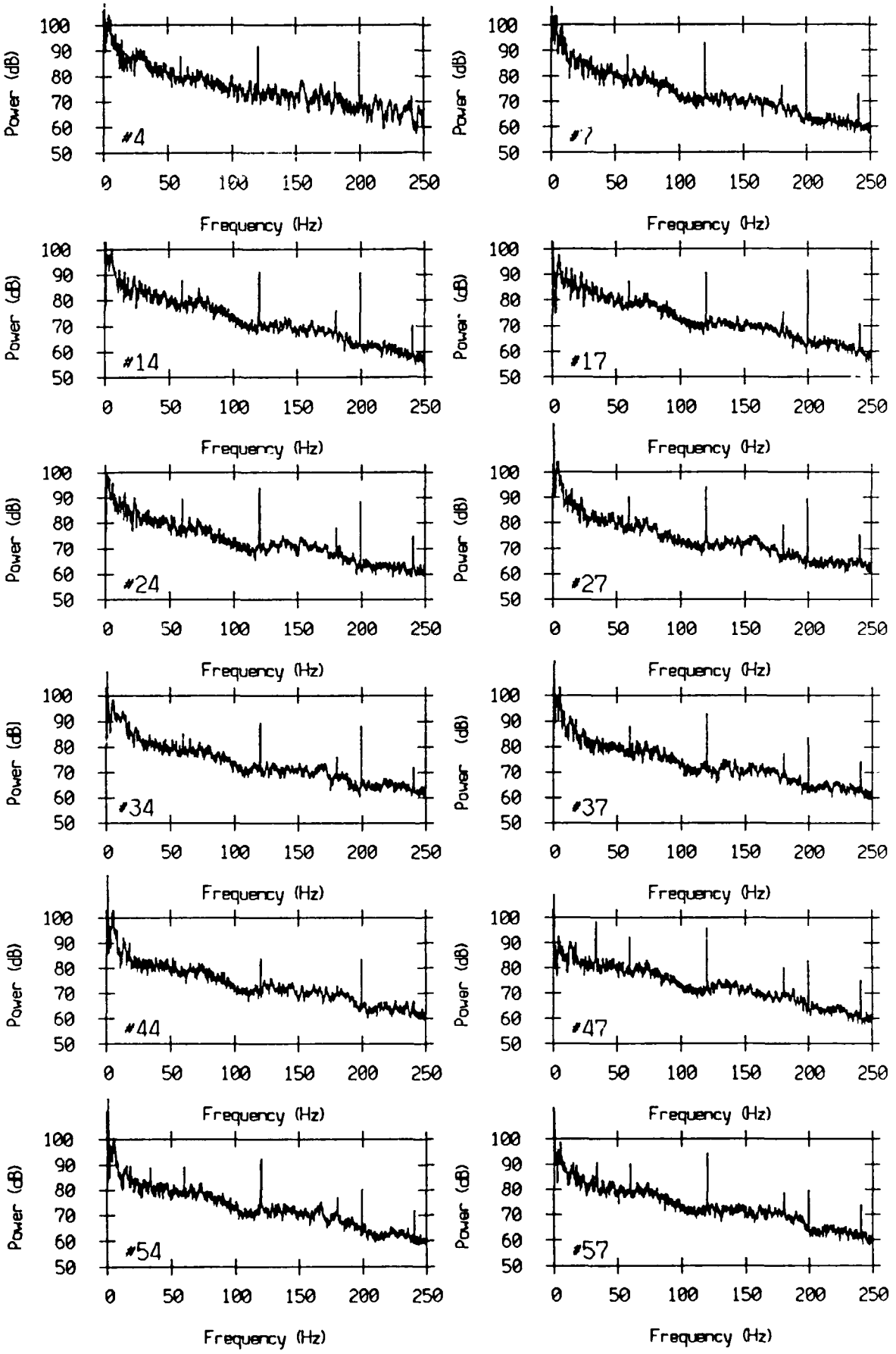

VLA Tape 986, Sept, 1987 - Time 07:51:12 GMT Cal. Pressure Spectra 1(
Data dur.: 2 min 11 sec. FFT Length: 16.38 sec. Samp Freq: 500 Hz

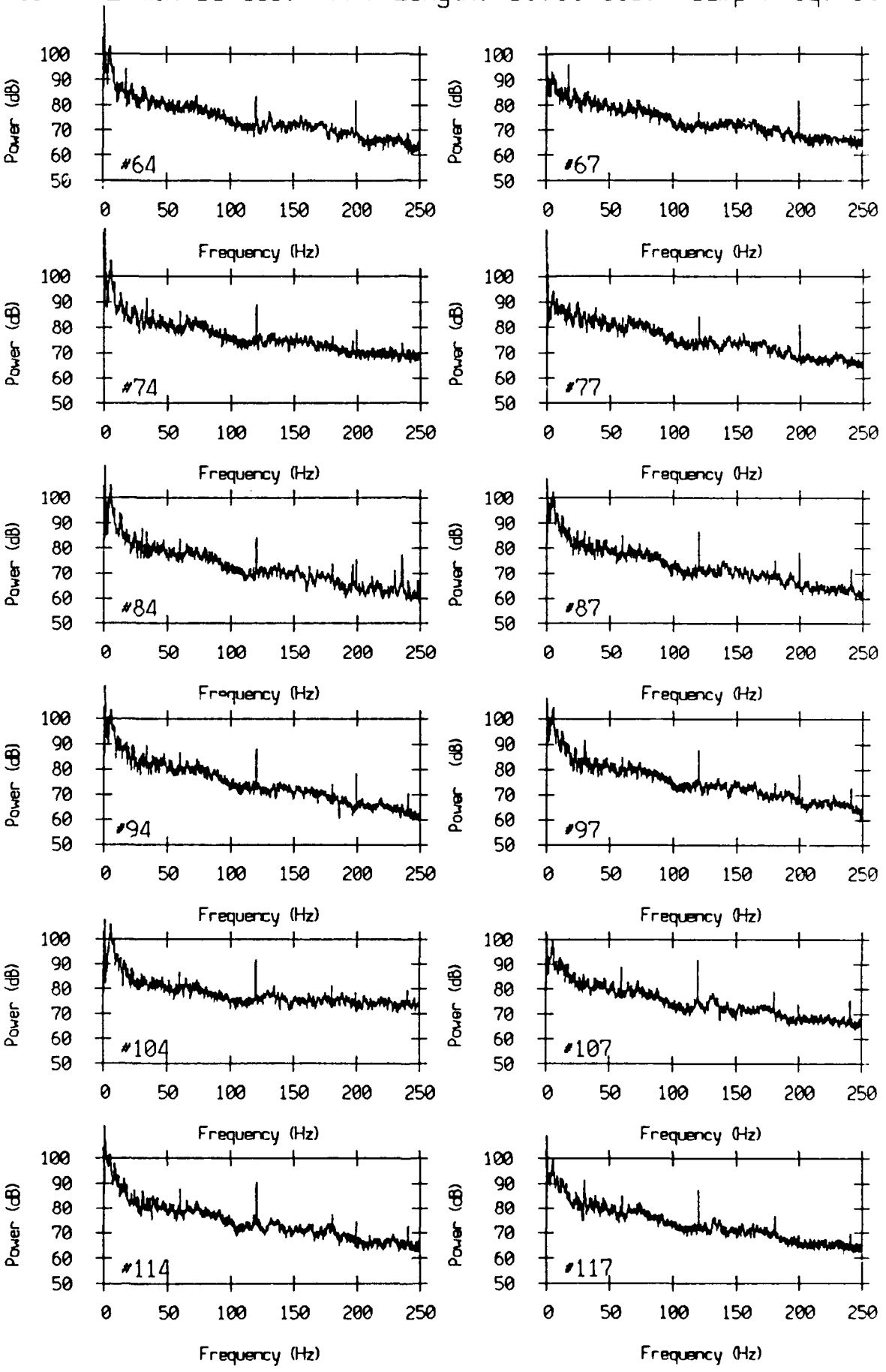

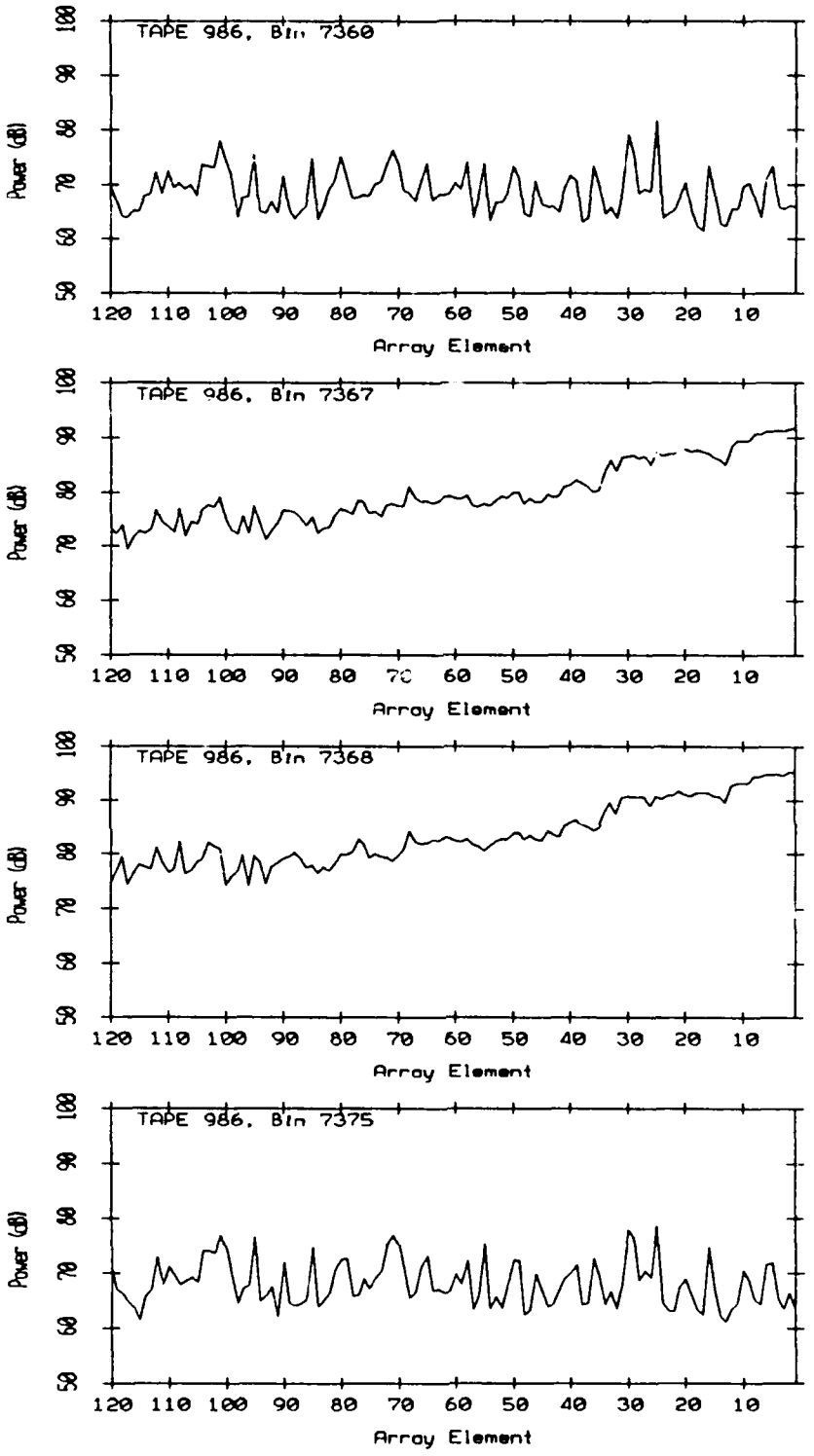
TAPE 986, Bin 7360
TAPE 986, Bin 7367
TAPE 986, Bin 7368
TAPE 986, Bin 7375
Power (dB)
100
90
80
70
60
50
120 110 100 90 80 70 60 50 40 30 20 10
Array Element

Tape 986 : Bin 7360

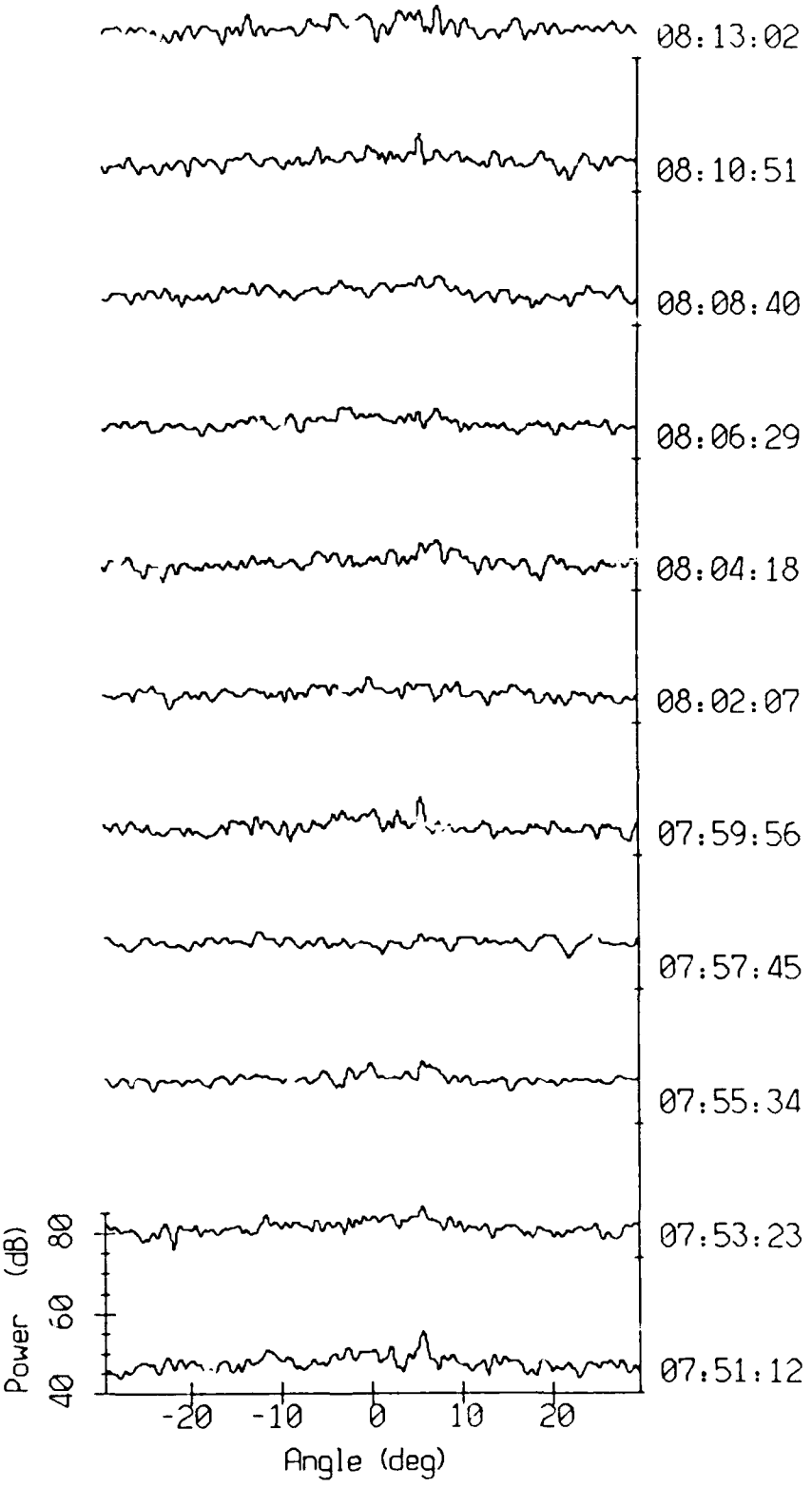

Tape 986 : Bin 7257

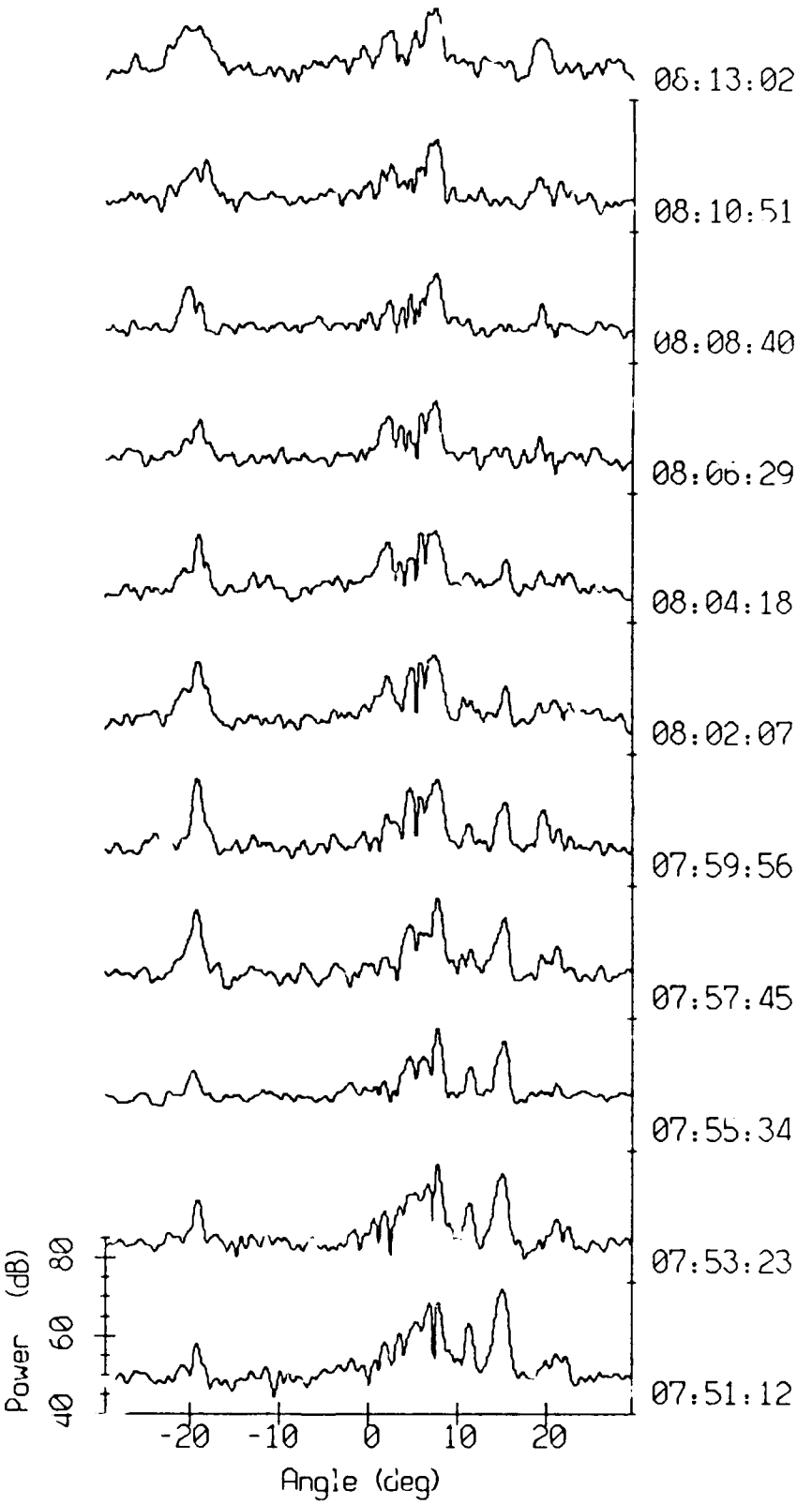

Tape 986 : Bin 7368

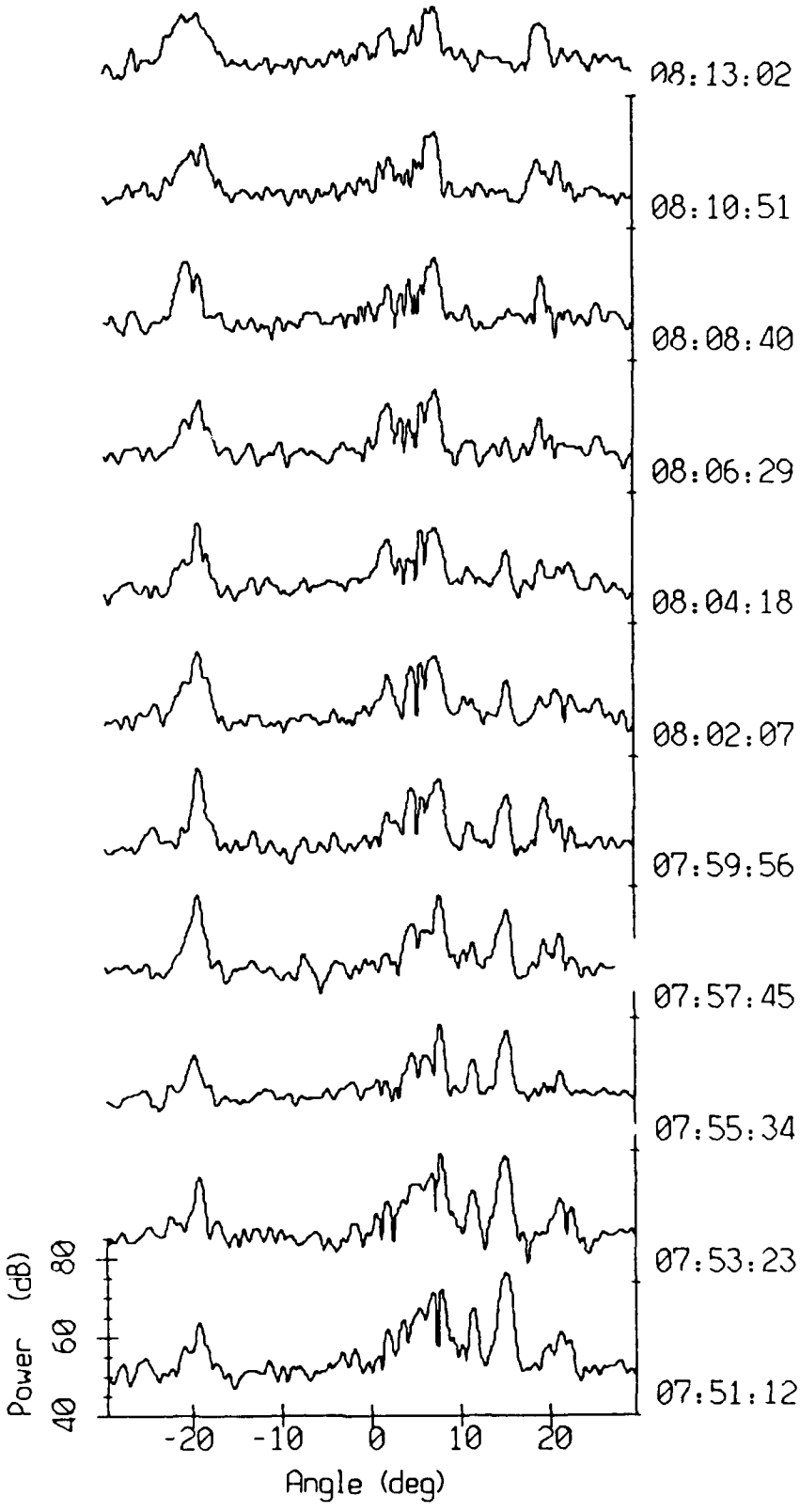

Tape 986 : Bin 7375

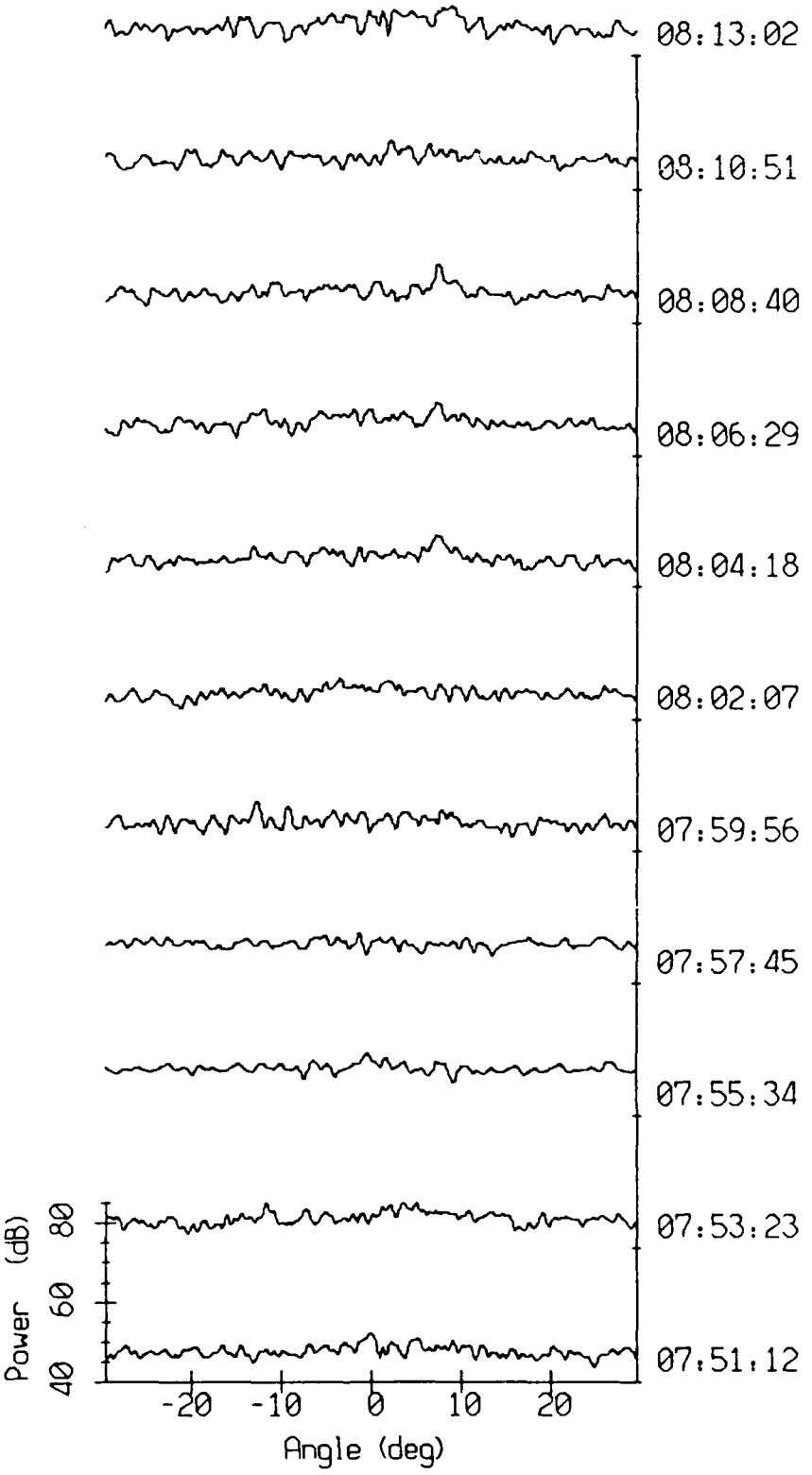

VLA Tape 990, Sept, 1987 - Time 09:31:23 GMT Cal. Pressure Spectra 10
Data dur.: 2 min 11 sec. FFT Length: 16.38 sec. Samp Freq: 500 Hz

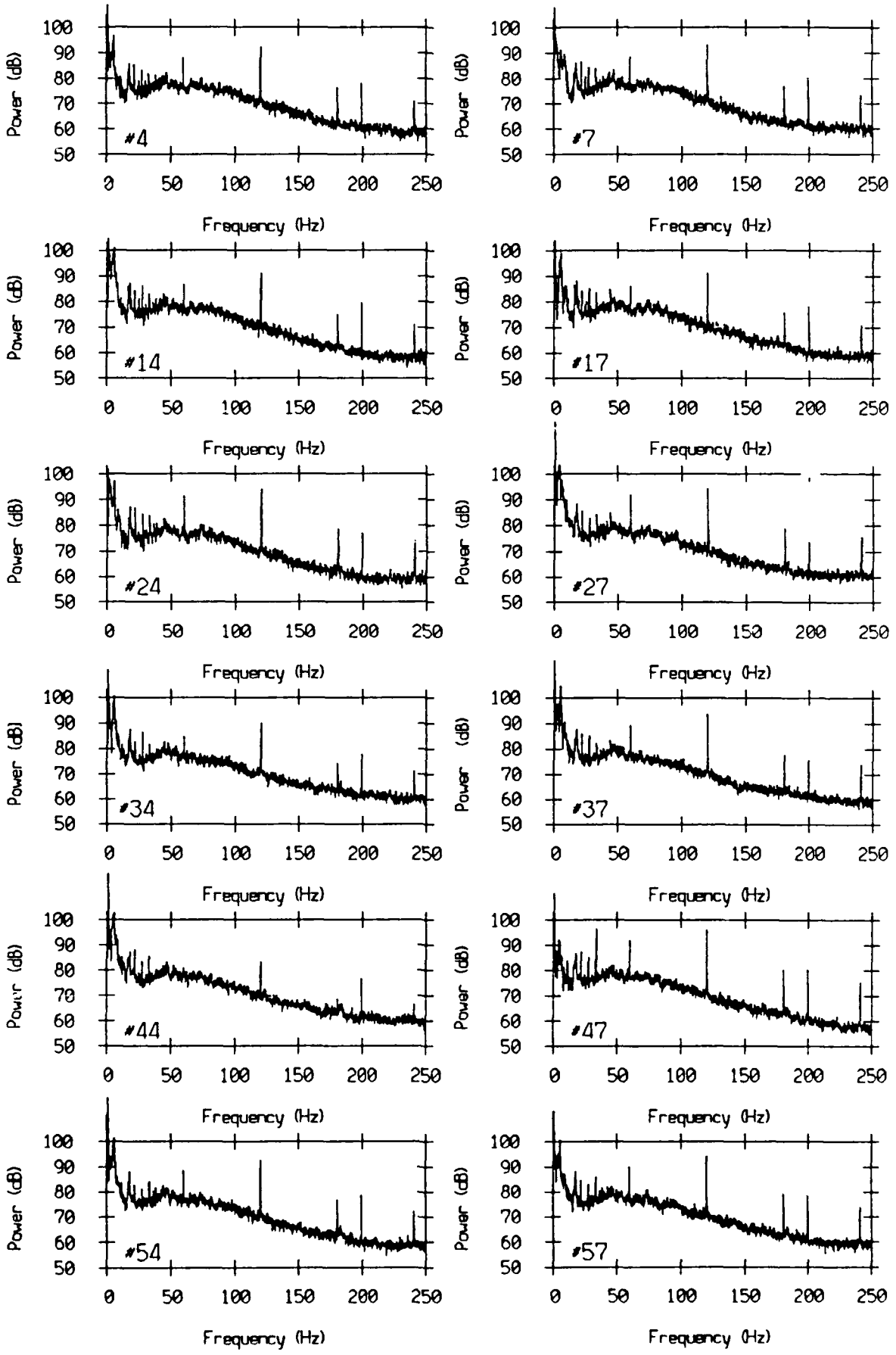

VLA Tape 990, Sept, 1987 - Time 09:31:23 GMT Cal. Pressure Spectra
Data dur.: 2 min 11 sec. FFT Length: 16.38 sec. Samp Freq: 500 Hz

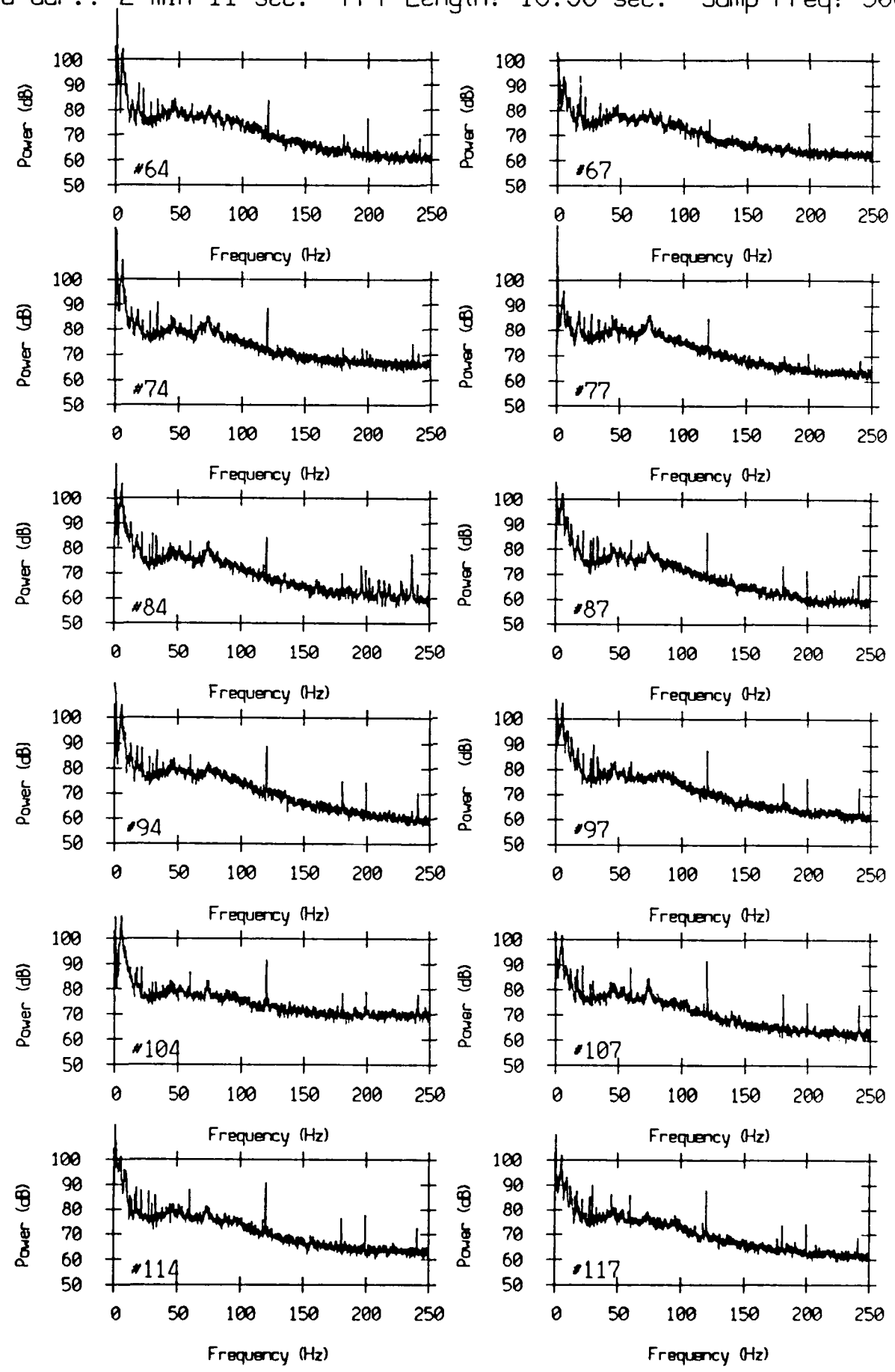

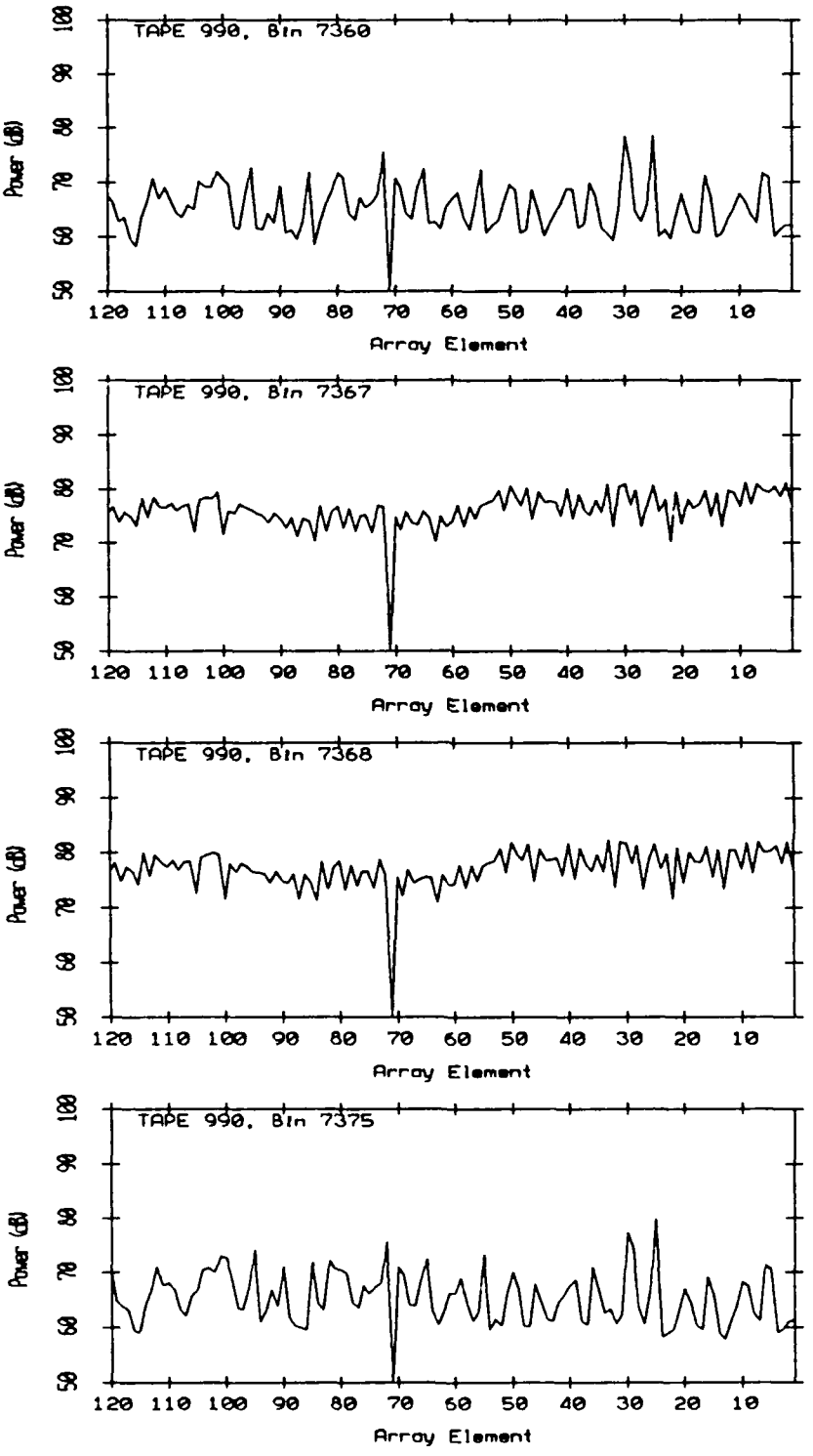
TAPE 990, Bin 7360
TAPE 990, Bin 7367
TAPE 990, Bin 7368
TAPE 990, Bin 7375
Power (dB)
100
90
80
70
60
50
120 110 100 90 80 70 60 50 40 30 20 10
Array Element

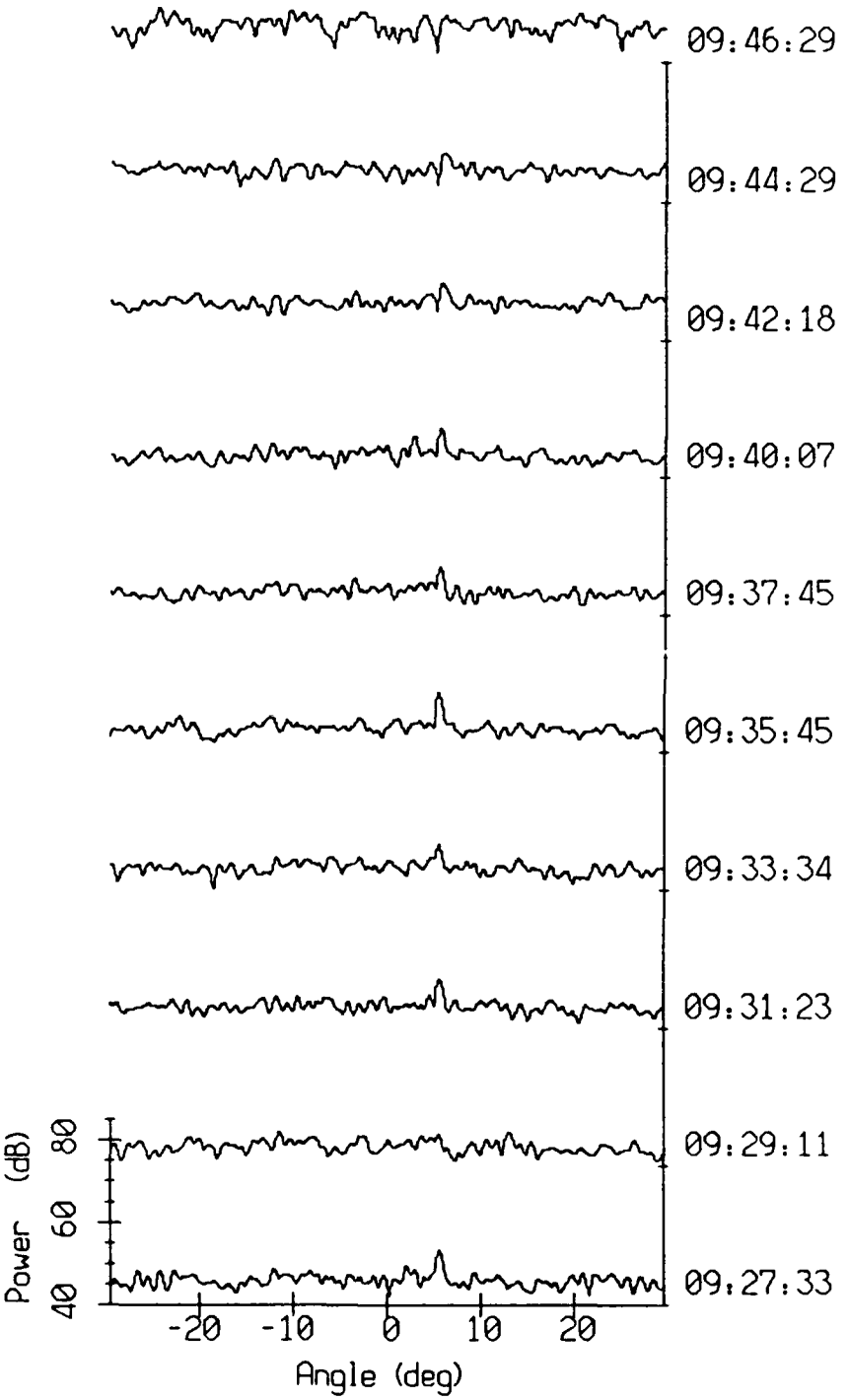
09:46:29
09:44:29
09:42:18
09:40:07
09:37:45
09:35:45
09:33:34
09:31:23
09:29:11
09:27:33
Power (dB)
40
60
80
-20
-10
0
10
20
Angle (deg)

Tape 990 : Bin 7367

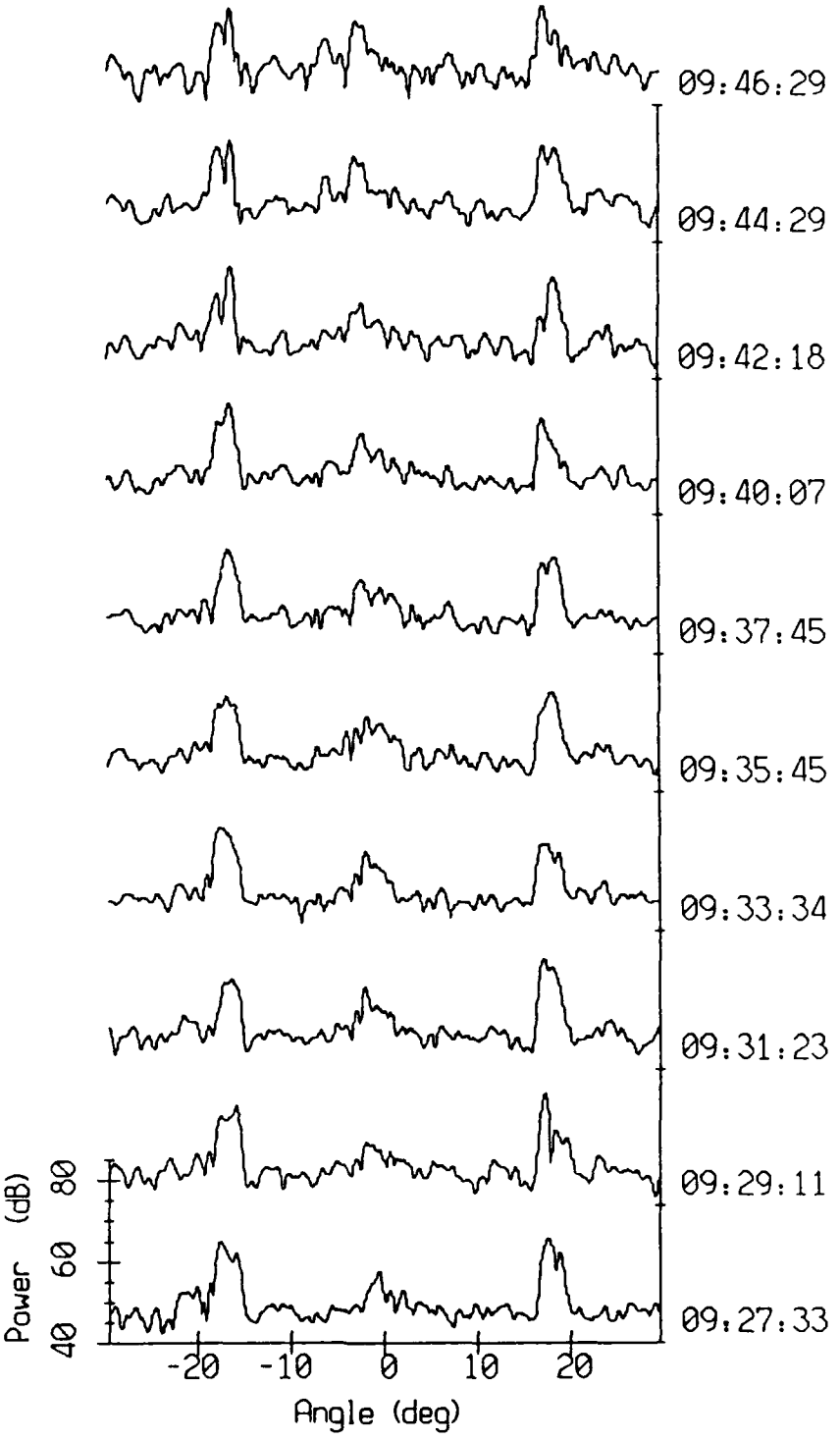

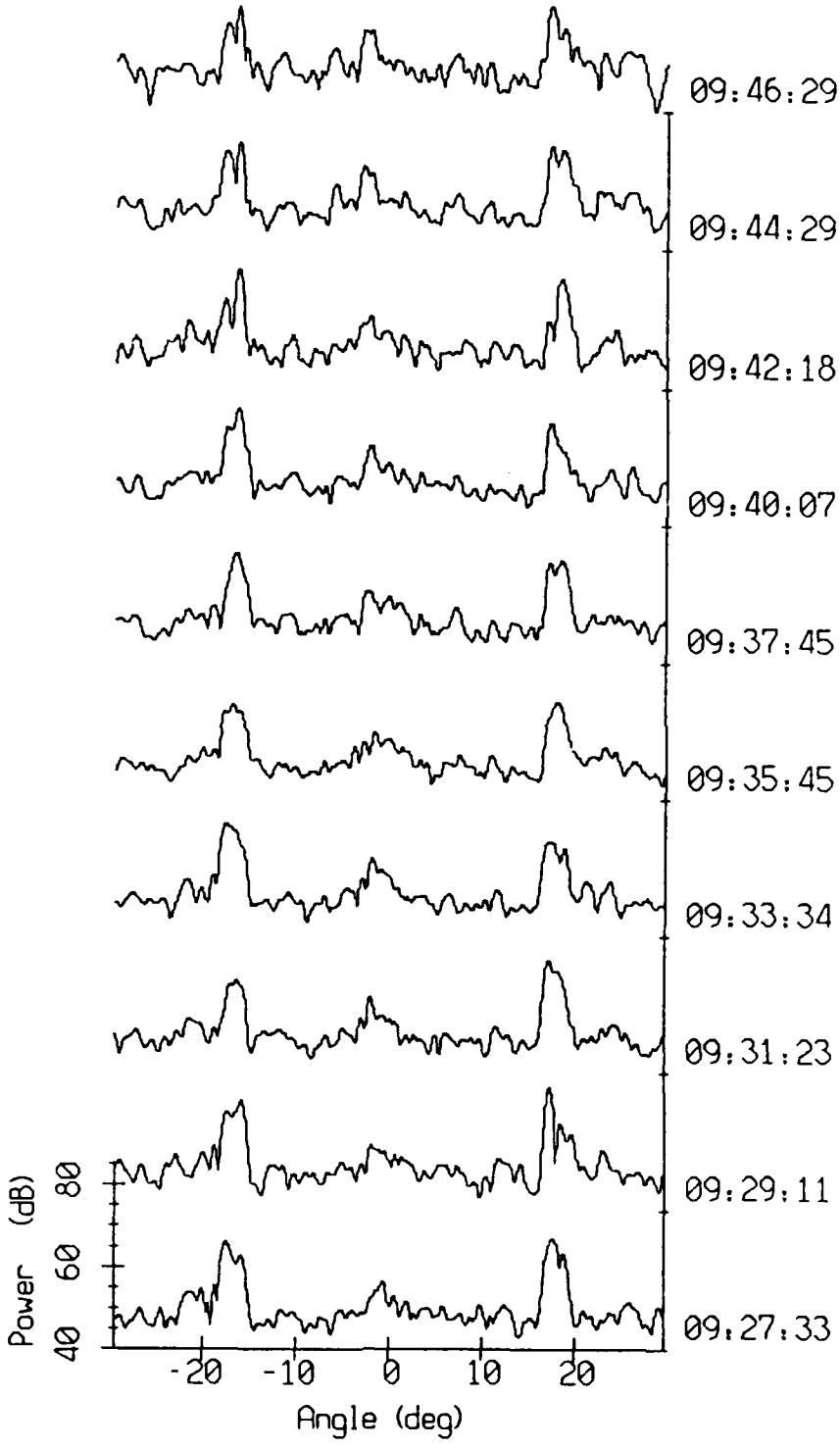
09:46:29
09:44:29
09:42:18
09:40:07
09:37:45
09:35:45
09:33:34
09:31:23
09:29:11
09:27:33
Power (dB)
40
60
80
-20
-10
0
10
20
Angle (deg)

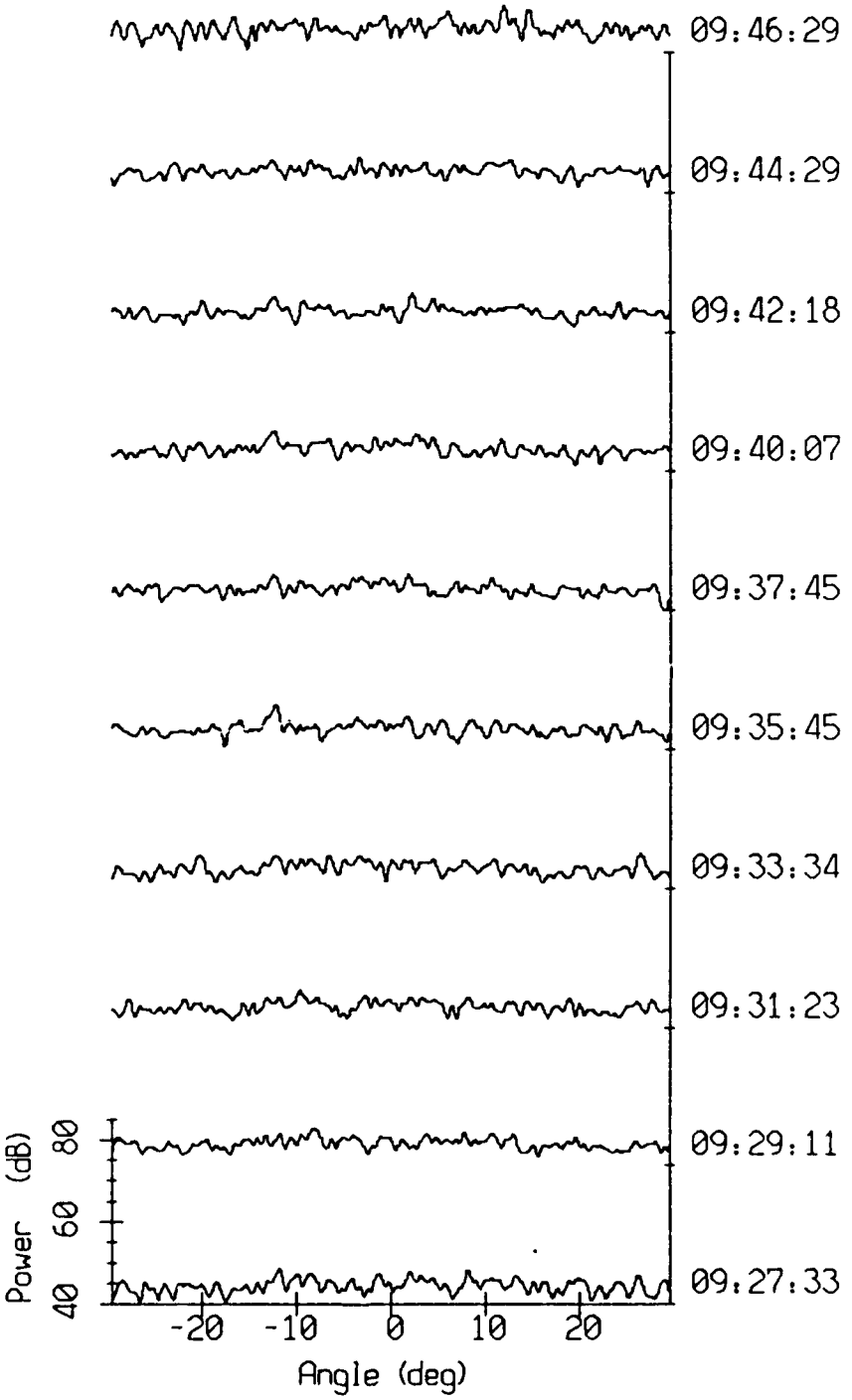
09:46:29
09:44:29
09:42:18
09:40:07
09:37:45
09:35:45
09:33:34
09:31:23
09:29:11
09:27:33
Power (dB)
40
60
80
-20
-10
0
10
20
Angle (deg)